Fisheries and Oceans Canada | Pêches et Océans Canada
Science | Sciences

Canadian Science Advisory Secretariat (CSAS)

Research Document 2014/062

Québec Region

Physical Oceanographic Conditions in the Gulf of St. Lawrence in 2013

P.S. Galbraith[1], J. Chassé[2], D. Gilbert[1], P. Larouche[1], C. Caverhill[3], D. Lefaivre[1], D. Brickman[3], B. Pettigrew[1], L. Devine[4], C. Lafleur[4]

[1] Fisheries and Oceans Canada, Québec Region,
Pelagic and Ecosystem Science Branch,
Maurice Lamontagne Institute,
P.O. Box 1000, Mont-Joli, Québec, G5H 3Z4

[2] Fisheries and Oceans Canada, Gulf Region,
P.O. Box 5030, Moncton, New Brunswick, E1C 9B6

[3] Fisheries and Oceans Canada, Maritimes Region,
Bedford Institute of Oceanography
P.O. Box 1006, Dartmouth, Nova Scotia, B2Y 4A2

[4] Fisheries and Oceans Canada, Québec Region,
Scientific advice, information and support Branch,
Maurice Lamontagne Institute,
P.O. Box 1000, Mont-Joli, Québec, G5H 3Z4

November 2014

Canada

Foreword

This series documents the scientific basis for the evaluation of aquatic resources and ecosystems in Canada. As such, it addresses the issues of the day in the time frames required and the documents it contains are not intended as definitive statements on the subjects addressed but rather as progress reports on ongoing investigations.

Research documents are produced in the official language in which they are provided to the Secretariat.

Published by:

Fisheries and Oceans Canada
Canadian Science Advisory Secretariat
200 Kent Street
Ottawa ON K1A 0E6

http://www.dfo-mpo.gc.ca/csas-sccs/
csas-sccs@dfo-mpo.gc.ca

ISSN 1919-5044

Correct citation for this publication:

Galbraith, P.S., Chassé, J., Gilbert, D., Larouche, P., Caverhill, C., Lefaivre, D., Brickman, D., Pettigrew, B., Devine, L., and Lafleur, C. 2014. Physical Oceanographic Conditions in the Gulf of St. Lawrence in 2013. DFO Can. Sci. Advis. Sec. Res. Doc. 2014/062. vi + 84 p.

This paper is dedicated to the memory of Sylvain Cantin and Daniel Dubé, who both left this world too soon in 2013. Sylvain, head technician in physical oceanography, was involved in all aspects of monitoring programs whose data are used in this series of reports. Daniel Dubé, Coast Guard helicopter pilot, flew the March monitoring survey six times including the last four years. Both were good friends and a pleasure to work with, and are greatly missed.

- *P. S. Galbraith*

TABLE OF CONTENTS

ABSTRACT

An overview of physical oceanographic conditions in the Gulf of St. Lawrence in 2013 is presented as part of the Atlantic Zone Monitoring Program (AZMP). AZMP data as well as data from regional monitoring programs are analysed and presented in relation to long term means. St. Lawrence River annual mean runoff was near-normal but the spring freshet was above-normal. It began early, in March, consistent with early melt associated with the warmest March air temperatures since 1873, and persisted much longer than usual with peak runoff in May and an average runoff nearly as high in June. The seasonal maximal volume of sea ice was 6th lowest since 1969. A large portion of the winter mixed layer remained above-freezing by at least 0.6°C in early March, preventing further sea-ice formation. The August-September cold intermediate layer (CIL) had the third lowest volume ($T < 1°C$) since at least 1985. The CIL minimum temperature index for the Gulf in August-September was the third highest since 1985. The sea-surface temperature averaged from May to November over the Gulf was above-normal by +0.4°C. Deep water temperatures and salinities are increasing overall in the Gulf, with inward advection from Cabot Strait where temperature and salinity reached a record high (since 1915) in 2012 at 200 and 300 m, respectively. Temperature averaged over the Gulf at 300 m increased slightly in 2013 to reach the highest value since 1980. Temperatures at the depth of the temperature maximum (approx. 250 m) were above-normal in Esquiman Channel and central Gulf, exceeding 6°C, causing large areas of the sea floor to be covered by waters with temperatures > 6°C in these areas. Salinity at Cabot Strait at 300 m decreased to normal in 2013, accompanied by a decrease in temperature. While this could have signified an important change to cooler water masses entering the Gulf at depth, waters just as warm as the record of 2012 were observed again in Cabot Strait in March 2014, reaching 7.5°C. The 2013 near-normal conditions were therefore perhaps only a respite.

Conditions océanographiques physiques dans le golfe du Saint-Laurent en 2013

RÉSUMÉ

Le présent document donne un aperçu des conditions d'océanographie physique qui ont prévalu dans le golfe du Saint-Laurent en 2013 et est un produit du Programme de monitorage de la zone Atlantique (PMZA). Les données du PMZA ainsi que de programmes de monitorage régionaux sont analysées et présentées en relation avec des moyennes à long terme. Le débit du fleuve Saint-Laurent était près de la normale, cependant la crue printanière était au-dessus de la normale. Celle-ci a débutée tôt, en mars, fort probablement causée par la fonte hâtive associée aux températures de l'air de mars les plus chaudes depuis au moins 1873. La crue a perdurée, avec un maximum tardif en mai et un débit presque qu'aussi élevé en juin. Le volume de glace de mer a atteint un volume qui en fait le sixième plus faible depuis 1969 tandis qu'une grande portion de l'étendue de la couche mélangée de surface demeurait au moins 0,6 °C au-dessus du point de congélation au début mars, empêchant la formation de glace à ces endroits. Le volume de la couche intermédiaire froide des mois d'août et septembre était à son troisième niveau le plus faible depuis le début de la série en 1985 pour T < 1 °C, tandis que sa température minimale était à son niveau le plus chaud depuis 1985. Les températures à la surface de l'eau moyennées de mai à novembre étaient au-dessus de la normale de +0,4 °C. Les températures et salinités des eaux profondes du golfe sont en augmentation avec l'advection depuis le détroit de Cabot d'eaux qui ont atteintes une température et une salinité record (depuis 1915) en 2012 à 200 m et 300 m respectivement. Globalement, les eaux de 300 m ont atteint un record de température depuis 1980. Les températures aux profondeurs du maximum profond de température ont dépassées le seuil de 6 °C, causant de larges étendues du fond du chenal Esquiman et du centre du golfe à être baignées par des températures > 6 °C. La salinité à 300 m au détroit de Cabot est descendue à un niveau normal en 2013, accompagnée d'une baisse notable de la température. Bien que cela ait pu signifier un important changement vers des masses d'eaux moins chaudes qui entrent dans le golfe, des températures tout aussi chaudes que le record de 2012 ont été observées dans le détroit de Cabot en mars 2014, atteignant 7,5 °C. Les conditions de 2013 ne furent donc possiblement qu'un court répit.

INTRODUCTION

This paper examines the physical oceanographic conditions and related atmospheric forcing in the Gulf of St. Lawrence in 2013 (Fig. 1). It complements similar reviews of the environmental conditions on the Newfoundland and Labrador Shelf and the Scotian Shelf and Gulf of Maine as part of the Atlantic Zone Monitoring Program (AZMP; see Therriault et. al., 1998 for background information on the program and Colbourne et al. 2013, and Hebert et al. 2013 for examples of past reviews in other AZMP regions). Specifically, it discusses air temperature, freshwater runoff, sea-ice volume, surface water temperature and salinity, winter water mass conditions (e.g., the near-freezing mixed layer volume, the volume of dense water that entered the Gulf through the Strait of Belle Isle), the summertime cold intermediate layer (CIL), and the temperature, salinity, and dissolved oxygen of the deeper layers. Some of the variables are spatially averaged over distinct regions of the Gulf (Fig. 2). The report uses data obtained from the Department of Fisheries and Oceans' (DFO) Atlantic Zone Monitoring Program (AZMP), other DFO surveys, and other sources. Environmental conditions are usually expressed as anomalies, i.e., deviations from their long-term mean. The long-term mean or normal conditions are calculated for the 1981–2010 reference period when possible. Furthermore, because these series have different units (°C, m^3, m^2, etc.), each anomaly time series is normalized by dividing by its standard deviation (SD), which is also calculated using data from 1981–2010 when possible. This allows a more direct comparison of the various series. Missing data are represented by grey cells, values within ±0.5 SD of the average as white cells, and conditions corresponding to warmer than normal (higher temperatures, reduced ice volumes, reduced cold-water volumes or areas) by more than 0.5 SD as red cells, with more intense reds corresponding to increasingly warmer conditions. Similarly, blue represents colder than normal conditions. Higher than normal freshwater inflow is shown as red, but does not necessarily correspond to warmer-than-normal conditions. Higher than normal stratification is shown in blue because it usually corresponds to lower salinity. The last detailed report of physical oceanographic conditions in the Gulf of St. Lawrence was produced for the year 2012 (Galbraith et al. 2013a).

The summertime water column in the Gulf of St. Lawrence consists of three distinct layers: the surface layer, the cold intermediate layer (CIL), and the deeper water layer (Fig. 3). Surface temperatures typically reach maximum values in mid-July to mid-August. Gradual cooling occurs thereafter, and wind forced mixing during the fall leads to a progressively deeper and cooler mixed layer, eventually encompassing the CIL. During winter, the surface layer thickens partly because of buoyancy loss (cooling and reduced runoff) and brine rejection associated with sea-ice formation, but mostly from wind-driven mixing prior to ice formation (Galbraith 2006). The surface winter layer extends to an average depth of 75 m and >150 m in places such as the Mécatina Trough (where intruding waters through the Strait of Belle Isle from the Labrador Shelf may extend from the surface to the bottom in depths >200 m) by the end of March when temperatures decrease to near freezing (-1.8 to 0°C) (Galbraith 2006). During spring, surface warming, sea-ice melt waters, and continental runoff produce a lower-salinity and higher-temperature surface layer, below which cold waters from the previous winter are partly isolated from the atmosphere and form the summer CIL. This layer will persist until the next winter, gradually warming up and deepening during summer (Gilbert and Pettigrew 1997; Cyr et al. 2011) and more rapidly during the fall as vertical mixing intensifies.

This report considers these three layers in turn. First, air temperature is examined because it is a significant driver of the surface layer, followed by the freshwater runoff. The winter sea ice and winter oceanographic conditions are described; these force the summer CIL, which is presented next. The deeper waters, mostly isolated from exchanges with the surface, are presented last

along with a summary of major oceanographic surveys. Quantities are often averaged over regions of the Gulf depicted in Fig. 2.

AIR TEMPERATURE

The monthly air temperature anomalies for several stations around the Gulf are shown in Fig. 4 for 2012–2013. Data up to 2012 are the Second Generation of Homogenized Surface Air Temperature Data, part of the Adjusted and Homogenized Canadian Climate Data (AHCCD), which accounts for shifts due to the relocation of stations, changes in observing practices and automation (Vincent et al. 2012). These are completed for 2013 using climate summaries from Environment Canada's National Climate Data and Information Archive (NCDIA). Comparisons between the two data sets are available for several stations around the Gulf in Galbraith and Larouche (2013) for April-November averages and in Galbraith et al. (2013b) for December-February averages. Several airport weather reporting stations have switched over to new NAV Canada sensors and reporting tool and have changed station identification numbers. Nevertheless these data have been merged with previous data if the station positions and altitudes are close to previous EC stations.

Fig. 5 shows the annual, winter (December-March), and April-November mean air temperature anomalies averaged over all stations shown in Fig. 4, since 1873. Record-high annual and winter conditions occurred in 2010 and record-high April-November temperatures in 2012. Galbraith et al. (2012) found the average NCDIA April-November air temperature over the Gulf to be a good proxy for May-November sea-surface temperature over the Gulf (but excluding the estuary) and found within the former a warming trend of 0.9°C per century between 1873 and 2011; the same trend is found here over the selected ACCHD stations between 1873 and 2013 (Fig. 5). Galbraith et al. (2010) found high correlations between NCDIA December-March air temperatures in the western Gulf and sea-ice properties, as well as with winter mixed layer volumes. Galbraith et al. (2013b) found slightly higher correlations with sea-ice using December-February ACCHD averages, possibly because March temperature are not important during low sea-ice cover since much of the sea-ice cover decrease has occurred much earlier in February.

March air temperatures were highest since 1958 at Natashquan, since 1962 at Chevery, since 1965 (series record) at Baie Comeau, and since 1999 at Plum Point, Daniel's Harbour, Stephenville and Port aux Basques. Overall, winter was cut short by a warm March with an average anomaly of +4.7°C (+2.3 SD), a series record since 1873. Combining this with warm air temperatures in December 2012 (+2.1°C anomaly, +0.9 SD) led to a short and mild winter over the Gulf. The December 2012 to March 2013 average air temperature anomaly over the Gulf was +2.3°C (+1.5 SD). April-November air temperatures were near-normal with an anomaly of +0.3°C (+0.5 SD). Air temperatures were below-normal in December 2013, by 6.3°C at Chevery (-2.2 SD, coldest since 1972 and fifth coldest since 1873), and by 5.1°C on average over available Gulf stations (-2.3 SD, coldest since 1972 and tenth lowest since 1873). Annually averaged air temperatures were near-normal overall, with an anomaly of +0.4°C (+0.4 SD).

PRECIPITATION AND FRESHWATER RUNOFF

Freshwater runoff data for the St. Lawrence River are updated monthly (Fig. 6, lower curve) using the water level method from Bourgault and Koutitonsky (1999) and are available from the St. Lawrence Global Observatory. A hydrological watershed model was used to estimate the monthly runoff since 1948 for all other major rivers flowing into the Gulf of St. Lawrence, with discharge locations as shown in Fig. 7. The precipitation data (NCEP reanalysis, six hourly intervals) used as input in the model were obtained from the NOAA-CIRES Climate Diagnostics

Center (Boulder, Colorado, USA; Kalnay et al. 1996). The data were interpolated to a ¼° resolution grid and the water routed to river mouths using a simple algorithm described here. When air temperatures were below freezing, the water was accumulated as snow in the watershed and later melted as a function of warming temperatures. Water regulation is modelled for three rivers that flow into the estuary (Saguenay, Manicouagan, Outardes) for which the annual runoff is redistributed following the climatology of the true regulated runoffs for 12 months thereafter. Runoffs were summed for each region shown and the climatology established for the 1981–2010 period. The waters that flow into the Estuary (region 1, Fig 7.) were added to the St. Lawrence River runoff measured at Québec City to produce what we label here as RIVSUM II although no advection lags were introduced (Fig. 6, upper curve).

Monthly anomalies of the summed runoffs for 2012 and 2013 are shown in Fig. 8. Rivers other than the St. Lawrence contribute about 5 000 $m^3 s^{-1}$ runoff to the Estuary, the equivalent of 40% of the St. Lawrence River, while the other tributaries distributed along the border of the GSL provide an additional 3 500 $m^3 s^{-1}$ in freshwater runoff to the system. River regulation has a strong impact on the relative contributions of sources. For example, in May 2012 the higher-than-average river runoff into the Estuary (an effect of the heavy precipitation in 2011 and river regulation) was almost as important as the then below-normal St. Lawrence run-off. The 2013 simulation shows that rivers in regions 3, 4, 5 and 8 behaved similarly, with higher-than-normal August and September runoff. The long term time series are shown, summed by large basins, in Fig. 9. Broad long-term patterns of runoff over the large basins were similar to that of the St. Lawrence River but interannual variability is low in the Northeast basin and Magdalen Shallows basin. The annual average runoff of the St. Lawrence River measured at Québec City and RIVSUM II both show a general downward trend from the mid-1970s until 2001, an upwards trend since 2001 but were near-normal in 2013 (Fig. 9) at 12 100 $m^3 s^{-1}$ and 17 100 $m^3 s^{-1}$ respectively (both at +0.1 SD). The spring freshet began early with above-normal runoff in March, consistent with early melt associated with above-normal air temperatures (Fig. 6). The freshet also persisted much longer than usual with peak runoff in May rather than April, and nearly as high still in June. The combined March-June observations combine to an above-normal freshet runoff (+0.5 SD and +0.6 SD for the St. Lawrence River and RIVSUM II respectively).

SURFACE LAYER

The surface layer conditions of the Gulf are monitored by various complementary methods. The shipboard thermosalinograph network (Galbraith et al. 2002) consists of temperature-salinity sensors (SBE-21; Sea-Bird Electronics Inc., Bellevue, WA) that have been installed on various ships starting with the commercial ship Cicero of Oceanex Inc. in 1999 (retired in 2006) and on the Cabot from 2006 to fall 2013. They sampled near-surface (3 m depth) water temperature and salinity along their year-round route between Montréal, QC, and St. John's, NL, making a return trip once per week. The data are especially useful for monitoring the winter freeze-up and the evolution of the spring thaw. Limitations of the network are that it does not provide data outside of the main shipping route and that semi-weekly ship tracks are irregular both in time and in the position where each longitude is crossed.

The second data source is the thermograph network (Gilbert et al. 2004, Galbraith et al. 2007), which consists of a number of stations with moored instruments recording water temperature every 30 minutes (Fig. 10). Most instruments are installed on Coast Guard buoys that are deployed in the ice-free season, but a few stations are monitored year-round. The data are typically only available after the instruments are recovered except for oceanographic buoys that transmit data in real-time. Data from Shediac station acquired by the DFO Gulf Region are also

shown. The network provides valuable near-surface temperature data at fixed sites and at short sampling intervals, but usually not in real-time nor during winter months.

The third data source are 1 km resolution monthly composite Sea Surface Temperature (SST) generated using National Oceanic and Atmospheric Administration (NOAA) and European Organisation for the Exploitation of Meteorological Satellites (EUMETSAT) Advanced Very High Resolution Radiometer (AVHRR) satellite images available from the Maurice Lamontagne Institute sea surface temperature processing facility (details in Galbraith and Larouche 2011, and Galbraith et al. 2012). These data are available for sea-ice free months with 1985-2010 climatologies computed for the months of May to November. Unfortunately, the MLI data processing has been on hold since September 2013 because of unresolved lack of hard disk space, and so the remaining four months were filled-in using AVHRR composites provided by the Bedford Institute of Oceanography (BIO) Operational Remote Sensing. However a thorough comparison of the data sets has not been completed.

SST SEASONAL CYCLE CLIMATOLOGY

The May to November cycle of weekly averaged surface temperature is illustrated in Fig. 11 using a 1985–2010 climatology based on AVHRR remote sensing data for ice-free months complemented by 2001–2010 thermosalinograph data for the winter months. Galbraith et al. (2012) have shown that Gulf-averaged air temperature and SST monthly climatologies match up quite well with SST lagging air temperature by half a month. Maximum sea-surface temperatures are reached on average during the second week of August but can vary by up to several weeks from year to year. The maximum surface temperature averages 15.6ºC over the Gulf during the second week of August (1985–2010), but there are spatial differences: temperatures on the Magdalen Shallows are the warmest of the Gulf, averaging 18.1ºC over the area, and the coolest are at the head of the St. Lawrence Estuary and upwelling areas along the lower North Shore.

Fig. 12 shows a mean annual cycle of water temperature at a depth of 3 m along the Montréal to St. John's shipping route based on thermosalinograph data collected from 2000 to 2013. Data were used from all instrumented ships that were within the main shipping route area to fill data gaps. The data were averaged for each day of the year at intervals of 0.1 degree of longitude to create a composite along the ship track. The most striking feature is the area at the head of the Laurentian Trough (69.5°W), where strong vertical mixing leads to cold summer water temperatures (around 5°C to 6°C and sometimes lower) and winter temperatures that are always above freezing (see also Fig. 11). The climatology shows the progression to winter conditions, first reaching near-freezing temperatures in the Estuary and then progressing eastward with time, usually reaching Cabot Strait by the end of the winter.

Temperature anomaly time series and 2000–2013 climatologies were constructed for selected sections that are crossed by the ship (Fig. 13). Although the anomalies are quite similar between the two sections, the near-surface temperature climatology at Tadoussac (head of the Laurentian Trough) contrasts with that nearby in the Estuary, as noted above. Winter temperatures are on average 0.6°C warmer at the Tadoussac section; the maximum monthly mean temperature in summer is only 6.8°C compared with 8.5°C at the nearby Estuary section and up to 13.1°C at the Mont-Louis section. The table provides a quick reference to the interannual near-surface temperature variations at the selected sections as well as monthly averages for the year in review.

SST IN 2013

Figs. 12 and 13 both show that near surface temperatures were close to freezing in winter over a shorter than normal period and over a smaller portion of the Gulf. The Estuary remained warm and spring warming occurred early everywhere, consistent with above-normal air temperatures in March. After a brief warm period in early May, the rest of the year was characterized mostly by cool surface waters within the Gulf until at least October. Conditions in Cabot Strait were however typically warm, similar to those found south of Newfoundland out to 55°W.

The 2013 monthly mean sea-surface temperatures from NOAA AVHRR imagery are shown in Fig. 14 as colour-coded maps and the corresponding temperature anomaly maps are shown in Fig. 15. These are referenced to the 1985–2010 monthly climatology for the months of January-August and 1999-2010 for September-November. The anomalies are shown only for the months of May to November, because ice cover biases the climatologies for the other months (even though December has been ice-free in recent years, it would be difficult to construct a valid climatology since 1985). April is included but is only accurate for the usually ice-free Northwest Gulf. The NOAA SST information is summarized in Fig. 16, showing the 2012 and 2013 monthly surface temperature anomalies spatially averaged over the Gulf and over each of the eight regions delimited by the areas shown in Fig. 2, and further into sub-regions of the Estuary as shown in Fig. 17 (Saguenay not available in data from BIO at this time). In sharp contrast to the generally above-normal temperatures of 2012, near-surface water temperatures were often below-normal in the Estuary and northwest Gulf, above-normal in Cabot Strait and near-normal elsewhere. October and November generally had above-normal temperatures.

Figures 18 and 19 show the 1985–2013 time series of monthly surface temperature anomalies spatially averaged over the Gulf of St. Lawrence and over the eight regions of the Gulf. These results show that Gulf-wide averaged temperatures in 2013 were near-normal from May to September and above-normal in October and November, similar to temperatures in 2011. October is shown to be the second warmest in the time series, however there may be a small bias between the two SST data sets used and so this should be considered to be a preliminary result. Averaged May-November over all regions, SST was above-normal by +0.4°C (+0.6 SD).

Sea-surface temperature monthly climatologies and time series were also extracted for more specific regions of the Gulf. The monthly average SST for the St. Lawrence Estuary as a whole (region 1) is repeated in Fig. 20 along with averages for the proposed Manicouagan Marine Protected Area (MPA), the proposed St. Lawrence Estuary MPA, and the Saguenay – St. Lawrence Marine Park. The overall pattern is similar across regions, but there are differences associated with episodic local events such as eddies and upwellings. The climatology averages also differ, for example the Manicouagan maximum monthly average temperature is 1.0°C warmer than for the Estuary as a whole.

The Magdalen Shallows, excluding Northumberland Strait, is divided into western and eastern areas as shown in Fig. 21. The monthly average SST for the Magdalen Shallows as a whole (region 8) is repeated in Fig. 22 along with averages for the western and eastern areas. Climatologies differ by roughly 0.5°C to 1°C between the western and eastern regions. Temperatures were typically near-normal before October and above-normal thereafter for both sub-regions.

Thermograph network observations are compared to daily average temperatures calculated using all available data for each day of the year at each station and depth (Figs. 23-25). The seasonal cycle of near-surface temperature is measured by shallow instruments, while Cold Intermediate Layer warming from spring to fall is captured by instruments moored between 30 and 120 m depth. Monthly average temperatures are also shown, with the magnitude of their anomaly colour-coded. Salinities are shown in a similar fashion in Fig. 26. The average monthly

temperatures for each station at shallow sampling depths (< 20 m) for 2012 and 2013 are also shown in Fig. 27.

Monthly anomalies were fairly consistent across all stations of each of the three regions listed in Fig. 27. As with AVHRR data sources and in spite of different climatological periods, the month of October is the only period showing widespread warm anomalies. The three stations recording winter temperatures showed near-normal or colder than normal values in mid-winter but shorter cold seasons.

Fig. 28 shows information similar to Fig. 27, but for thermograph sensors moored deeper than 20 m. The deep (>300 m) waters of the Estuary show above-normal temperatures in 2013 after near-normal temperatures in 2012 and below-normal values in 2011 (not shown; see Galbraith et al. 2013a).

Fig. 29 shows the history of monthly averaged temperature anomalies for selected stations both in the northeastern and southern Gulf. There are large differences in springtime bottom temperature at the Strait of Belle Isle (71 m) depending on how late the cold inflow of Labrador Shelf Water persists. The Shediac Valley (82 m) and Irwing Whale (67 m) stations both show interannual variability and the seasonality of bottom temperature on the Magdalen Shallows, and the Île Shag (10 m) and La Perle (26 m) stations both show bottom temperature close to Îles-de-la-Madeleine that are important to the lobster fishery.

SEA ICE

Ice volume is estimated from a gridded database of ice cover and ice categories obtained from the Canadian Ice Service, consisting of weekly estimates for 1969–1997 and daily with higher spatial resolution thereafter. Standard average thicknesses are attributed to each ice category to estimate the volume. Offshore sea ice is typically produced in the northern parts of the Gulf and drifts towards Îles-de-la-Madeleine and Cabot Strait during the ice season. The maximum ice volume that occurred within the Gulf (delimited at Cabot Strait) in 2013 is shown and compared with previous minimum and maximum conditions observed in 2010 and 1993 (Fig. 30). This differs from last year's report where the total volume including the Scotian Shelf was considered, picking out 2003 as the maximum of the time series rather than 1993.

Fig. 31 shows the daily evolution of the estimated sea-ice volume in relation to the climatology and historical extremes. It clearly shows why the high interannual variability in ice cover leads to weak normalized anomalies even in cases of near-absence of sea-ice. Fig. 32 shows the estimated seasonal maximum ice volumes within the Gulf as well as on the Scotian Shelf. Processing differs from last year's report in that the land fraction within each cell is not counted as ice in the relatively coarse grid prior to 1988 (e.g. see coarser resolution grid in the map for 1993 in Fig. 30) and daily values from 1998 onwards were low-pass filtered using a 7-day running mean prior to identifying the seasonal maximum in order to be more comparable with the pre-1998 weekly charts. The combined Gulf and Scotian Shelf ice volume shown separately as top and bottom panels of Fig. 32 is indicative of the total volume of ice produced in the Gulf, including the advection out of the Gulf, but it also includes the thicker sea ice that drifts into the Gulf from the Strait of Belle Isle. The volume shown on the bottom panel of Fig. 32 corresponds to that found seaward of Cabot Strait (defined by its narrowest crossing). It would represent the volume of ice exported from the Gulf provided that no melt had already occurred. Fig. 33 shows the day of first and last occurrence of ice in each of the regions of the Gulf of St. Lawrence, extracted from the same database, as well as duration of the ice season and maximum observed volume during each season. Caution should be used in over interpreting the values since the database from which it is produced is only at weekly resolution prior to 1998. Fig. 34 shows the time series of seasonal maximum ice volume and area (excluding thin new ice), ice

season duration and December-to-March air temperature anomaly (from Fig. 5). The figure shows declining trends in ice cover severity since 1990. The correlation between annual maximum ice volume (including the Scotian Shelf) and the December-February air temperature averaged over five Western Gulf stations (Sept-Îles, Mont-Joli, Gaspé, Charlottetown and Îles-de-la-Madeleine) accounted for 72% of the variance using the 1969–2012 time series (Galbraith et al. 2013b). Fig. 34 shows a similar comparison using only ice volume within the Gulf and the ACCHD December-to-March air temperature anomaly from Fig. 5. The correlation coefficient is reduced to $R^2 = 0.58$ between the ice volume and air temperature anomaly, however including ice exported to the Scotia Shelf would yield $R^2 = 0.72$ as in Galbraith et al, 2013b. The correlation between air temperature and the ice parameters season duration and area are very high ($R^2 = 0.78$ and 0.74). Correlation coefficients are slightly higher when using January to February air temperatures, perhaps because March air temperatures have no effect on ice cover that has almost disappeared by then during very mild winters.

In 2013, the Gulf seasonal maximum ice volume was 26 km³ (Fig. 30), more than double the volume of the record low of the 1969–2010 time series observed three years earlier (11 km³ in 2010), still 1.4 SD below the 63 km³ climatological average and 6th lowest of the time series (Fig. 32). In fact, four of the six lowest maximum ice volumes of the time series have occurred in the last four years. Almost no ice was exported from the Gulf of St. Lawrence onto the Scotian Shelf for the fourth consecutive year. This low maximum ice is consistent with the December-March Gulf air temperature anomaly of +2.3°C (+1.5 SD, Fig. 5 and Fig. 34). The sea-ice cover throughout the season was typically at or below the -1 SD level from the 1981-2010 climatology (Fig. 31). The duration of the 2011–12 ice season was much shorter than normal in all regions except the Magdalen Shallows and Cabot Strait, due to late ice formation and early melt (Fig. 33).

WINTER WATER MASSES

A wintertime survey of the Gulf of St. Lawrence waters (0–200 m) has been undertaken in early March since 1996 using a Canadian Coast Guard helicopter. This has added a considerable amount of data to the previously very sparse winter data for the region. The survey, sampling methods, and results concerning the cold-water volume formed in the Gulf and the estimate of the water volume advected into the Gulf via the Strait of Belle Isle over the winter are described in Galbraith (2006) and in Galbraith et al. (2006). One hundred and seven stations were sampled during the 5–14 March 2013 survey. Fig. 35 and Fig. 36 show gridded interpolations of near-surface temperature, temperature above freezing, salinity, cold layer thickness and where it contacts the bottom, and thickness of the Labrador Shelf water intrusion for 2012 and 2013.

During winters prior to 2010, the surface mixed layer was usually very close (within 0.1°C) to the freezing point in most regions of the Gulf but thickness of the surface layer varied, leading to variability in the cold-water volume between mild and severe winters. This was not the case in 2010 for the first time since the inception of the winter survey, when the mixed layer was on average 1°C above freezing. Similar conditions to those of 2010 were observed in March 2011, although not quite as warm. The winter surface mixed layer returned to near-normal conditions in 2012, as observed prior to 2010, whereby waters were near-freezing at the end of winter over a large portion of the Gulf (Fig. 35). However in March 2013 such conditions were limited to Mécatina Trough and shallow portions of the Magdalen Shelf.

During typical winters, surface waters in the temperature range of ~ 0°C to -1°C are only found on the northeast side of Cabot Strait. Some of these warm waters have presumably entered the Gulf during winter and flowed northward along the west coast of Newfoundland, however it is also possible that local waters could have simply not cooled close to freezing. The area of warm

water was fairly extensive in 2013, reaching Anticosti Island with temperatures generally < -0.5°C, and extending over the Laurentian Channel with temperatures between -0.5°C and -1°C. Near-freezing waters with salinities of around 32 are responsible for the (local) formation of the CIL since that is roughly the salinity at the temperature minimum during summer. These are coded in blue in the salinity panel of Fig. 35 and are typically found to the north and east of Anticosti Island. Surface salinities were generally lower than usual in this part of the Gulf during the winter of 2013 although higher than the same period in 2012.

Near-freezing waters with salinity >32.35 (colour-coded in violet) are considered to be too saline to have been formed from waters originating within the Gulf (Galbraith 2006) and are presumed to have been advected from the Labrador Shelf through the Strait of Belle Isle. These waters were only present at the surface close to and in the Strait of Belle Isle (Fig. 35) in March 2013. A T-S water mass criterion from Galbraith (2006) was used to identify intruding Labrador Shelf waters that have exhibited no evidence of mixing with warm and saline deep Gulf water. These waters occupied the sub-surface of the northern portion of Mécatina Trough in March 2013 (top-right panel of Fig. 36). The recent history of Labrador Shelf water intrusions is shown in Fig. 37, where its volume is shown as well as the fraction it represents of all the cold-water volume in the Gulf. This volume was below normal in March 2013, at 1000 km³ (-0.6 SD), but near-normal as the percentage of cold water it represents, at 12% (-0.3 SD).

The cold mixed layer depth typically reaches about 75 m in the Gulf and is usually delimited by the -1°C isotherm because the mixed layer is typically near-freezing and deeper waters are much warmer (Galbraith 2006). In March 2010 and 2011 much of the mixed layer was warmer than -1°C such that the criterion of T<0°C was also introduced (see middle panels of Fig. 36). The cold surface layer is the product of local formation as well as cold waters advected from the Labrador Shelf, and can consist either of a single water mass or of layers of increasing salinity with depth. Integrating the cold layer depth over the area of the Gulf (including the Estuary but excluding the Strait of Belle Isle) yields a cold-water (<- 1°C) volume of 8 200 km³ (Fig. 36), 1.0 SD below the 1999–2013 average and similar to the volume observed in 2011. The mixed layer volume increases to 15 500 km³ when water temperatures <0°C are considered which is 0.3 SD above the 1999–2013 average. This volume of cold water corresponds to 46% of the total water volume of the Gulf (33 500 km³, including the Estuary). The time series of winter cold-water (<-1°C) volume observed in the Gulf (this time excluding the estuary to extend the time series to years when sampling wasn't as complete) is shown in Fig. 38.

COLD INTERMEDIATE LAYER

PREDICTION FROM THE MARCH SURVEY

The summer CIL minimum temperature index (Gilbert and Pettigrew 1997) has been found to be highly correlated with the Gulf (excluding the estuary) volume of cold water (<-1°C) measured the previous March when much of the mixed layer was near-freezing (Galbraith 2006, updated relation in right panel of Fig. 38). This is expected because the CIL is the remnant of the winter cold surface layer. A measurement of the volume of cold water present in March is therefore a valuable tool for forecasting the coming summer CIL conditions. Based on the similarities of the mixed layer in terms of temperature and volumes colder than 1°C and 0°C with those observed in 2011, we forecasted in last year's report warm summertime CIL conditions in 2013 with an index of between +0.2°C and +0.4°C, similar to CIL conditions in the previous two years.

AUGUST CIL BASED ON THE MULTI-SPECIES SURVEY

The CIL minimum temperature, thickness and volume for T<0°C and <1°C were estimated using temperature profiles from all sources for August and September. Most data are mostly from the multi-species surveys in September for the Magdalen Shallows and August for the rest of the Gulf. Using all available temperature profiles, each 1-m depth layer of the Gulf was spatially interpolated for temperature, with the interpolated field bound between the minimum and maximum values observed within each of the different regions of the Gulf (Fig. 2) to avoid spurious extrapolations. The CIL thickness at each grid point is simply the sum of depth bins below the threshold temperature, and the CIL minimum temperature is only defined at grid points where temperature rises by at least 0.5°C at depths greater than that of the minimum, or if the grid point minimum temperature is below the CIL spatial average of the Gulf.

Fig. 39 shows the gridded interpolation of the CIL thickness <1°C and <0°C and the CIL minimum temperature for August–September 2013 as well their 1985-2010 climatology (1994-2010 for Mécatina Trough). The CIL thickness for T<1°C was generally less and core temperatures generally warmer in 2013 than in 2012, similar to conditions in 2011 (not shown). Similar maps were produced for all years back to 1971 (although some years have no data in some regions), allowing the calculation of volumes for each region for each year as well as the climatologies shown on the left side of Fig. 39. The 2013 CIL is thinner and warmer than the 1985-2010 climatologies.

The time series of the regional CIL volumes are shown in Fig. 40 (for <0°C and <1°C). The CIL defined by <0°C all but disappeared except for the Mécatina Trough and its surrounding influence in Esquiman Channel. Most regions show an increased CIL <1°C volume in 2013 compared to 2012. Fig. 41 shows the average CIL core temperature and the total volume of CIL water (<0°C and <1°C) from the August–September interpolated grids (e.g., Fig. 39). The CIL areal minimum temperature average and volume shown in Fig. 41 exclude data from Mécatina Trough which has very different water masses from the rest of the Gulf; it is influenced by inflow through the Strait of Belle Isle and is therefore not indicative of the climate in the rest of the Gulf. The CIL volume as defined by T<1°C increased significantly (to -2.1 SD) compared to 2012 conditions (-3.2 SD) and reached a volume similar to 2011 (-2.3 SD), but still only the 3rd lowest since at least 1985. In the case of the volume delimited by 0°C, there was only a slight decrease compared to the already low 2012 conditions, reaching a new record-low (since 1985).

The time series of the CIL regional average minimum core temperatures are shown in Fig. 42. All regions show a decrease in core temperature except in Anticosti Channel and Mécatina Trough. The 2013 average temperature minimum (excluding Mécatina Trough, the Strait of Belle Isle and the Magdalen Shallows) was +0.48°C, a decrease of 0.30°C, and is shown in Fig. 41 (bottom panel, green line). The overall 2013 CIL water mass properties are similar to observations of 2011.

NOVEMBER CIL CONDITIONS IN THE ST. LAWRENCE ESTUARY

The AZMP November survey provides a high resolution conductivity-temperature-depth (CTD) sampling grid in the St. Lawrence estuary since 2006 although measurements are sparser in 2013. This allows the finer display of the CIL minimum temperature in the Estuary (Fig. 43) that usually highlights the CIL erosion and warming spatially towards the head of the channel, although this effect is not apparent in 2013. The data also show the temporal warming (Fig. 40) and thinning (Fig. 42) since the August survey. The CIL was colder in November 2013 than in 2012. Fig. 42 shows that the fairly rapid increase of the CIL minimum temperature occurring between August and November is fairly constant inter-annually in spite of the differences in August temperature.

GILBERT AND PETTIGREW (1997) CIL INDEX

The Gilbert and Pettigrew (1997) CIL index is defined as the mean of the CIL minimum core temperatures observed between 1 May and 30 September of each year, adjusted to 15 July. It was updated using all available temperature profiles measured within the Gulf between May and September inclusively since 1947 (black line of the bottom panel of Fig. 41). As expected, the CIL core temperature interpolated to 15 July is almost always colder than the estimate based on August and September data for which no temporal corrections were made. This is because the CIL is eroded over the summer and therefore its core warms over time.

This CIL index for summer 2013 was +0.09°C, 1.3 SD above normal. The 0.33°C decrease from the summer 2012 CIL index of +0.42°C is consistent with the increase in CIL volume between August 2012 and 2013 discussed above and the decrease of 0.3°C in the areal average of the minimum temperature in August. The warm winter conditions since 2010 led to CIL indices that were still far below the record high observed in the 1960s and 1980s. The earlier CIL temperature minimums will be re-examined to confirm that they were calculated using data with sufficient vertical resolution to correctly resolve the core minimum temperature. While we previously reported that other indicators show some years in that period to be warm such as the Estuary regional averages recorded in 1980 (Fig. 40 for volume and Fig. 42 for core temperature) and bottom temperatures in the June survey (see below), mechanical bathythermograph data were since found to be possibly erroneous and were excluded from the analysis, leading to not-as-warm and more voluminous 1980 CIL estimates. It is also becoming increasingly clear that the winter mixed layer is not the only factor explaining summertime CIL conditions and that mechanisms having a multi-year cumulative effect are required to explain the interannual autocorrelations observed. For example, this may be linked to the summertime thermocline being shallower than normal, decreasing the thickness of the CIL.

As a summary, Fig. 44 shows selected time series of winter and summertime CIL conditions (June bottom temperatures also related to the CIL are outlined below) and highlights the strong correlations between these various time series. Although the CIL was colder and thicker in 2013 than in 2012, the latter year was a record warm year and the 2013 CIL was still generally warm, similar to 2011 conditions.

MAGDALEN SHALLOWS JUNE SURVEY

A long-standing assessment survey covering the Magdalen Shallows has taken place in June for mackerel and since merged with the June AZMP survey. It provides good coverage of the temperature conditions that are greatly influenced by the cold intermediate layer that reaches the bottom at roughly half of the surface area at this time of time.

Near-surface waters warm quickly in June, mid-way between the winter minimum and the annual maximum in early August. This can introduce a bias if the survey dates are not the same each year. To account for this, the seasonal warming observed at the Shediac Valley AZMP monitoring station was evaluated. A linear regression was performed of temperature versus time for each meter of the water column for each year with monitoring data at Shediac Valley between May and July. Visual inspection showed that the depth-dependent rate was fairly constant for all years and an average was computed for every depth. Warming is maximal at the surface at 20°C per 100 days and decreases almost proportionally with depth to reach 2.7°C per 100 days at 40 m. In spite of some uncertainties between 40 and 55 m, the warming rate is well approximated by a further linear decrease reaching 1°C per 100 days at 82 m.

All available temperature casts taken in June from a given year are binned at 1m depth intervals (or interpolated if the resolution is too coarse) and then adjusted according to the sampling date

to offset them to June 15th according to the depth-dependent warming rate extracted from Shediac Valley monitoring data. An interpolation scheme is used to estimate temperature at each 1 m depth layer on a 2 km resolution grid. Fig. 45 shows temperatures and anomalies at depths of 10, 20 and 50 m. Fig. 46 shows averages over the grids at 0, 10, 20, 30, 50 and 75 m for all years when interpolation was possible, as well as SST June averages since 1985, for both western and eastern regions of the Magdalen Shallows (Fig. 21). Temperatures were normal at 10 m and normal to above-normal at 20 m and 50 m (Fig. 45). On average, temperatures were normal or above-normal at all depths in both western and eastern regions with generally higher anomalies on the western Shelf (Fig. 46).

BOTTOM WATER TEMPERATURES

Bottom temperature is also estimated at each point of the above grids by looking up the interpolated temperature at the depth level corresponding to a bathymetry grid provided by the Canadian Hydrographic Service with some corrections applied (Dutil et al. 2012). The method is fully described in Tamdrari et al. (2012). A climatology was constructed by averaging all available temperature grids between 1981 and 2010 and anomaly grids were computed for each year. The June bottom temperature climatology as well as the 2013 reconstructed temperature and anomaly fields are shown in Fig. 47. Temperature anomalies are typically greater than +2.0°C in shallow waters, but in deeper waters the bottom area occupied by waters colder than 0°C is only slightly less than the climatology, leading to near-normal temperatures in the deepest portions of the Magdalen Shallows.

The same method was applied to the entire Gulf by combining all available CTD data from August and September, thus including the multispecies surveys for the northern Gulf in August and for the Magdalen Shallows in September into a single map (Fig. 48). Most of the northeastern Gulf had above normal bottom temperatures, with large areas of Anticosti and Esquiman Channels above 6°C.

Time series of the bottom area covered by water in various temperature intervals were estimated from the gridded data for the June surveys as well as for the September multispecies survey on the Magdalen Shallows (Fig. 49). Unlike the very cold conditions observed on the bottom in 2008, none of the bottom of the Magdalen Shallows was covered by water with temperatures <-1°C in June 2013 and only a small area <0°C was left in September 2013; these conditions are similar to those in 2005-07, and 2009-12. The bottom area covered by waters colder than 0°C in June has been in an upward trend since the series minimum in 2010. The time series of areas of the Magdalen Shallows covered by water colder than 0, 1, 2, and 3°C in September are also shown in Fig. 44. The area covered by water temperatures <1°C had reached a low not seen since 1983 in 2012 but rebounded to a larger area not seen in the previous four years, although still a (warm) anomaly of -0.6 SD (Fig. 44). Areas with T< 2°C increased since the same period in 2012 to reach near-normal conditions. The thermograph network (Fig. 25) also showed bottom temperatures at Shediac Valley (82 m) and at Irwing Whale stations (67 m) to be below-normal and near-normal in June, respectively. Fig. 29 shows bottom temperatures at the Irwing Whale station (67 m) colder in 2013 than the prior three summers.

Time series of the bottom area covered by water in various temperature intervals were also estimated for the other regions of the Gulf based on August-September temperature profile data (Figs. 50 and 51). Mécatina Trough and Esquiman Channel, areas affected by the winter intrusion of cold Labrador Shelf water, were the only regions to have bottom waters colder than 0°C, although the area was very small in Esquiman Channel compared with prior cold years. Bottom waters are colder in Mécatina Trough in 2013 compared to the same period in 2012.

While some years Anticosti Channel is also affected by the winter intrusion, for the first time since 1983 no waters colder than 0°C occupied the bottom. The figures also show compression of the bottom habitat area in the temperature range of 5–6°C in 1992. The 2012 return of >6°C temperatures to the sea floor increased in area in 2013 in Anticosti Channel, Esquiman Channel and Central Gulf and reduced the bottom habitat area in the temperature range of 5–6°C in Anticosti Channel, while the decrease appears more in the 3–5°C habitat in Esquiman Channel.

SEASONAL AND REGIONAL AVERAGES OF TEMPERATURE PROFILES

In order to show the seasonal progression of temperature profiles, regional averages are shown in Figs. 52 to 55 based on the data collected during the March helicopter survey, the June AZMP and mackerel surveys, the August multi-species survey (September survey for the Magdalen Shallows), and the October AZMP survey (November survey not shown) and including all additional archived CTD data for those months. The temperature scale was adjusted to highlight the CIL and deep water features; the display of surface temperature variability is best suited to other tools such as remote sensing and thermographs. During the surveys, a total of 107 CTD casts in March, 126 casts in June, 306 casts in August, 249 in September, 123 in October and 89 in November were obtained within the regions shown in Fig. 2. Average discrete depth layer conditions are summarized for the months of the 2012 and 2013 AZMP surveys in Fig. 56 for temperature and in Fig. 57 for salinity and 0-50 m stratification. For each survey the anomalies were computed relative to monthly temperature and salinity climatologies calculated for each region.

Monthly temperature and salinity climatologies for 1981–2010 were constructed for various depths using a method similar to that used by Petrie et al. (1996) but using the geographical regions shown in Fig. 2. All available data obtained during the same month within a region and close to each depth bin are first averaged together for each year. Monthly averages from all available years and their standard deviations are then computed. This two-fold averaging avoids the bias that occurs when the numbers of profiles in any given year are different. The temperature climatologies are shown in grey as the mean value ± 1 SD (Figs. 52 to 55).

The March water temperature conditions were discussed at length in earlier sections and are included here for completeness (Fig. 52), but caution is needed in interpreting the mean profiles. Indeed, regional averaging of winter profiles does not work very well in the northeast Gulf (regions 4 and 5) because very different water masses are present in the area such as the cold Labrador Shelf intrusion with saltier and warmer deeper waters of Anticosti Channel or Esquiman Channel. For example, the sudden temperature decrease near the bottom of Mécatina Trough resulted from the deepest cast used in each of the averages, which contained colder Labrador Shelf intrusion water. Large changes near 200 m are due to our usual sampling cutoff near 200 m for the March airborne survey, with some casts being slightly deeper than others. In particular, the unusual shifts in temperature below 200 m in the mean profiles for the Estuary (region 1) and Northwest Gulf (region 2) appears because only one station in each region is sampled beyond 200 m. The highlights of March water temperatures shown in Fig. 52 include the previously discussed winter mixed layer, with above-normal temperatures in regions other than Mécatina Trough and the Magdalen Shallows. The thermocline was much shallower than usual in central Gulf and Esquiman Channel regions, but much deeper than usual in the Estuary, the Northwest Gulf and Anticosti Channel. One profile was sampled beyond 200 m depth on the Newfoundland side of Cabot Strait to sample the inflow into the Gulf; temperatures at ≥200 m were above normal, yet 1°C cooler than in March 2012 (See also Fig. 56).

Temperatures in June 2013 (Fig. 53 and summary in Fig. 56) were characterized by CIL conditions that were below normal in thickness and above-normal in minimum temperature, yet

colder and thicker than in 2012. Deep water temperatures were above-normal in all regions along the Laurentian Channel, with the warm anomaly that had begun to affect the Northwest Gulf in 2012 having finally reached the Estuary in 2013. Warming is expected to continue in these two regions through 2014. Temperatures at the depth of the temperature maximum (250+ m) were above-normal in Esquiman Channel and central Gulf, exceeding 6°C at depth, presumably advected in from Cabot Strait 2012 record-high conditions. By August, deep temperatures exceeding 6°C were also observed due to deeper sampling in Anticosti Channel (Fig. 54). By October (Fig. 55) some waters warmer than 6°C also reappeared in Cabot Strait at a surprisingly shallow maximum temperature depth of 200 m. The peculiar temperature structure there between 200 and 325 m was also observed in Central Gulf (where stations reaching this depth were sampled at the mouth of Esquiman Channel). It must be noted however that the 7°C waters observed in 2012 in Cabot Strait do not appear to have propagated far into the Gulf in 2013 and may have been associated with a gyre that circulated back out (see later Fig. 62 for examples of such recirculation gyres), although measurements indicate their continued presence off the southern coast of Newfoundland and up to Cabot Strait in 2013.

DEEP WATERS (>150 M)

The deeper water layer (>150 m) below the CIL originates at the entrance of the Laurentian Channel at the continental shelf and circulates towards the heads of the Laurentian, Anticosti, and Esquiman channels without much exchange with the upper layers. The layer from 150 to 540 m is characterized by temperatures between 1 and >7°C and salinities between 32.5 and 35 (except for Mécatina Trough where near-freezing waters may fill the basin to 235 m in winter and persist throughout the summer). Interdecadal changes in temperature, salinity, and dissolved oxygen of the deep waters entering the Gulf at the continental shelf are related to the varying proportion of the source cold–fresh and high dissolved oxygen Labrador Current water and warm–salty and low dissolved oxygen slope water (McLellan 1957, Lauzier and Trites 1958, Gilbert et al. 2005). These waters travel from the mouth of the Laurentian Channel to the Estuary in roughly three to four years (Gilbert 2004), decreasing in dissolved oxygen from in situ respiration and oxidation of organic material as they progress to the channel heads. The lowest levels of dissolved oxygen are therefore found in the deep waters at the head of the Laurentian Channel in the Estuary.

TEMPERATURE AND SALINITY

The calculation of monthly temperature and salinity climatologies mentioned earlier using a method similar to that of Petrie et al. (1996) also provides time series of monthly averaged values. These monthly averages were further averaged into regional yearly time series that are presented in Fig. 58 for 200 and 300 m. The 300 m observations in particular suggest that temperature anomalies are advected up-channel from Cabot Strait to the northwestern Gulf in two to three years, consistent with the findings of Gilbert (2004). The regional averages are weighted into a Gulf-wide average in accordance to the surface area of each region at the specified depth. These Gulf-wide averages are shown for 200 and 300 m in Fig. 58 as well as for 150, 200, and 300 m in Fig. 59. Linear trends in temperature and salinity at 300 m of respectively 2.2°C and 0.3 per century are shown on Fig. 59 (See also Galbraith et al. 2013b for other long term trends). Some older values have changed since last year's report from the removal of some anomalously suspect historical temperature-salinity profiles.

In 2013, the gulf-wide average temperatures and salinities were above normal at all depths. Temperature at 300 m increased slightly overall to reach 5.8°C (+1.8 SD); the highest since 1980. It increased in central Gulf to reach +1.9 SD, a high since 1994. The 300 m depth waters of the Estuary warmed between 2012 and 2013 as expected based on the change observed

between 2011 and 2012 in the northwest Gulf although not by as much (see also Fig. 28 for the deep thermograph at Rimouski station). The warm anomaly present since 2010 at Cabot Strait should continue to progress up the channel towards the Estuary for a few years; already the temperature in the Northwest Gulf is above normal (+1.2 SD). Salinity decreased overall by 0.6 SD at 200 m and by 0.5 SD at 300 m but remained above-normal at +0.5 SD at both depths. However, salinity at Cabot Strait at 300 m decreased to normal from the record high (since 1915) of +1.8 SD or 34.81 of 2012, while temperature at 200 m decreased to 5.4°C (+0.9 SD) from the record high of 6.4 (+2.5 SD), suggesting an important change in water masses entering the Gulf at depth (but see *Outlook for 2014*).

DISSOLVED OXYGEN AND HYPOXIA IN THE ST. LAWRENCE ESTUARY

Fig. 59 shows an update of the Gilbert et al. (2005) oxygen time series, providing the mean dissolved oxygen value at depths ≥295 m in the St. Lawrence Estuary expressed as a percentage of saturation at surface pressure. Since some of the variability is associated with changing water masses, the temperature at 300 m in the Estuary is also shown. The deep waters of the Estuary were briefly hypoxic in the early 1960s and have consistently been hypoxic since 1984. Dissolved oxygen decreased slightly from 21.3 percent saturation (67.6 $\mu mol\ l^{-1}$) in 2012 to 21.0 percent saturation (66.5 $\mu mol\ l^{-1}$) in 2013.

Inflow of warmer (colder) waters to the Estuary are expected to deteriorate (ameliorate) the hypoxic conditions since these waters are typically poorer (richer) in dissolved oxygen (McLellan 1957, Lauzier and Trites 1958, Gilbert et al. 2005) similarly to changes that have occurred over interdecadal time scales. While the slight decrease just described is consistent with source water mass changes and the 0.09°C temperature increase at 300 m between 2012 and 2013 (A change of dissolved oxygen of 147.4 $\mu mol\ l^{-1}$ is accounted for by a 10.09°C temperature difference in source water masses in Gilbert et al 2005, implying that a change of 1.3 $\mu mol\ l^{-1}$ would be expected with the 0.09°C temperature increase), this might be coincidental. Recent interannual variability in the Gilbert et al. 2005 updated time series and CTD-based regional time series shown in Fig. 58 (bottom block) do not show changes in dissolved oxygen that would have been expected to be associated with changes in temperature. Differences between the Gilbert et al. 2005 updated time series and the CTD-based time series from the Estuary should also be investigated (bottom panel of Fig. 58).

CURRENTS AND TRANSPORTS

Currents and transports are derived from a numerical model of the Gulf of St. Lawrence, Scotian Shelf, and Gulf of Maine. The model is prognostic, i.e., it allows for evolving temperature and salinity fields. It has a spatial resolution of 1/12° with 46 depth-levels in the vertical. The atmospheric forcing is taken from the Global Environmental Multiscale (GEM) model run at the Canadian Meteorological Center (CMC). Freshwater runoff is obtained from observed data and the hydrological model, as discussed in the freshwater runoff section. A simulation was run for 2006–2013 from which transports were calculated. The reader is cautioned that the results outlined below are not measurements but simulations and that improvement in the model may lead to changes in the transport values.

Figs. 60–62 show seasonal depth-averaged currents for 0–20 m, 20–100 m, and 100 m to the bottom for 2013. Currents are strongest in the surface mixed layer, generally 0–20 m, except in winter months when the 20–100 m and the 100m to bottom averages are almost as high (note the different scale for this depth). Currents are also strongest along the slopes of the deep channels. The Anticosti Gyre is always evident but strongest during winter months, when it even extends strongly into the bottom-average currents.

Monthly averaged transports across seven sections of the Gulf of St. Lawrence are shown for sections with estuarine circulation in Fig. 63, and in Fig. 64 for sections where only net transports are relevant. In Fig. 63, the net transport integrates both up and downstream circulation and, for example, corresponds to freshwater runoff at the Pointe-des-Monts section. The outflow transport integrates all currents heading toward the ocean, while the estuarine ratio corresponds to the outflow divided by the net transports.

Transports on sections under the direct estuarian influence of the St. Lawrence River (e.g., Pointe-des-Monts) have a more direct response to change in freshwater runoff while others (e.g., Cabot Strait, Bradelle Bank) have a different response, presumably due to redistribution of circulation in the GSL under varying runoff. The estuarine circulation ratio is determined by the mixing intensities within the estuary and is greatly influenced by stratification. It is on average greatest during winter months and weakest during the spring freshet. In fact, it is sufficiently reduced in spring that the overall outward transport at Pointe-des-Monts reaches its minimum value in June even though this month corresponds to the third highest net transport of the year, i.e. the estuary becomes sufficiently stratified that fresh water runoff tends to slip on top of the denser salty waters underneath. In 2013, the estuarine ratio at Pointe-des-Monts was much above-normal in winter.

HIGH FREQUENCY SAMPLING AZMP STATIONS

Sampling by the Maurice Lamontagne Institute began in 1996 at two stations that were to become part of the AZMP (Therriault et al. 1998) in the northwest Gulf of St. Lawrence: the Anticosti Gyre and the Gaspé Current. Both stations were to be sampled at 15-day intervals, but logistical problems have often led to less frequent sampling. A station offshore of Rimouski (48° 40' N 68° 35' W) has also been sampled regularly since 1993 (Plourde et al. 2009), typically once a week during summer and less often during spring and fall but almost never in winter (Fig. 65). In 2013, following several analyses that identified good correlations and correspondences between the Anticosti Gyre and Gaspé Current stations with the Rimouski station, it was decided to drop sampling efforts at the logistically difficult stations and integrate the Rimouski station officially in the AZMP program.

The AZMP station in the Shediac Valley (47° 46.8' N, 64° 01.8' W) is sampled on a regular basis by the Bedford Institute of Oceanography as well as occasionally by DFO Gulf Region and by the Maurice Lamontagne Institute during their Gulf-wide surveys (Fig. 65). This station has been sampled irregularly since 1947, nearly every year since 1957, and more regularly during the summer months since 1999 when the AZMP program began. However, observations were mostly limited to temperature and salinity prior to 1999.

Isotherms and isohalines as well as monthly averages of layer temperature and salinity, stratification, and CIL core temperature and thickness at <1°C are shown for 2009-2013 for the Rimouski station in Fig. 66 and for the Shediac Valley station in Fig. 67. The scorecard climatologies are calculated from all available data at all stations except for Shediac Valley, where the time series from 1981-2013 is considered.

At the Rimouski station, the CIL typically had a normal thickness from March until August, but was thinner than normal from September onwards. Its minimum temperature was typically above-normal. At 200-300 m, the gradual shift of cold-fresh waters present in 2010 to warmer-saltier waters advected from Cabot Strait lead to a shift to warm anomalies by May 2013. At the Shediac Valley station, a mix of conditions tends to average out to above-normal temperatures averaged over the water column starting from July onwards. March salinities were above-normal while summertime salinities were generally below normal. Stratification was above-normal in July and August in agreement with the above-normal (+0.5 SD) spring freshet runoff.

Fig. 68 shows the interannual variability of some bulk layer averages from May to October for the two stations. Bulk surface layer temperature and salinity was normal at Rimouski station while CIL minimum temperature and stratification were above-normal. Bulk surface layer temperature has been above-normal at Shediac Valley station for four consecutive years, but the high early summer stratifications were not enough to yield a positive anomaly when averaged over the May to October period.

OUTLOOK FOR 2014

Air temperatures averages from December 2013 to March 2014 were the coldest over the Gulf since 1993, and March 2014 was the coldest since 1948. This was the setting for the March 2014 survey which provides an outlook for CIL conditions expected for the remainder of 2014. Fig. 69 shows the surface mixed layer temperature, salinity, and thickness (at T<-1°C and T<0°C), as well as the thickness and extent of the cold and saline layer that has intruded into the Gulf from the Labrador shelf. The winter mixed layer was thick and near-freezing throughout the Gulf, up to Cabot Strait, after four consecutive winters with warmer conditions. The overall thickness and volume of the layer colder than -1°C was second highest in the 1996-2014 time series after the record of 2003, a year when a record volume of Labrador Shelf Water also contributed towards the high overall volume. The Cold Intermediate Layer for summer 2014 is therefore forecasted to be colder than during the previous four summers and resemble conditions of 2009 with a Gilbert & Pettigrew (1997) index of around -0.5°C.

Conditions are quite different at depth. Recall that a return to near-normal conditions was observed in 2013 at 200-300 m in Cabot Strait after record high temperatures were recorded there in 2012. This could have signaled a reprieve of increasingly warm waters that are then advected into the Gulf interior by estuarine circulation. However waters just as warm as the record of 2012 were observed again in Cabot Strait in March 2014, reaching 7.5°C. The 2013 near-normal conditions were only a respite.

SUMMARY

Fig. 70 summarizes SST, CIL and deep water average temperatures. For May-November SST, a proxy is used prior to 1985 using the April-November air temperature anomaly averaged over all stations of Fig. 4 except the two from the Estuary, similar to the index developed in Galbraith et al. (2012). Fig. 70 shows decreases from 2012 values for May-November average SST, CIL minimum temperature and average temperature at 200 m, but an increase at 300 m to reach a maximum since 1980.

To further summarize the temperature state of the Gulf of St. Lawrence, nine time series are chosen to represent surface and deep conditions (Fig. 71). Here, the CIL is grouped as a shallow feature since it is generated by the winter surface mixed layer. Fig. 72 shows three annual composite index time series (Petrie et al. 2007) constructed as the sum of these anomalies, representing the state of different parts of the system, with each time series contribution shown as stacked bars. The first anomaly sum represents the entire water column, whereas the second and third sums represent the state of the shallow and deep parts of the water column, which are decoupled. These composite indices measure the overall state of the climate system with positive values representing warm conditions and negative representing cold conditions. The plot also indicates the degree of correlation between the various measures of the environment. The record combined high occurred in 1980 from the record deep anomalies and the near-record shallow anomalies, whereas the record high shallow anomaly occurred in 2012. The record low occurred in 1992, combining records in both shallow and deep anomalies. In 2013, both shallow and deep indices decreased from 2011 but remained above-

normal at +1.2 SD and +1.5 SD respectively, with all components in phase (positive). The shallow index was 6th highest of the series and the deep index was 4th highest. This lead to an overall index of +1.6 SD, the fourth highest of the series.

HIGHLIGHTS

- Annual mean air temperatures in 2013 were near-normal over the Gulf (+0.4°C, +0.4 SD). Winter (December-March) air temperatures were above normal by 2.3°C (+1.5 SD), including the third warmest March since at least 1873 (+4.7°C, + 2.3 SD), cutting the winter short and leading to early sea-ice melt and spring runoff.
- Annual average runoff of the St. Lawrence River was near-normal but the spring freshet was above-normal. It began early in March, consistent with early melt associated with above-normal air temperatures, and persisted much longer than usual with peak runoff in May that was nearly as high in June.
- Sea ice maximum volume was 6th lowest since 1969. A large portion of the winter mixed layer remained above-freezing by at least 0.6°C in early March, limiting sea-ice formation.
- The August-September cold intermediate layer (CIL) had the third lowest volume since at least 1985, and the CIL minimum temperature index for the Gulf was the third highest since 1985.
- May-November sea-surface temperature averaged over the Gulf was above-normal by +0.4°C (+0.6 SD).
- Deep water temperatures and salinities are increasing overall in the Gulf, with inward advection from Cabot Strait where temperature and salinity reached a record high (since 1915) in 2012 at 200 and 300 m, respectively. Temperature averaged over the Gulf at 300 m increased slightly to reach 5.8°C (+1.8 SD); the highest since 1980.
- Temperatures at the depth of the temperature maximum (250+ m) were above-normal in Esquiman Channel and central Gulf, exceeding 6°C, causing large areas of the sea floor to be covered by waters with temperatures > 6°C in these areas. However, salinity at Cabot Strait at 300 m decreased to normal in 2013, accompanied by a decrease in temperature. This could have signaled a reprieve of increasingly warm waters that are then advected into the Gulf interior by estuarine circulation, however waters just as warm as the record of 2012 were observed again in Cabot Strait in March 2014, reaching 7.5°C. The 2013 near-normal conditions were perhaps only a respite.

ACKNOWLEDGEMENTS

We are grateful to the people responsible for CTD data acquisition during the surveys used in this report:

- Rimouski station monitoring: Chief scientist Pierre Joly, Roger Pigeon & Yves Gagnon; scientific personnel Jean-François St-Pierre, Félix St-Pierre, Marjorie Hudon, Jean-Yves Couture, Marie-Lyne Dubé, Caroline Lafleur, Sylvain Chartrand, Lily St-Amand.
- March 2013 helicopter survey: Chief scientist Peter Galbraith; scientific personnel Rémi Desmarais; helicopter pilot Daniel Dubé; aircraft technician Tommy Levesque.
- March 2014 helicopter survey: Chief scientist Peter Galbraith; scientific personnel Rémi Desmarais; helicopter pilot Robert Delisle; aircraft technician David Gauvin.
- June AZMP transects: Chief scientists: François Villeneuve; scientific personnel: Isabelle St-Pierre, Yves Gagnon, Roger Pigeon, Sylvain Chartrand, Johanne Guérin, Rémi Desmarais, Marie-Lyne Dubé, Jean-Pierre Allard, Benoît Légaré; the officers and crew of the CCGS Teleost.

- August Multi-species survey: Chief scientists: Diane Archambault and Philippe Schwab; scientific personnel: Caroline Lafleur, Bernard Pettigrew Jean-Yves Couture and Sylvain Chartrand; the officers and crew of the CCGS Teleost.
- October-November AZMP survey: Chief scientists : Pierre Joly and François Villeneuve; scientific personnel: Jean-François St-Pierre, Sylvain Chartrand, Yves Gagnon, Roger Pigeon, Laure Devine, Marie-Lyne Dubé, Bernard Pelchat, Sonia Michaud, Félix St-Pierre, Caroline Lafleur; the officers and crew of the CCGS Hudson.
- September Multi-species survey: Tom Hurlbut for providing the CTD data.
- Northumberland Strait survey: Chief scientists Mark Hanson and Joël Chassé.

Data from the following sources are also gratefully acknowledged:

- Air temperature: Environment Canada.
- Runoff at Québec City: Denis Lefaivre.
- Runoff from hydrological modelling: Joël Chassé and Diane Lavoie.
- Thermograph network: Bernard Pettigrew, Rémi Desmarais.
- Thermosalinograph: Denis Lefaivre, Roger Pigeon, Sylvain Cantin, Peter Galbraith.
- AVHRR SST remote sensing (IML): Pierre Larouche, Bernard Pettigrew.
- AVHRR SST remote sensing (BIO): Carla Caverhill.
- Dissolved oxygen: Caroline Lafleur, Laure Devine, Pierre Joly, Marie-Lyne Dubé.

All figures were made using the free software Gri (Kelley and Galbraith 2000).

We are grateful to David Hebert and Eugene Colbourne for reviewing the manuscript and providing insightful comments.

REFERENCES

Benoît, H.P., C. Savenkoff, P. Ouellet, P.S. Galbraith, J. Chassé and A. Fréchet, 2012. Impacts of fishing and climate-driven changes in exploited marine populations and communities with implications for management, in State-of-the-Ocean Report for the Gulf of St. Lawrence Integrated Management (GOSLIM) Area, H. P. Benoît, J. A. Gagné, C. Savenkoff, P. Ouellet and M.-N. Bourassa, Eds. Can. Manuscr. Rep. Fish. Aquat. Sci. 2986: viii + 73 pp.

Bourgault, D. and V.G. Koutitonsky. 1999. Real-time monitoring of the freshwater discharge at the head of the St. Lawrence Estuary. Atmos. Ocean, 37 (2): 203–220.

Colbourne, E., Craig, J., Fitzpatrick, C., Senciall, D., Stead, P., and Bailey, W. 2013. An assessment of the physical oceanographic environment on the Newfoundland and Labrador Shelf during 2012. DFO Can. Sci. Advis. Sec. Res. Doc. 2013/052. v + 35 p.

Cyr, F., D. Bourgault and P. S. Galbraith, 2011. Interior versus boundary mixing of a cold intermediate layer. J. Gephys. Res. (Oceans), 116, C12029, doi:10.1029/2011JC007359.

Dutil, J.-D., S. Proulx, P.S. Galbraith, J. Chassé, N. Lambert and C. Laurian, 2012. Coastal and epipelagic habitats of the estuary and Gulf of St. Lawrence. Can. Tech. Rep. Fish. Aquat. Sci. 3009: ix + 87 p.

Galbraith, P.S. 2006. Winter water masses in the Gulf of St. Lawrence. J. Geophys. Res., 111, C06022, doi:10.1029/2005JC003159.

Galbraith, P.S. and P. Larouche, 2011. Sea-surface temperature in Hudson Bay and Hudson Strait in relation to air temperature and ice cover breakup, 1985-2009. J. Mar. Systems, 87, 66-78.

Galbraith, P.S. and P. Larouche. 2013. Trends and variability in eastern Canada sea-surface temperatures. Ch. 1 (p. 1-18) In: Aspects of climate change in the Northwest Atlantic off Canada [Loder, J.W., G. Han, P.S. Galbraith, J. Chassé and A. van der Baaren (Eds.)]. Can. Tech. Rep. Fish. Aquat. Sci. 3045: x + 190 p.

Galbraith, P.S., F.J. Saucier, N. Michaud, D. Lefaivre, R. Corriveau, F. Roy, R. Pigeon and S. Cantin. 2002. Shipborne monitoring of near-surface temperature and salinity in the Estuary and Gulf of St. Lawrence. Atlantic Zone Monitoring Program Bulletin, Dept. of Fisheries and Oceans Canada. No. 2: 26–30.

Galbraith, P.S., R. Desmarais, R. Pigeon and S. Cantin. 2006. Ten years of monitoring winter water masses in the Gulf of St . Lawrence by helicopter. Atlantic Zone Monitoring Program Bulletin, Dept. of Fisheries and Oceans Canada. No. 5: 32–35.

Galbraith, P.S., D. Gilbert, C. Lafleur, P. Larouche, B. Pettigrew. 2007. Physical oceanographic conditions in the Gulf of St. Lawrence in 2006. DFO Can. Sci. Advis. Sec. Res. Doc. 2007/024, iv + 51 pp.

Galbraith, P. S., P. Larouche, D. Gilbert, J. Chassé, and B. Petrie. 2010. Trends in sea-surface and CIL temperatures in the Gulf of St. Lawrence in relation to air temperature. Atlantic Zone Monitoring Program Bulletin, 9: 20-23.

Galbraith P.S., P. Larouche, J. Chassé, B. Petrie, 2012. Sea-surface temperature in relation to air temperature in the Gulf of St. Lawrence: interdecadal variability and long term trends. Deep Sea Res. II, V77–80, 10–20.

Galbraith, P.S., Chassé, J., Larouche, P., Gilbert, D., Brickman, D., Pettigrew, B., Devine, L., and Lafleur, C. 2013a. Physical Oceanographic Conditions in the Gulf of St. Lawrence in 2012. DFO Can. Sci. Advis. Sec. Res. Doc. 2013/026. v + 89 p.

Galbraith. P.S., D. Hebert, E. Colbourne and R. Pettipas. 2013b. Trends and variability in eastern Canada sub-surface ocean temperatures and implications for sea ice. Ch.5 In: Aspects of climate change in the Northwest Atlantic off Canada [Loder, J.W., G. Han, P.S. Galbraith, J. Chassé and A. van der Baaren (Eds.)]. Can. Tech. Rep. Fish. Aquat. Sci. 3045: x + 192 p.

Gilbert, D. 2004. Propagation of temperature signals from the northwest Atlantic continental shelf edge into the Laurentian Channel. ICES CM, 2004/N:7, 12 pp.

Gilbert, D. and B. Pettigrew. 1997. Interannual variability (1948-1994) of the CIL core temperature in the Gulf of St. Lawrence. Can. J. Fish. Aquat. Sci., 54 (Suppl. 1): 57–67.

Gilbert, D., P.S. Galbraith, C. Lafleur and B. Pettigrew. 2004. Physical oceanographic conditions in the Gulf of St. Lawrence in 2003. DFO Can. Sci. Advis. Sec. Res. Doc. 2004/061, 63 pp.

Gilbert, D., B. Sundby, C. Gobeil, A. Mucci and G.-H. Tremblay. 2005. A seventy-two-year record of diminishing deep-water oxygen in the St. Lawrence estuary: The northwest Atlantic connection. Limnol. Oceanogr., 50(5): 1654–1666.

Hammill, M.O. and P.S. Galbraith, 2012. Changes in seasonal sea-ice cover and its effect on marine mammals, in State-of-the-Ocean Report for the Gulf of St. Lawrence Integrated Management (GOSLIM) Area, H. P. Benoît, J. A. Gagné, C. Savenkoff, P. Ouellet and M.-N. Bourassa, Eds. Canadian Manuscript Report of Fisheries and Aquatic Sciences 2986: viii + 73 pp.

Hebert, D., Pettipas, R., Brickman, D., and Dever M. 2013. Meteorological, Sea Ice and Physical Oceanographic Conditions on the Scotian Shelf and in the Gulf of Maine during 2012. DFO Can. Sci. Advis. Sec. Res. Doc. 2013/058. v + 46 p.

Kalnay, E., M. Kanamitsu, R. Kistler, W. Collins, D. Deaven, L. Gandin, M. Iredell, S. Saha, G. White, J. Woollen, Y. Zhu, M. Chelliah, W. Ebisuzaki, W. Higgins, J. Janowiak, K. Mo, C. Ropelewski, J. Wang, A. Leetmaa, R. Reynolds, R. Jenne and D. Josephé. 1996. The NCEP/NCAR 40-year reanalysis project. Bull. Am. Meteorol. Soc. 77, 437–470.

Kelley, D.E. and P.S. Galbraith. 2000. Gri: A language for scientific illustration, Linux J., 75, 92 101.

Lauzier, L.M. and R.W. Trites. 1958. The deep waters of the Laurentian Channel. J. Fish. Res. Board Can. 15: 1247–1257.

McLellan, H.J. 1957. On the distinctness and origin of the slope water off the Scotian Shelf and its easterly flow south of the Grand Banks. J. Fish. Res. Board. Can. 14: 213–239.

Petrie, B., K. Drinkwater, A. Sandström, R. Pettipas, D. Gregory, D. Gilbert and P. Sekhon. 1996. Temperature, salinity and sigma-t atlas for the Gulf of St. Lawrence. Can. Tech. Rep. Hydrogr. Ocean Sci., 178: v + 256 pp.

Petrie, B., R. G. Pettipas and W. M. Petrie. 2007. An overview of meteorological, sea ice and sea surface temperature conditions off eastern Canada during 2006. DFO Can. Sci. Advis. Sec. Res. Doc. 2007/022.

Plourde, S., P. Joly, L. St-Amand and M. Starr. 2009. La station de monitorage de Rimouski : plus de 400 visites et 18 ans de monitorage et de recherche. Atlantic Zone Monitoring Program Bulletin, Dept. of Fisheries and Oceans Canada. No. 8: 51-55.

Tamdrari, H., M. Castonguay, J.-C. Brêthes, P. S. Galbraith and D. E. Duplisea, 2012. The dispersal pattern and behaviour of cod in the northern Gulf of St. Lawrence: results from tagging experiments, Can. J. of Fisheries and Aquatic Sciences, 69: 112-121.

Therriault, J.-C., B. Petrie, P. Pépin, J. Gagnon, D. Gregory, J. Helbig, A. Herman, D. Lefaivre, M. Mitchell, B. Pelchat, J. Runge and D. Sameoto. 1998. Proposal for a Northwest Atlantic zonal monitoring program. Can. Tech. Rep. Hydrogr. Ocean Sci., 194: vii + 57 pp.

Vincent, L. A., X. L. Wang, E. J. Milewska, H. Wan, F. Yang, and V. Swail. 2012. A second generation of homogenized Canadian monthly surface air temperature for climate trend analysis. *J. Geophys. Res.* 117, D18110, doi:10.1029/2012JD017859.

FIGURES

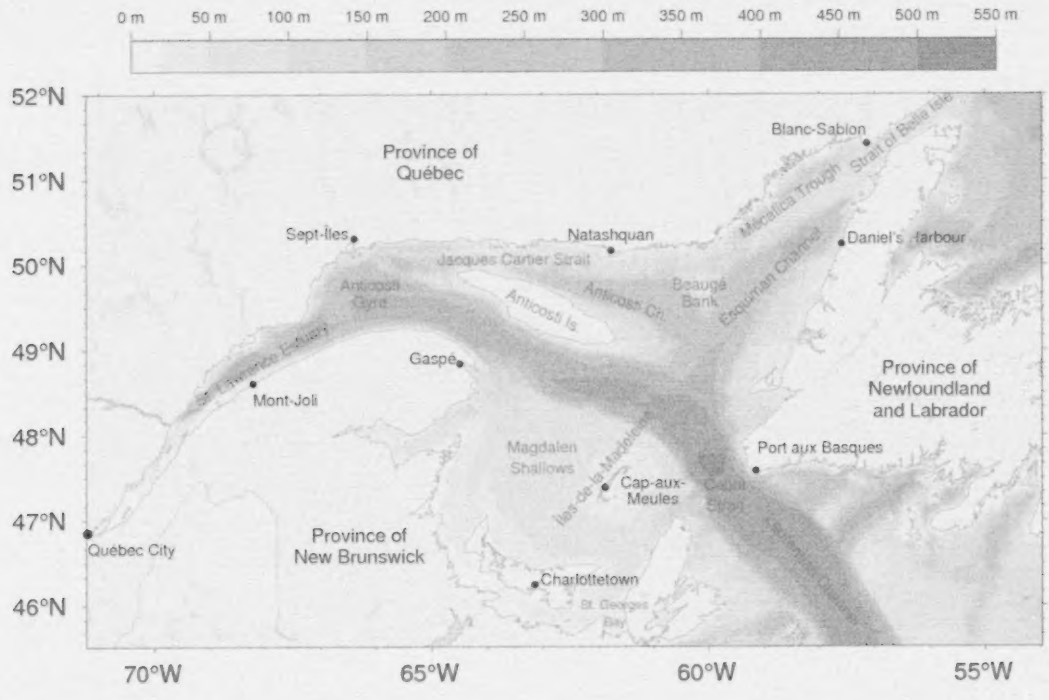

Fig. 1. The Gulf of St. Lawrence. Locations discussed in the text are indicated. Bathymetry datasets used are from the Canadian Hydrographic Service to the west of 56°47' W (with some corrections applied to the baie des Chaleurs and Magdalen Shallows) and TOPEX data to the east.

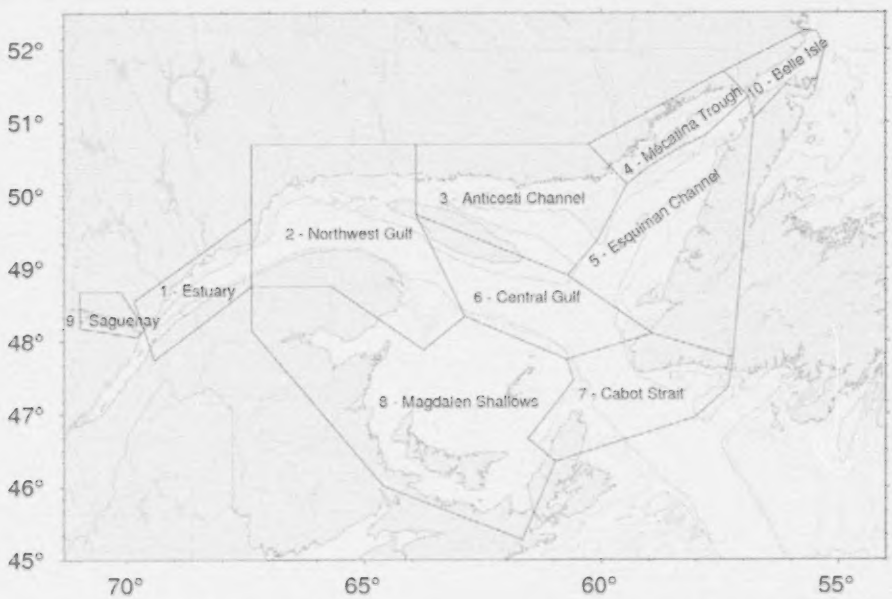

Fig. 2. Gulf of St. Lawrence divided into oceanographic regions. The first eight are typically used in this report.

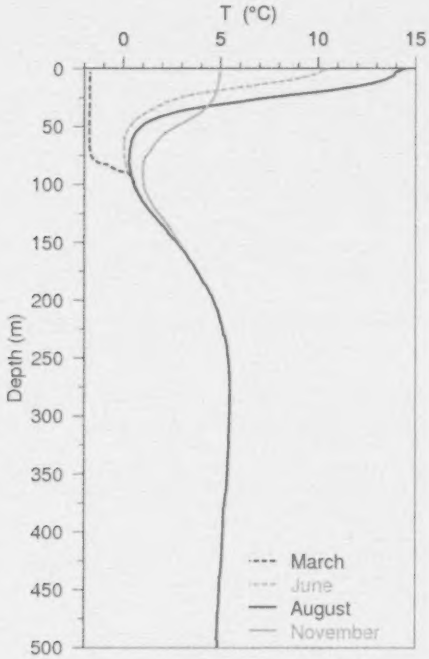

Fig. 3. Typical seasonal progression of the depth profile of temperature observed in the Gulf of St. Lawrence. Profiles are averages of observations in August, June and November 2007 in the northern Gulf. The dashed line at left shows a single winter temperature profile (March 2008), with near freezing temperatures in the top 75 m. The cold intermediate layer (CIL) is defined as the part of the water column that is colder than 1°C, although some authors use a different temperature threshold. Figure from Galbraith et al. (2012).

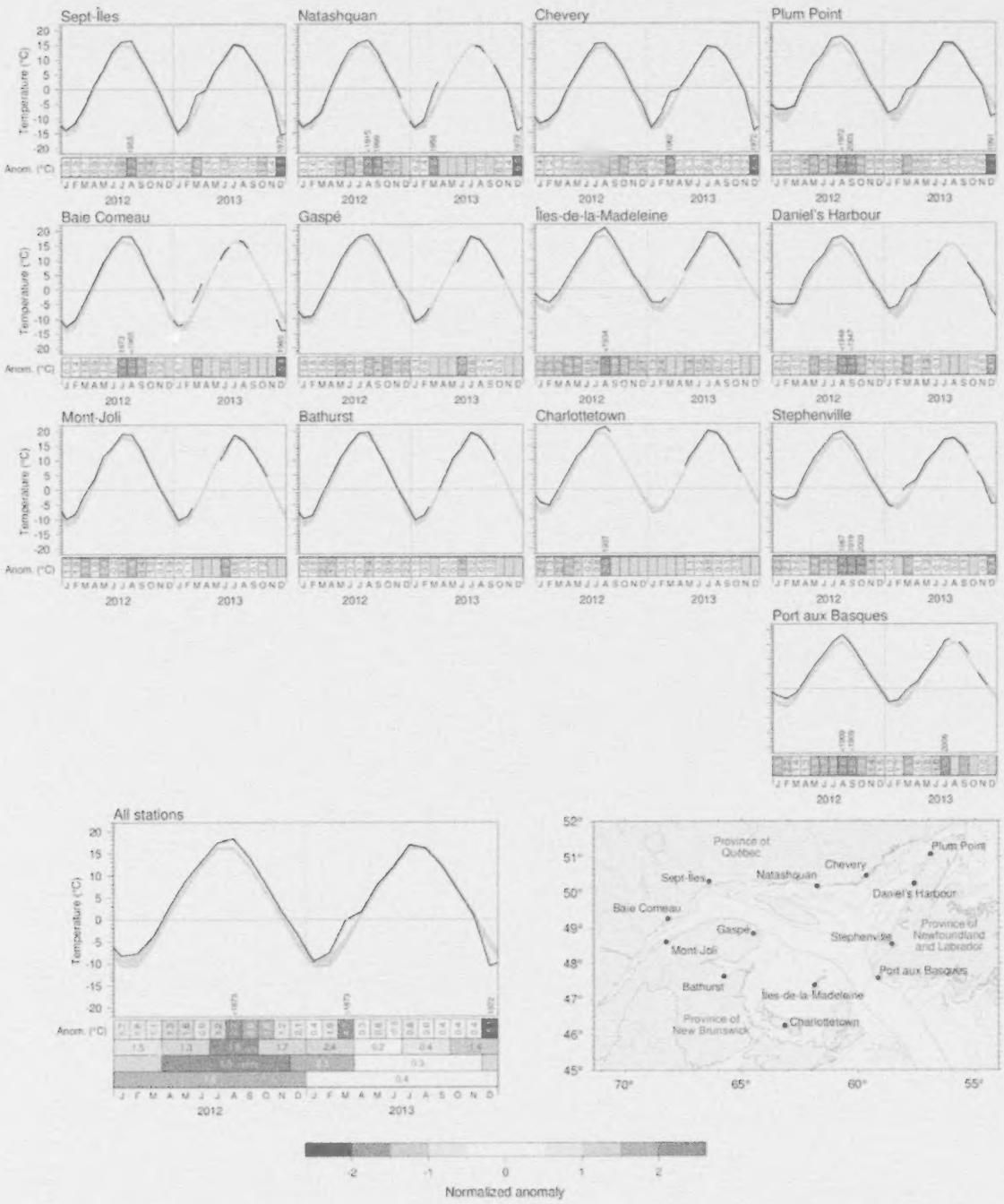

Fig. 4. Monthly air temperatures and anomalies for 2012 and 2013 at selected stations around the Gulf as well as the average for all stations. The blue area represents the 1981–2010 climatological monthly mean ± 0.5 SD. Months with 4 or more days of missing data are omitted. The bottom scorecards are colour-coded according to the monthly normalized anomalies based on the 1981–2010 climatologies for each month, but the numbers are the monthly anomalies in °C. For anomalies greater than 2 SD from normal, the prior year with a greater anomaly is indicated. Seasonal, December-March, April-November and annual anomalies are included for the all-station average.

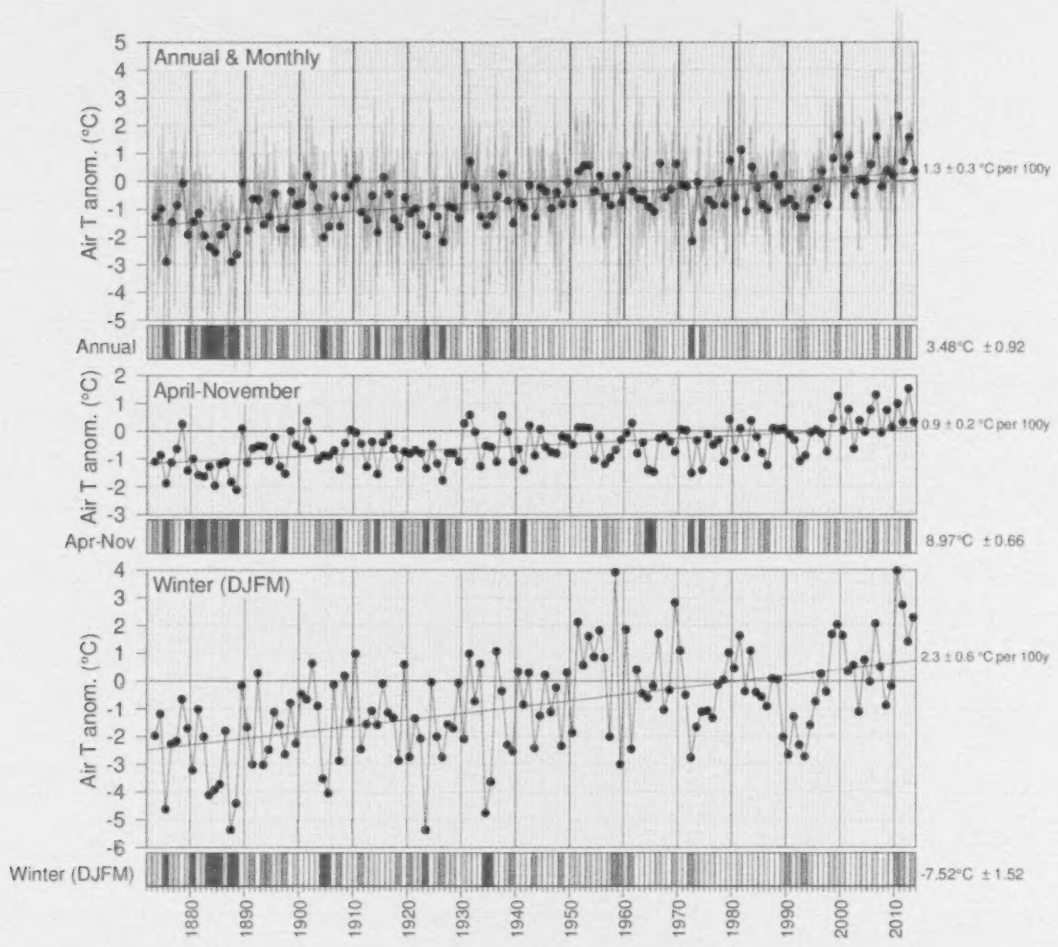

Fig. 5 Annual, April-November December-March mean air temperature anomalies averaged for the selected stations around the Gulf from Fig. 4. The bottom scorecards are colour-coded according to the normalized anomalies based on the 1981–2010 climatology. Trends plus and minus their 95% confidence intervals are shown. April-November air temperature anomalies tend to be highly-correlated with May-November sea-surface temperature anomalies (Galbraith et al. 2012; Galbraith and Larouche 2013) whereas winter air temperature anomalies correlate highly with sea-ice cover parameters and winter mixed-layer volumes (Galbraith et al. 2010; Galbraith et al.2013b)

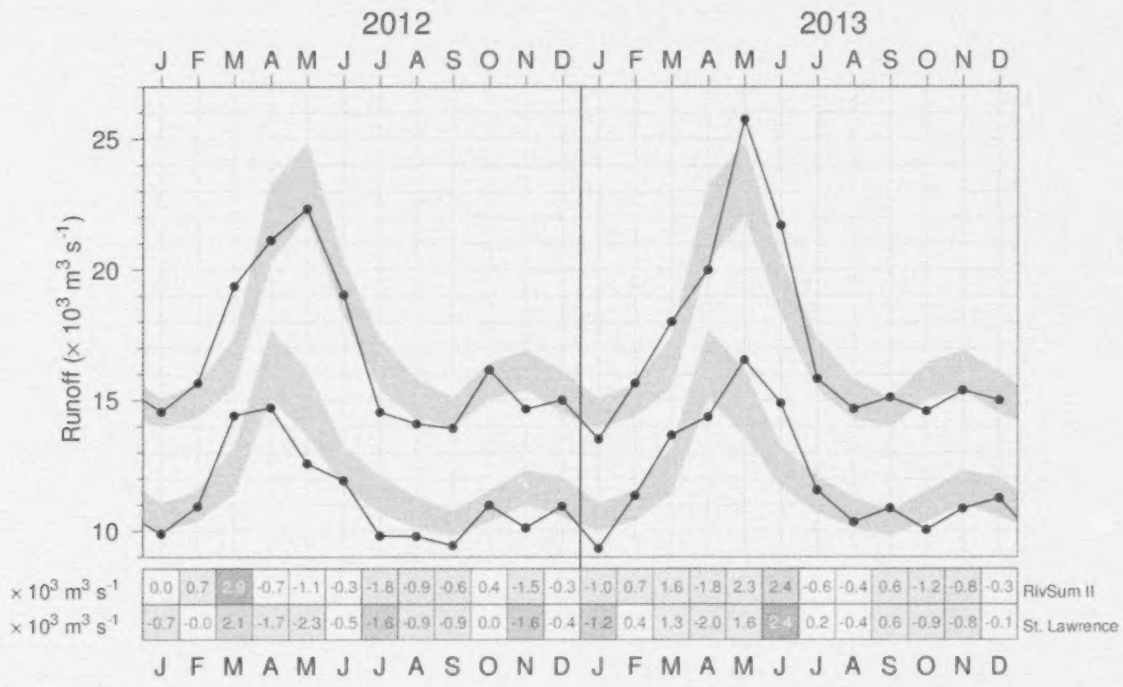

Fig. 6. Monthly mean freshwater flow of the St. Lawrence River at Québec City (lower curve) and its sum with rivers flowing into the St. Lawrence Estuary (RIVSUM II, upper curve). The 1981–2010 climatological mean (± 0.5 SD) is shown (blue shading). The scorecards are colour-coded according to the monthly anomalies normalized for each month of the year, but the numbers are the actual monthly anomalies in 10^3 $m^3 s^{-1}$.

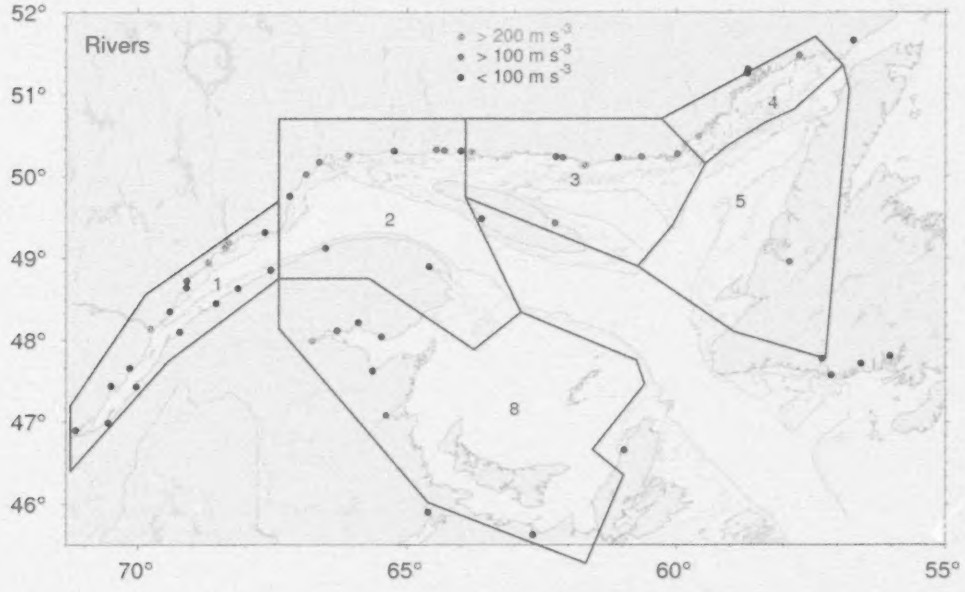

Fig. 7. River discharge locations for the regional sums of runoffs listed in Table 2. Red and blue dots indicate rivers that have climatological mean runoff greater than 200 m3 s-1 and between 100 and 200 $m^3 s^{-1}$, respectively.

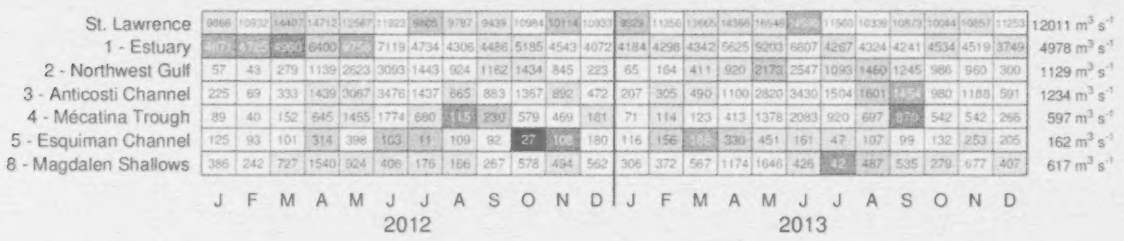

Fig. 8. Monthly anomalies of the St. Lawrence River runoff and sums of all other major rivers draining into separate Gulf regions for 2012 and 2013. The scorecards are colour-coded according to the monthly normalized anomalies based on the 1981–2010 climatologies for each month, but the numbers are the monthly average runoffs in m3 s-1. Numbers on the right side are annual climatological means. Runoff regulation is simulated for three rivers that flow into the Estuary (Saguenay, Manicouagan, Outardes).

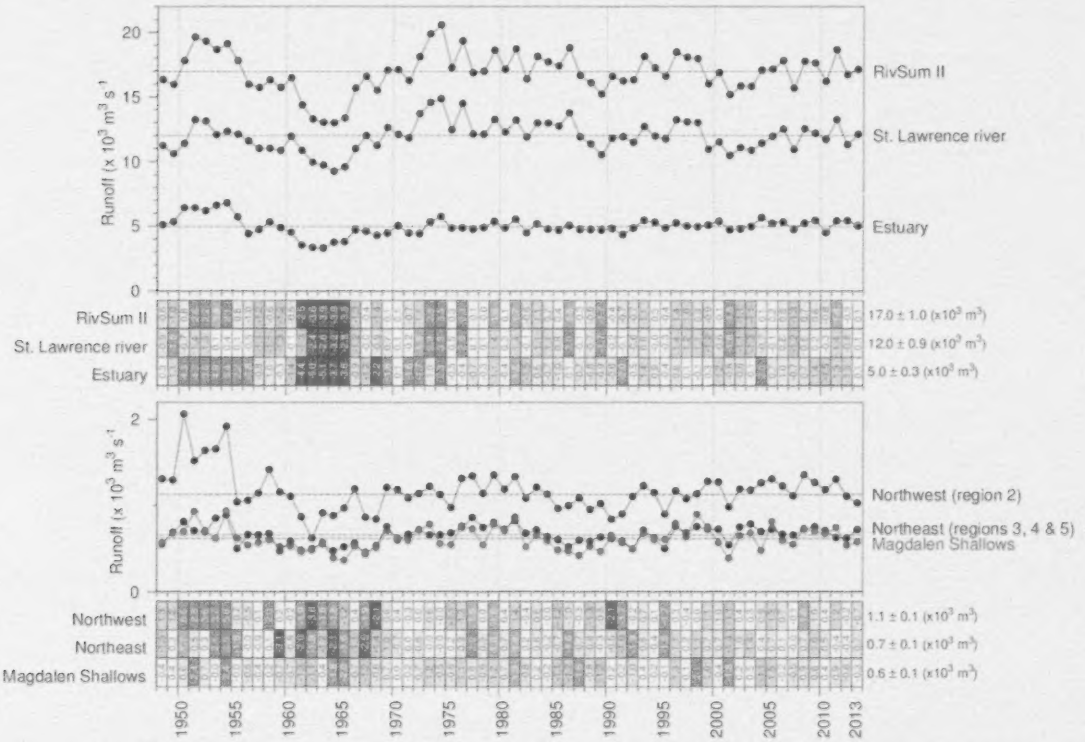

Fig. 9. Annual mean freshwater flow of the St. Lawrence River at Québec City and of the sum of all rivers flowing into regions of the Estuary and Gulf. The 1981–2010 climatological mean is shown as horizontal lines and indicated on the right side of the scorecards. Numbers in scorecards are normalized anomalies.

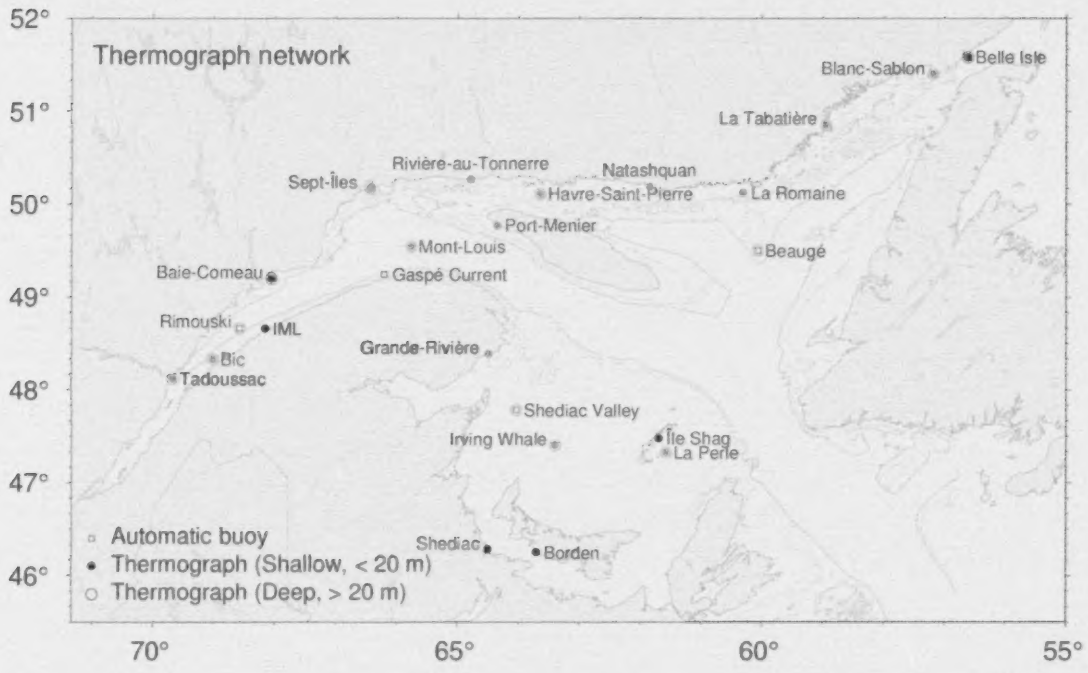

Fig. 10. Locations of the Maurice Lamontagne Institute thermograph network stations in 2013, including oceanographic buoys that transmit data in real time (squares). Deep and shallow instruments are denoted by open circles and dots, while seasonal and year-round deployments are denoted by gray and black symbols. Shediac station from DFO Gulf Region is also shown.

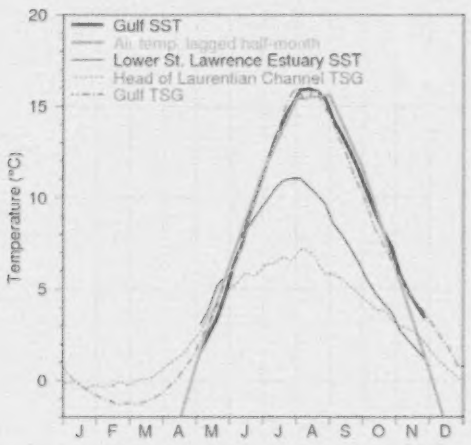

Fig. 11. Sea-surface temperature climatological seasonal cycle in the Gulf of St. Lawrence. AVHRR temperature weekly averages for 1985 to 2010 are shown from May to November (ice-free months) for the entire Gulf (thick black line) and the cooler Lower St. Lawrence Estuary (thin black line), defined as the area west of the Pointe-des-Monts section and east of approx 69°30'W. Thermosalinograph data averages for 2000 to 2010 are shown for the head of the Laurentian Channel (at 69°30'W, grey dashed line) and for the average over the Gulf waters along the main shipping route between the Pointe-des-Monts and Cabot Strait sections (gray dash-dotted line). Monthly air temperature averaged over eight stations in the Gulf of St. Lawrence are shown offset by 2 weeks into the future (thick grey line; winter months not shown). Figure from Galbraith et al. (2012).

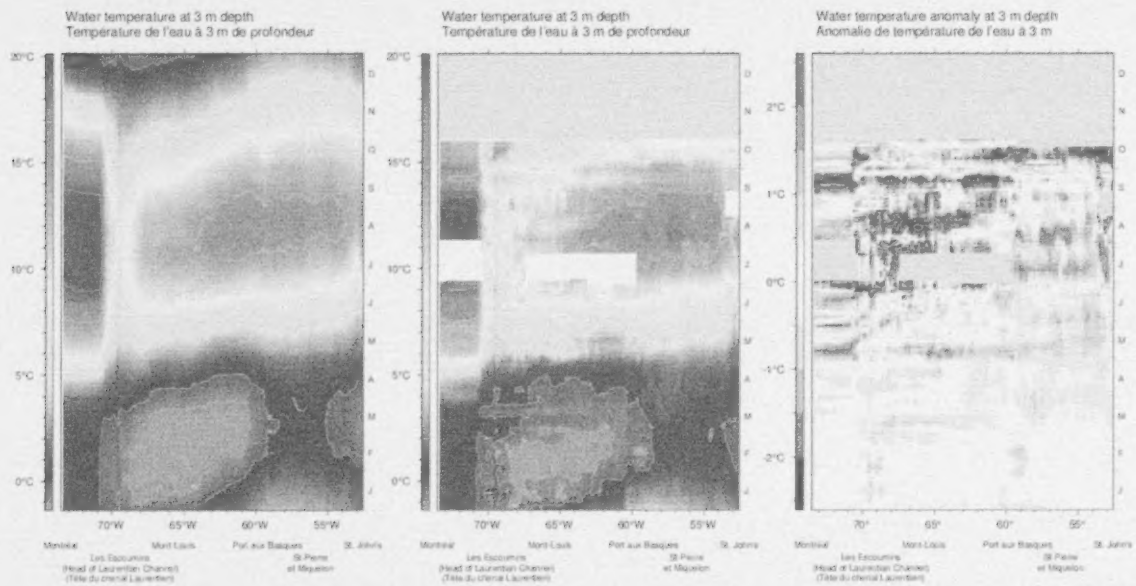

Fig. 12. Thermosalinograph data at 3 m depth along the Montréal to St. John's shipping route:composite mean annual cycle of the water temperature for the 2000–2013 period (left panel),composite annual cycle of the water temperature for 2013 (middle panel), and water temperature anomaly for 2013 relative to the 2000–2013 composite (right panel).

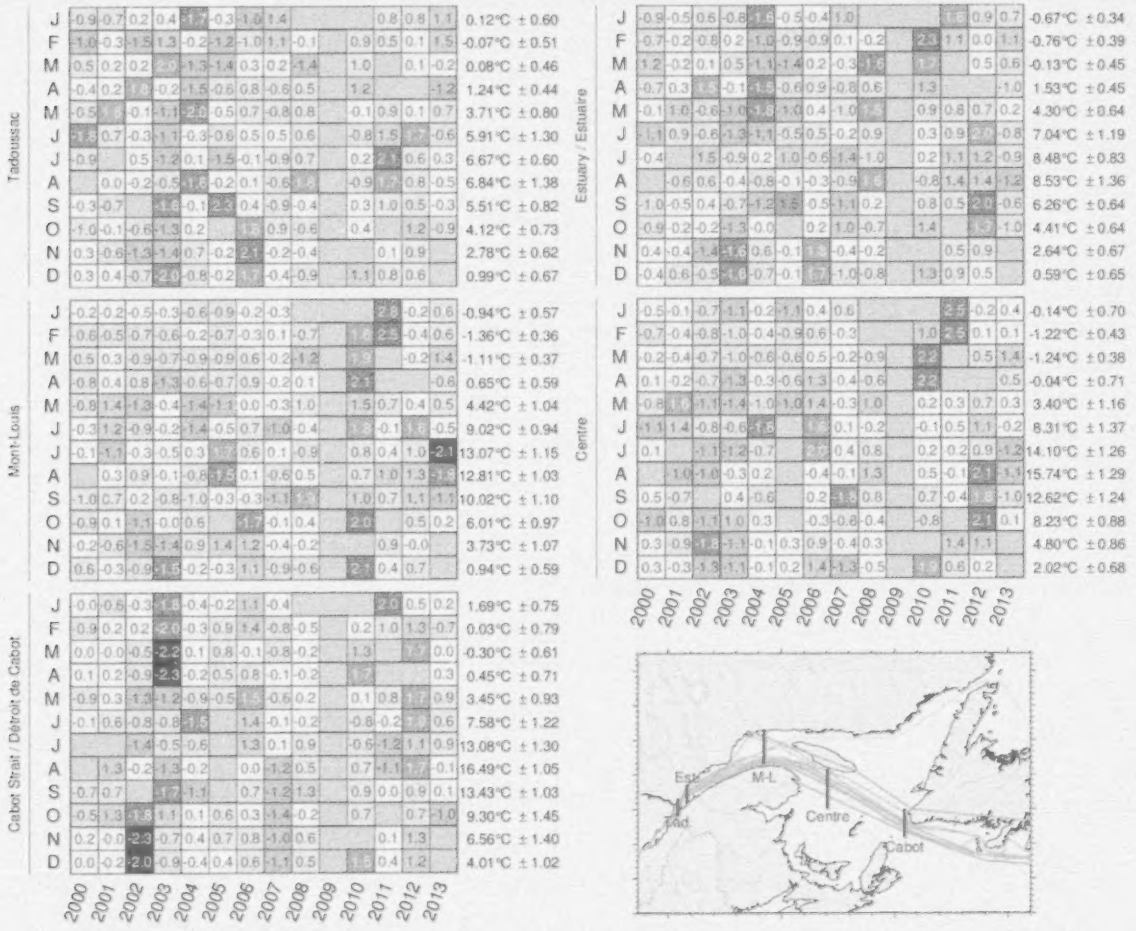

Fig. 13. Thermosaligraph near-surface temperature monthly anomalies for various sections along the main shipping lane. The numbers on the right are the 2000–2013 climatological means and standard deviations. The numbers in the boxes are normalized anomalies. The map shows all TSG data sampled in 2013. Those drawn in colour are within the main shipping corridor and are used in this report. Monthly average anomalies of temperatures measured close to the indicated blue section lines are shown in the other scorecard panels.

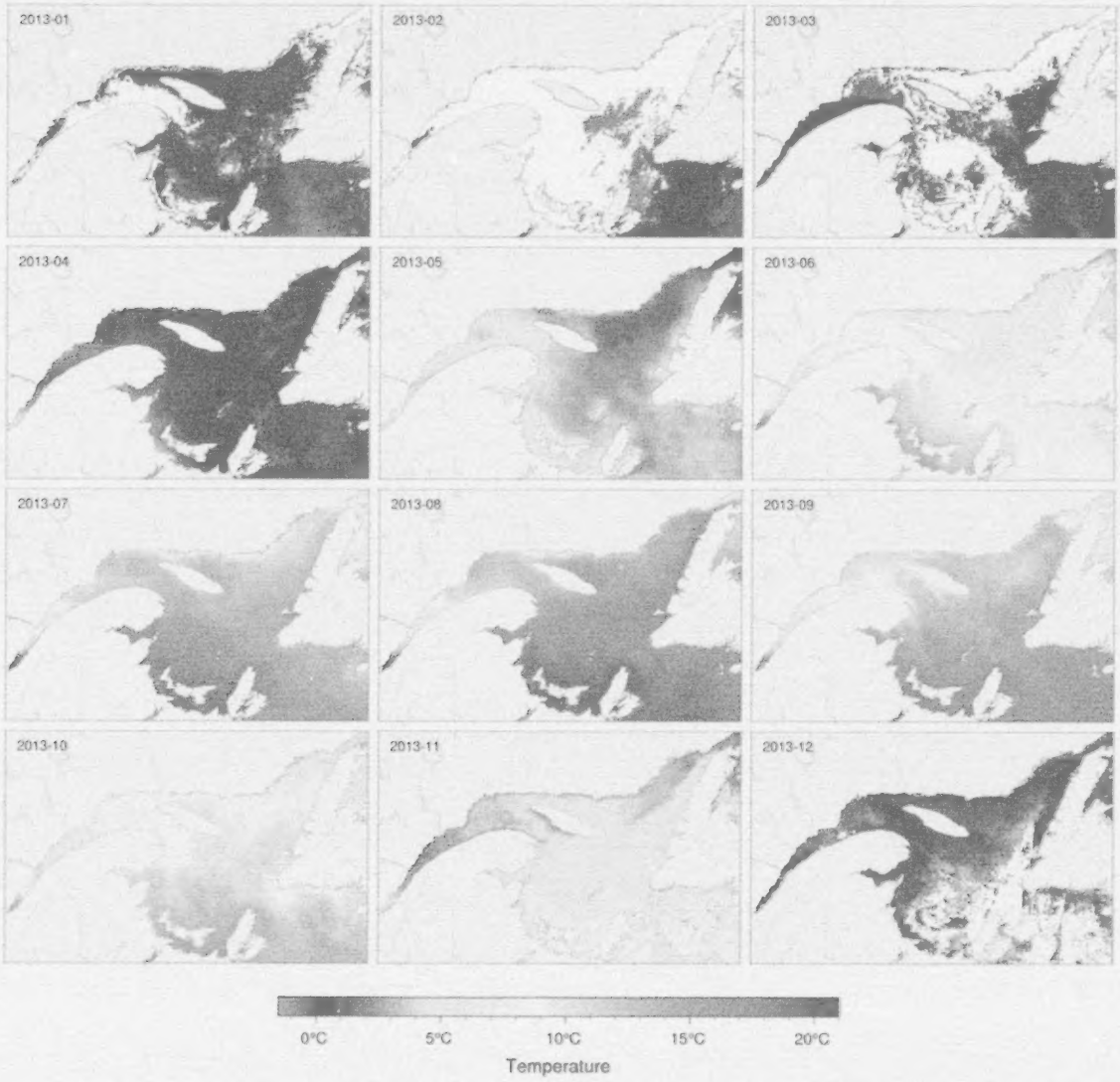

Fig. 14. Sea-surface temperature monthly averages for 2013 as observed with NOAA AVHRR remote sensing. White areas have no data for the period due to ice cover or clouds. January-August data are from MLI's Remote Sensing Laboratory (P. Larouche) while September-December are from BIO Operational Remote Sensing (C. Caverhill).

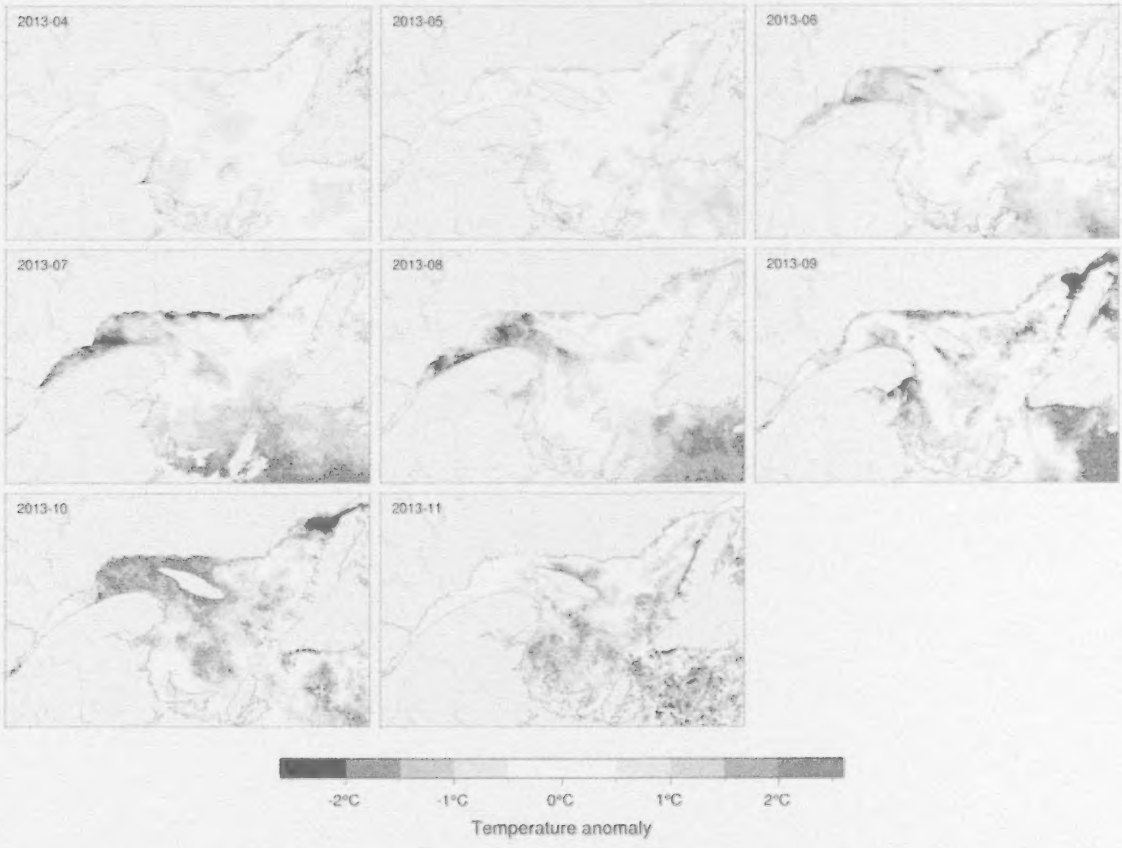

Fig. 15. Sea-surface temperature monthly anomalies for April through November 2013 based on monthly climatologies calculated for the 1985–2010 period observed with NOAA AVHRR remote sensing. Only ice-free months are shown. January-August data are from MLI's Remote Sensing Laboratory (P. Larouche) and are based on a climatology for 1985-2010 while September-November are from BIO's Operational Remote Sensing (C. Caverhill) and use a 1999-2010 climatological period here.

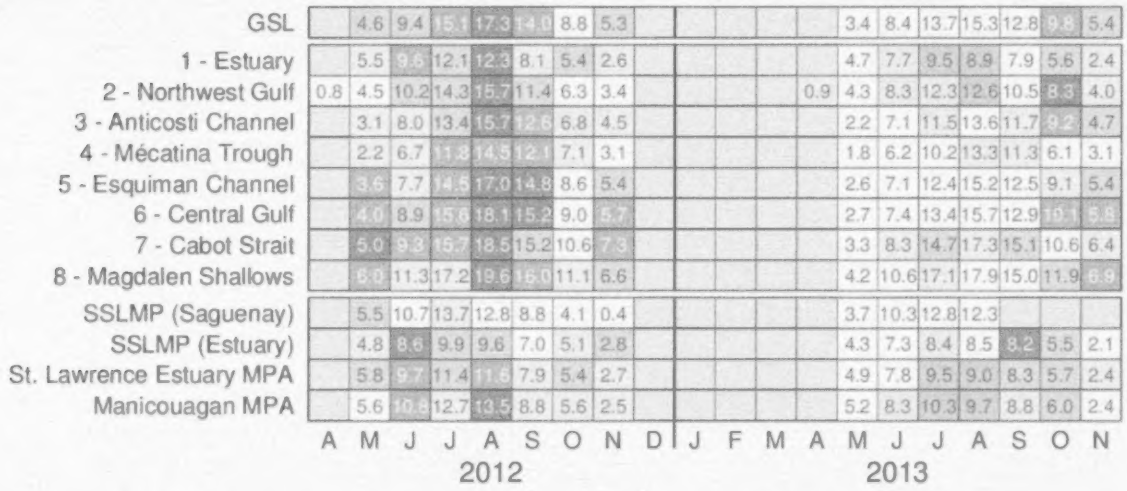

Fig. 16. NOAA SST May to November monthly anomalies averaged over the Gulf, the eight regions of the Gulf, and management regions of the St. Lawrence Estuary for 2012 and 2013 (April results are also shown for the Northwest Gulf). The scorecards are colour-coded according to the monthly normalized anomalies based on the 1985–2010 climatologies for each month, but the numbers are the monthly average temperatures.

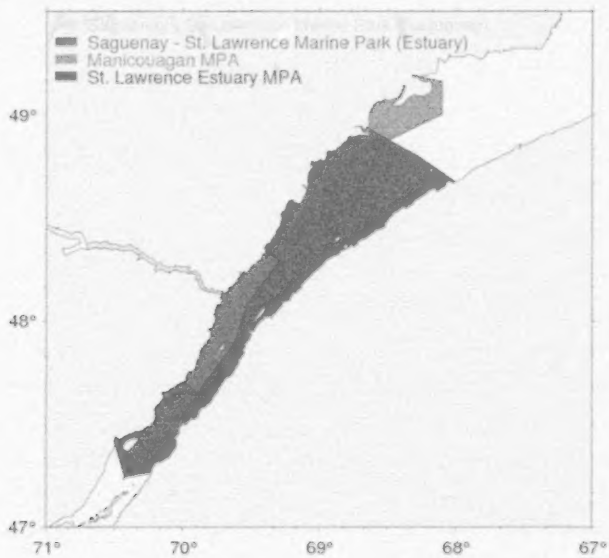

Fig. 17. Map showing the proposed Manicouagan MPA, the proposed St. Lawrence Estuary MPA, and the Saguenay – St. Lawrence Marine Park for the purpose of SST extraction from NOAA imagery (Fig. 16).

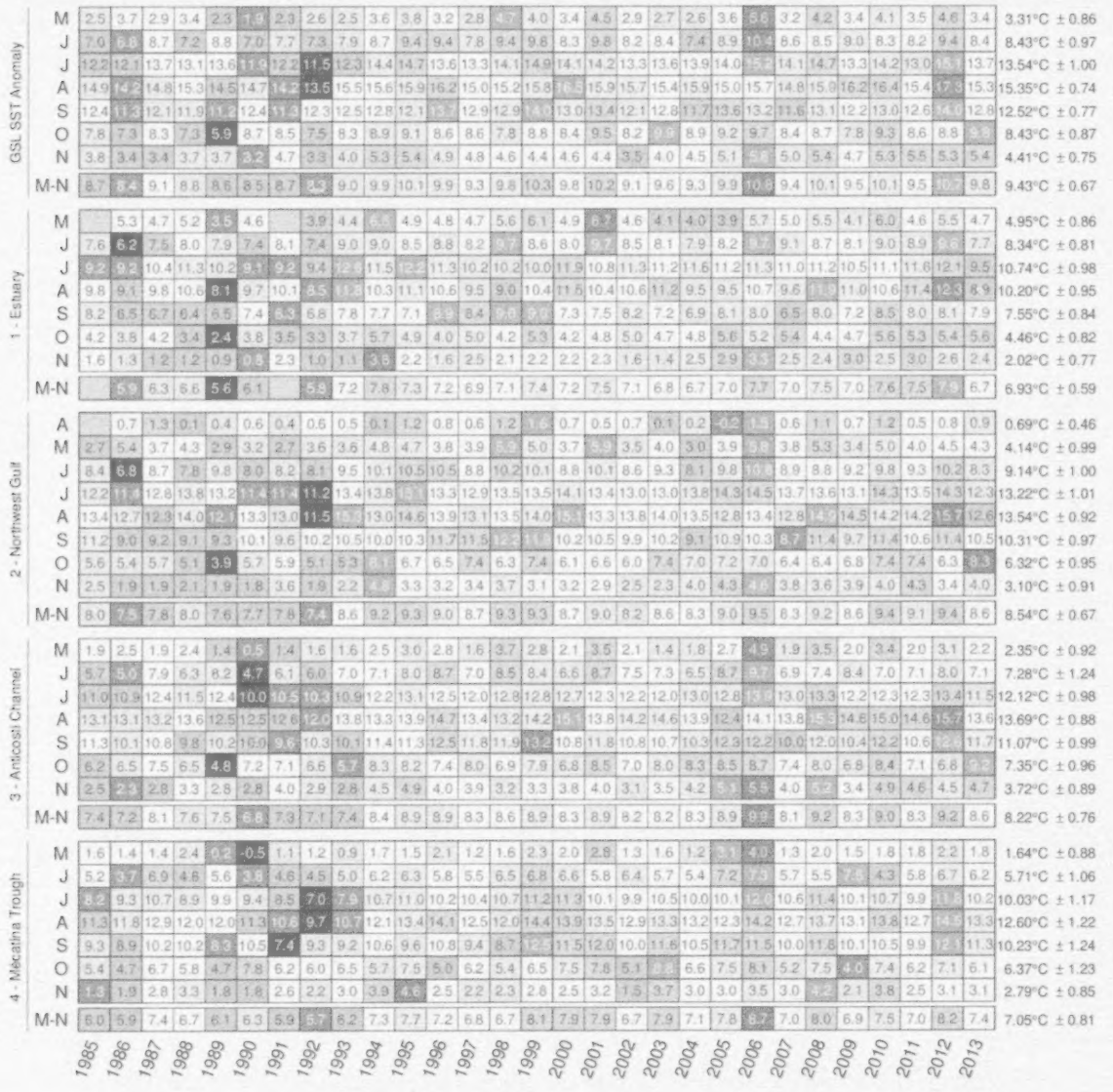

Fig. 18. NOAA SST May to November monthly anomalies averaged over the Gulf of St. Lawrence and over the first four regions of the Gulf. The scorecards are colour-coded according to the monthly normalized anomalies based on the 1985–2010 climatologies for each month, but the numbers are the monthly average temperatures in °C. The 1985-2010 mean and standard deviation are indicated for each month on the right side of the table. April anomalies are included for the Northeast Gulf because those regions are typically ice-free by then. The May to November average is also included.

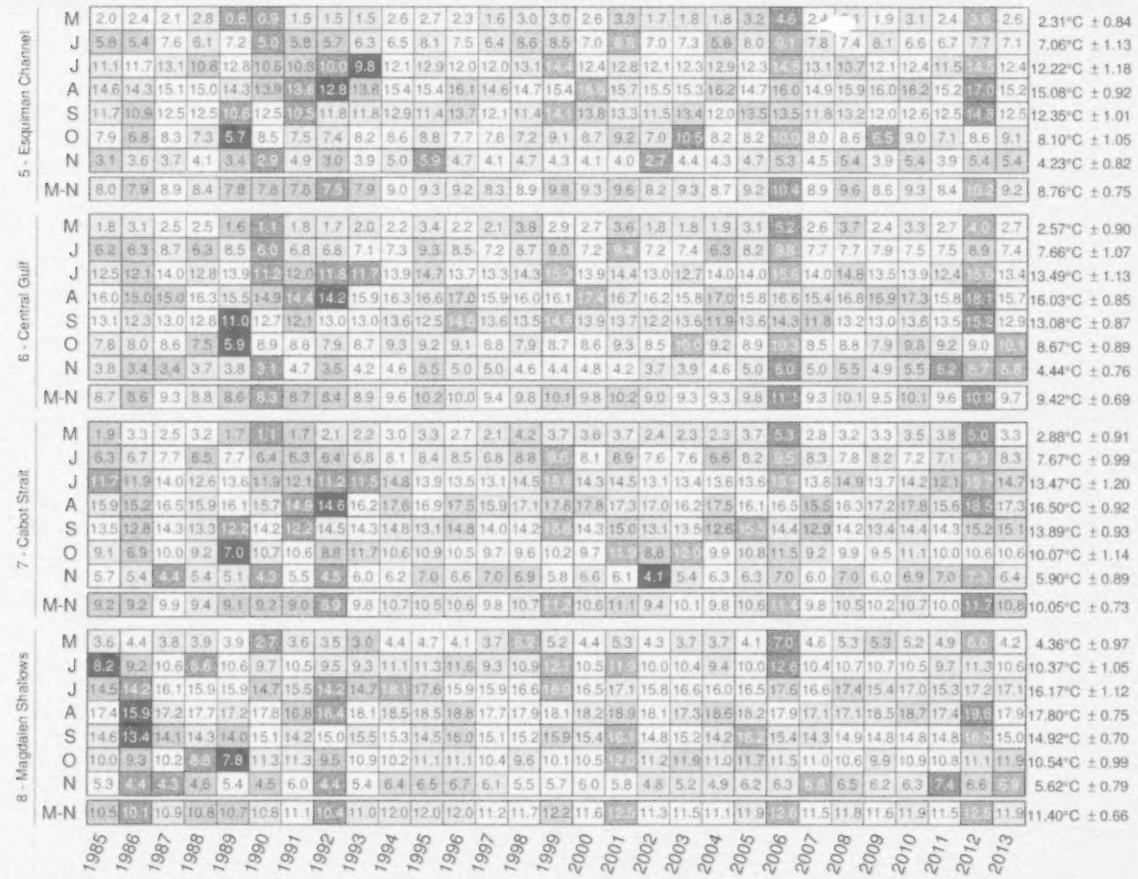

Fig. 19. NOAA SST May to November monthly anomalies averaged over the remaining four regions of the Gulf. The scorecards are colour-coded according to the monthly normalized anomalies based on the 1985–2010 climatologies for each month, but the numbers are the monthly average temperatures in °C. The 1985-2010 mean and standard deviation are indicated for each month on the right side of the table. The May to November average is also included.

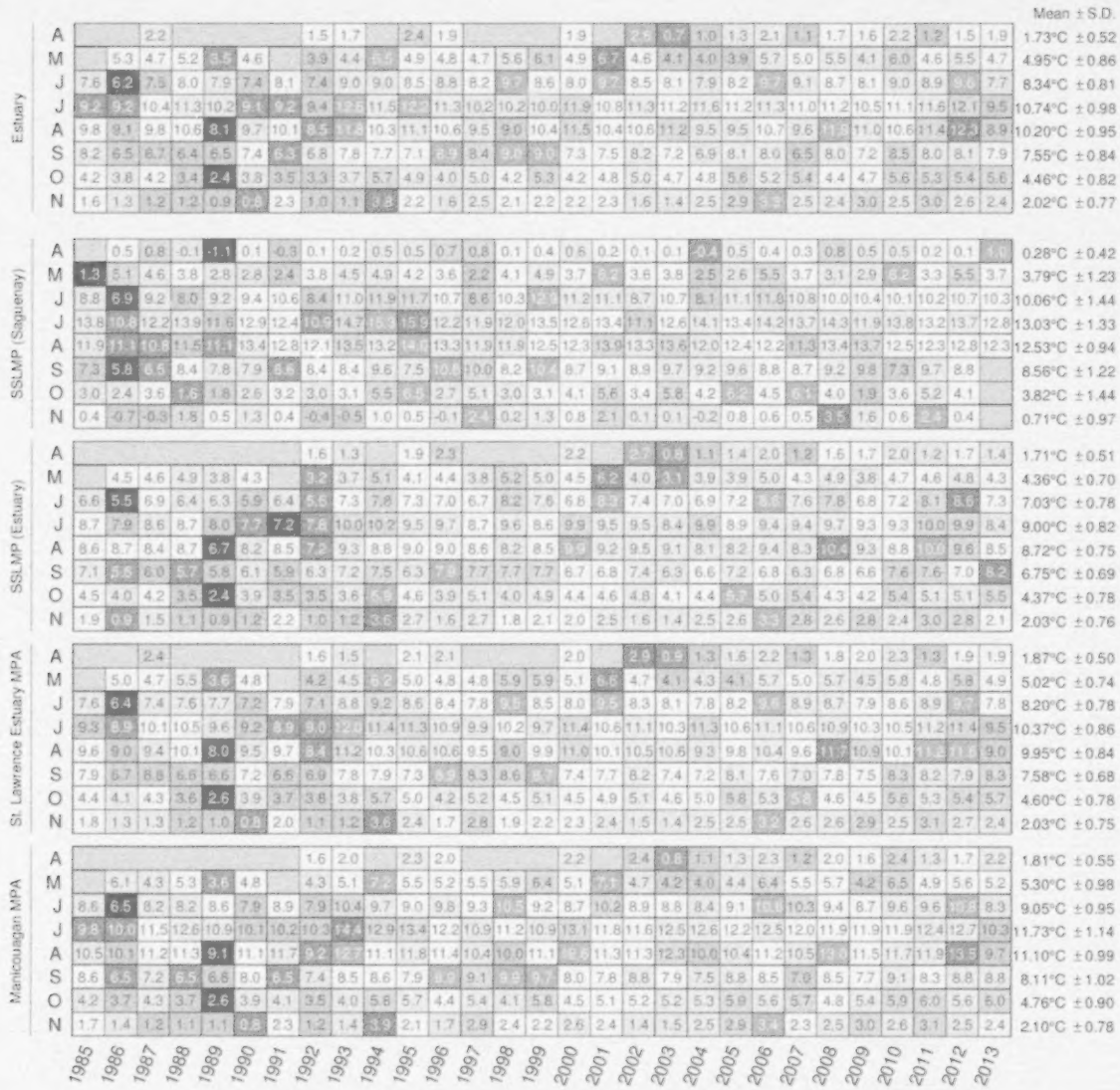

Fig. 20. NOAA SST April to November monthly anomalies averaged over the Estuary (region 1 of the Gulf) and subregions for the Saguenay – St. Lawrence Marine Park (PMSSL), the proposed St. Lawrence Estuary Marine Protected Area (MPA), and Manicouagan MPA. The scorecards are colour-coded according to the monthly normalized anomalies based on the 1985–2010 climatologies for each month, but the numbers are the monthly average temperatures in °C. The 1985-2010 mean and standard deviation are indicated for each month on the right side of the table.

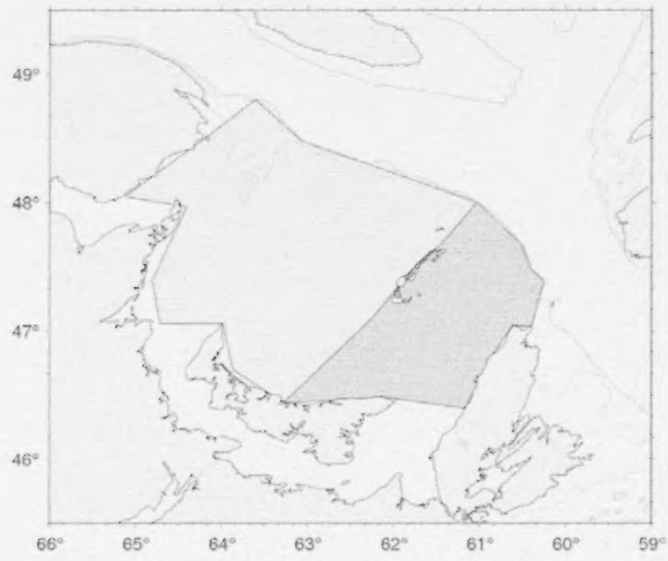

Fig. 21. Areas defined as the western and eastern Magdalen Shallows.

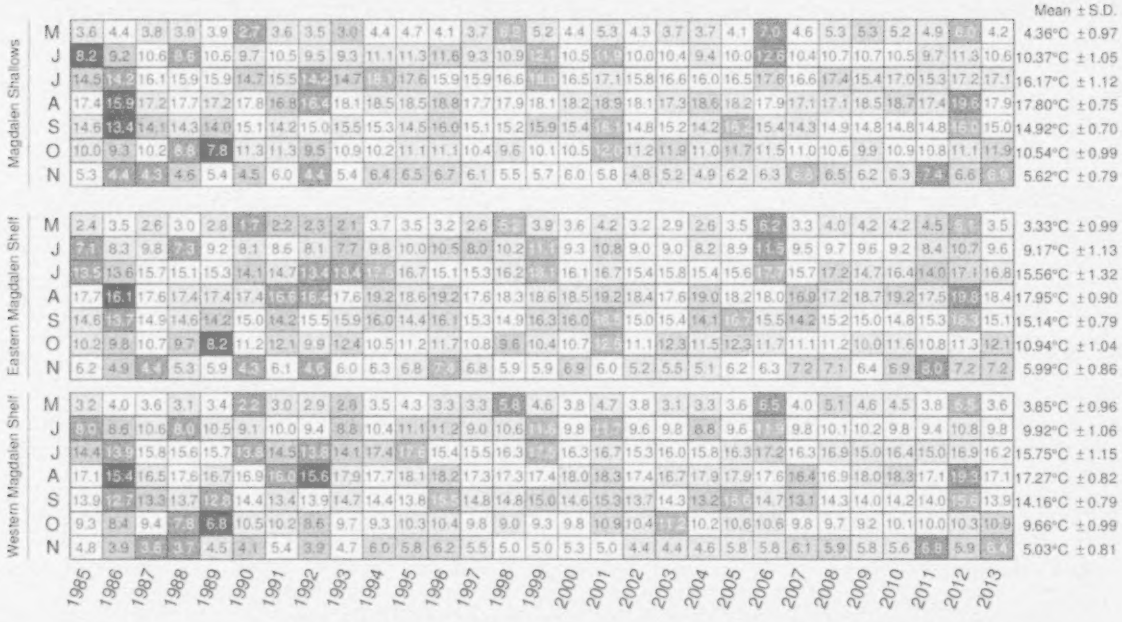

Fig. 22. NOAA SST May to November monthly anomalies averaged over the Magdalen Shallows (region 8 of the Gulf) and the eastern and western subregions of the Magdalen Shallows. The scorecards are colour-coded according to the monthly normalized anomalies based on the 1985–2010 climatologies for each month, but the numbers are the monthly average temperatures in °C. The 1985-2010 mean and standard deviation are indicated for each month on the right side of the table.

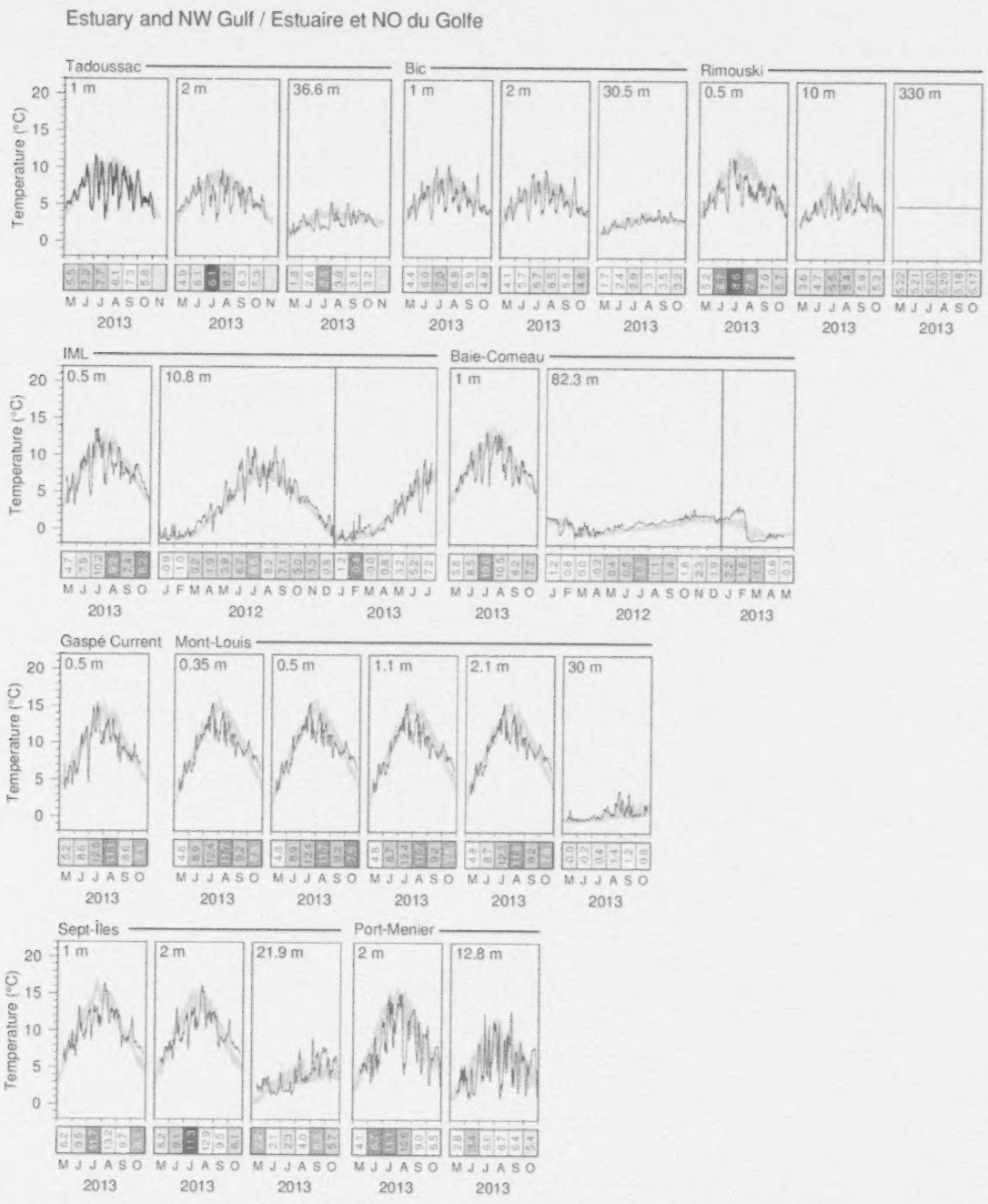

Fig. 23. Thermograph network data. Daily mean 2013 temperatures compared with the daily climatology (daily averages ± 0.5 SD; blue areas) for stations in the Estuary and northwestern Gulf. Scorecards show monthly average temperature. Data from 2012 are included if they were not all shown in last year's report.

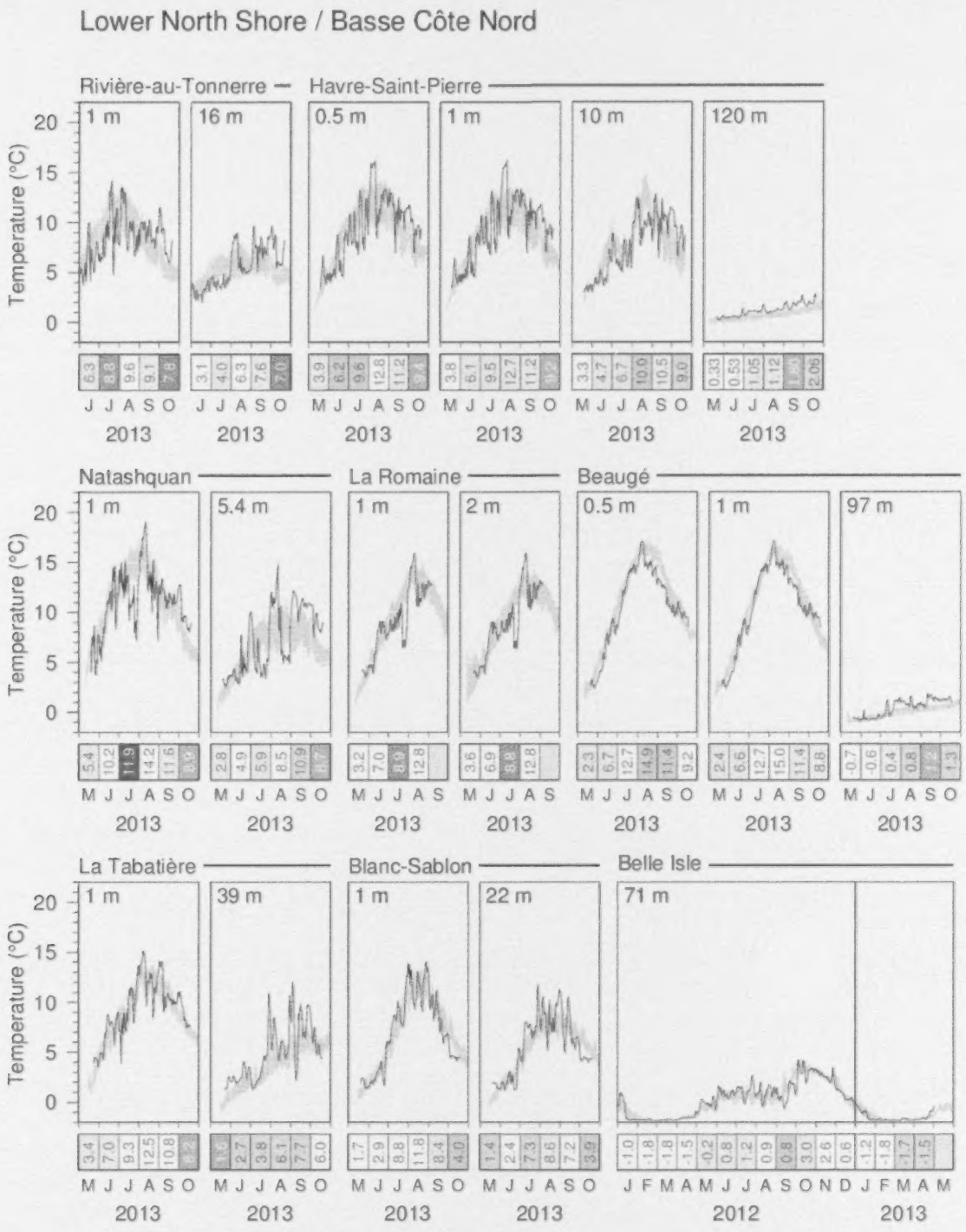

Fig. 24. Thermograph network data. Daily mean 2013 temperatures compared with the daily climatology (daily averages ± 0.5 SD; blue areas) for stations of the lower north shore. Data from 2012 are included if they were not all shown in last year's report.

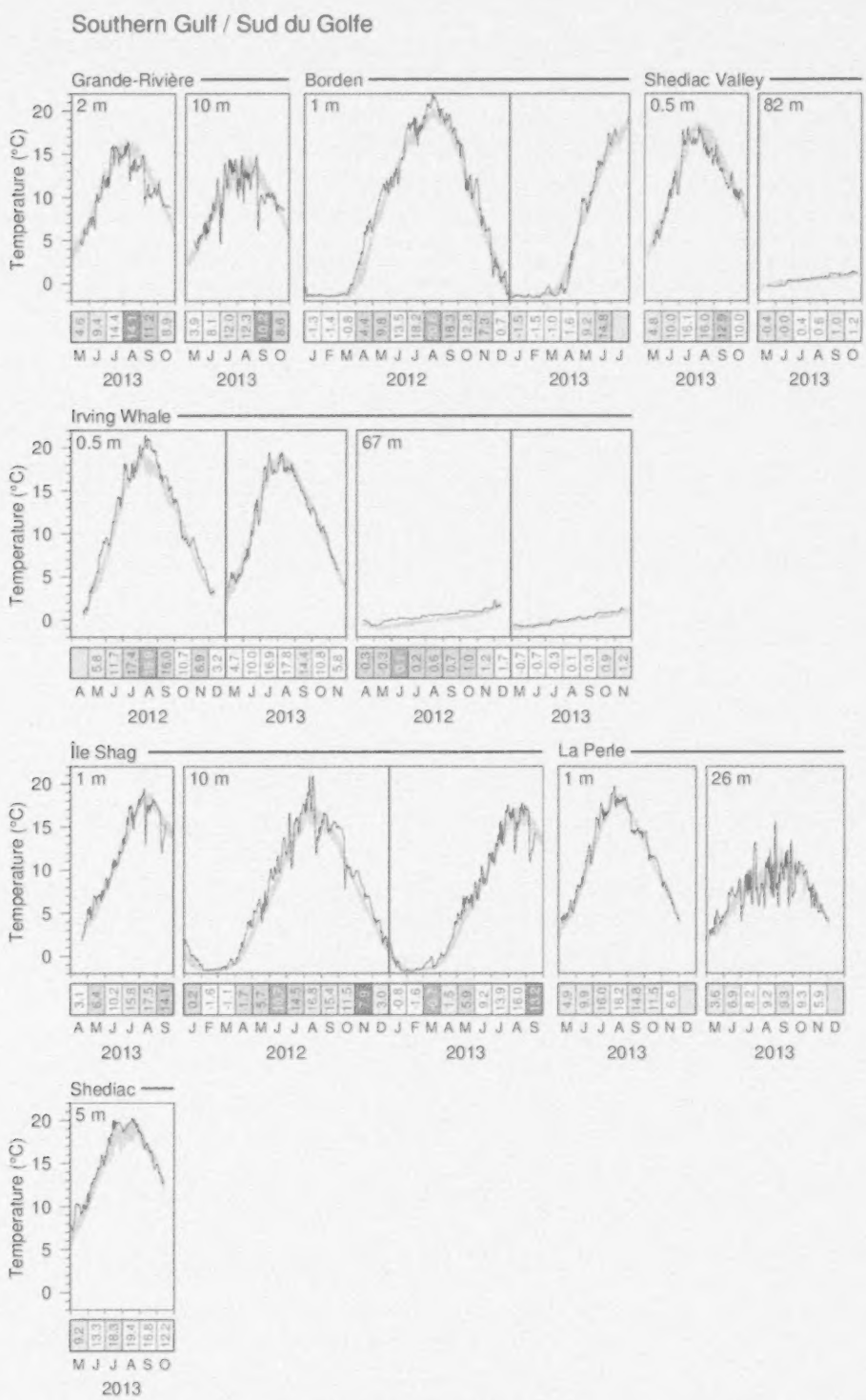

Fig. 25. Thermograph network data. Daily mean 2013 temperatures compared with the daily climatology (daily averages ± 0.5 SD; blue area) for stations of the southern Gulf. Data from 2012 are included if they were not all shown in last year's report.

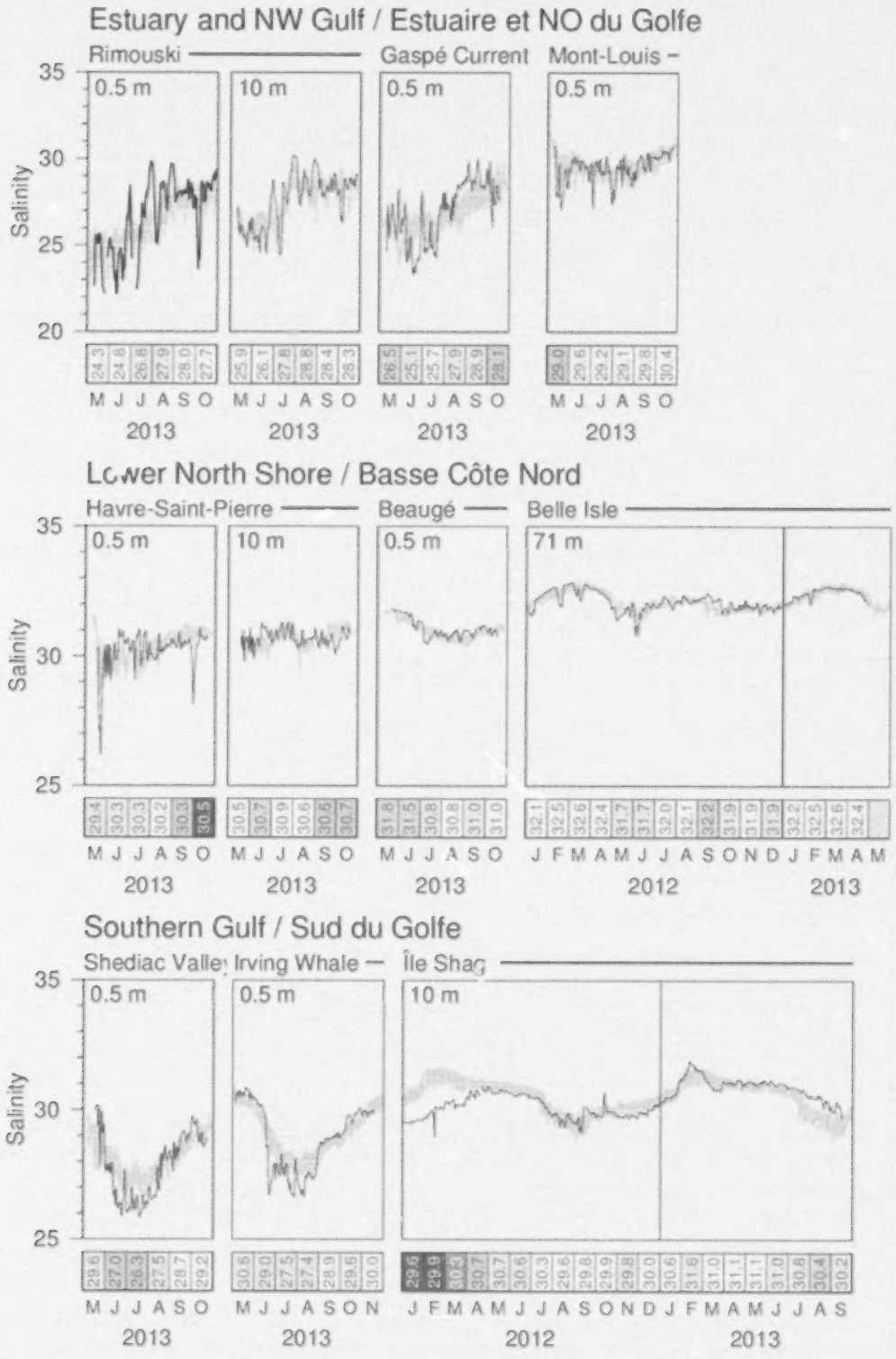

Fig. 26. Thermograph network data. Daily mean 2013 salinities compared with the daily climatology (daily averages ± 0.5 SD; blue area) computed from all available stations.

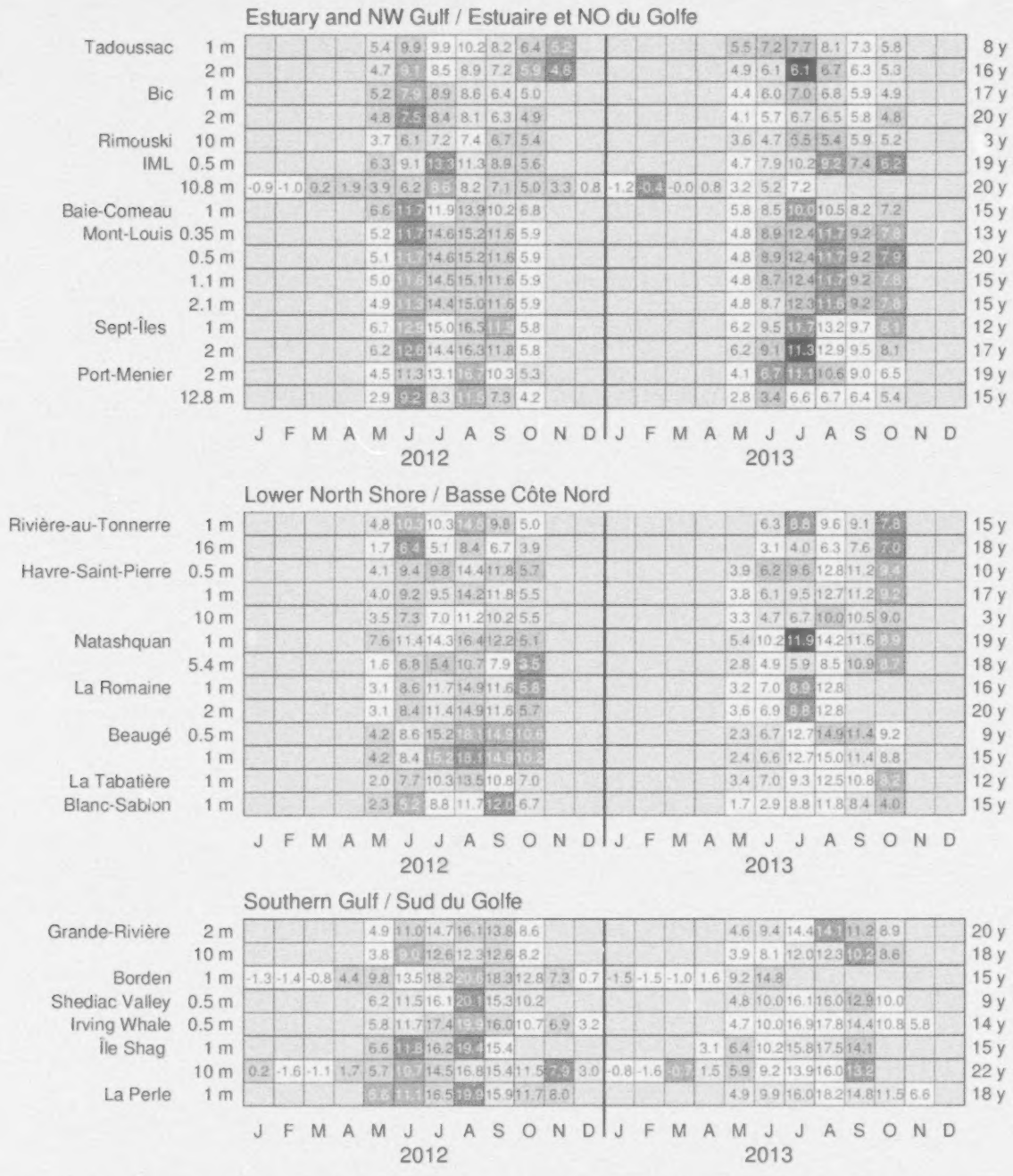

Fig. 27. Monthly mean temperatures at all shallow sensors of the Maurice Lamontagne Institute thermograph network in 2012 and 2013. The number of years that each station and depth has been monitored is indicated on the far right. The colour-coding is according to the temperature anomaly relative to the climatology of each station for each month. Numbers are monthly average temperatures.

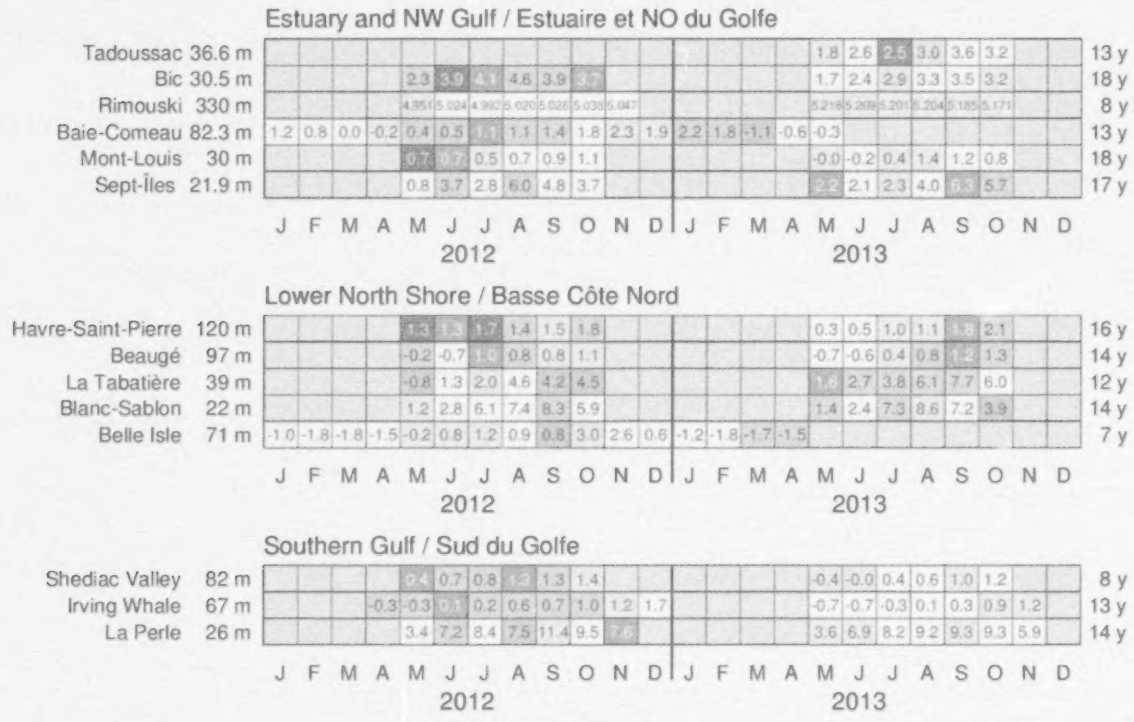

Fig. 28. Monthly mean temperatures at all sensors deeper than 20 m of the Maurice Lamontagne Institute thermograph network in 2012 and 2013.The number of years that each station and depth has been monitored is indicated on the far right. The colour-coding is according to the temperature anomaly relative to the climatology of each station for each month. Numbers are monthly average temperatures, with greater number of significant digits included when variance is lower.

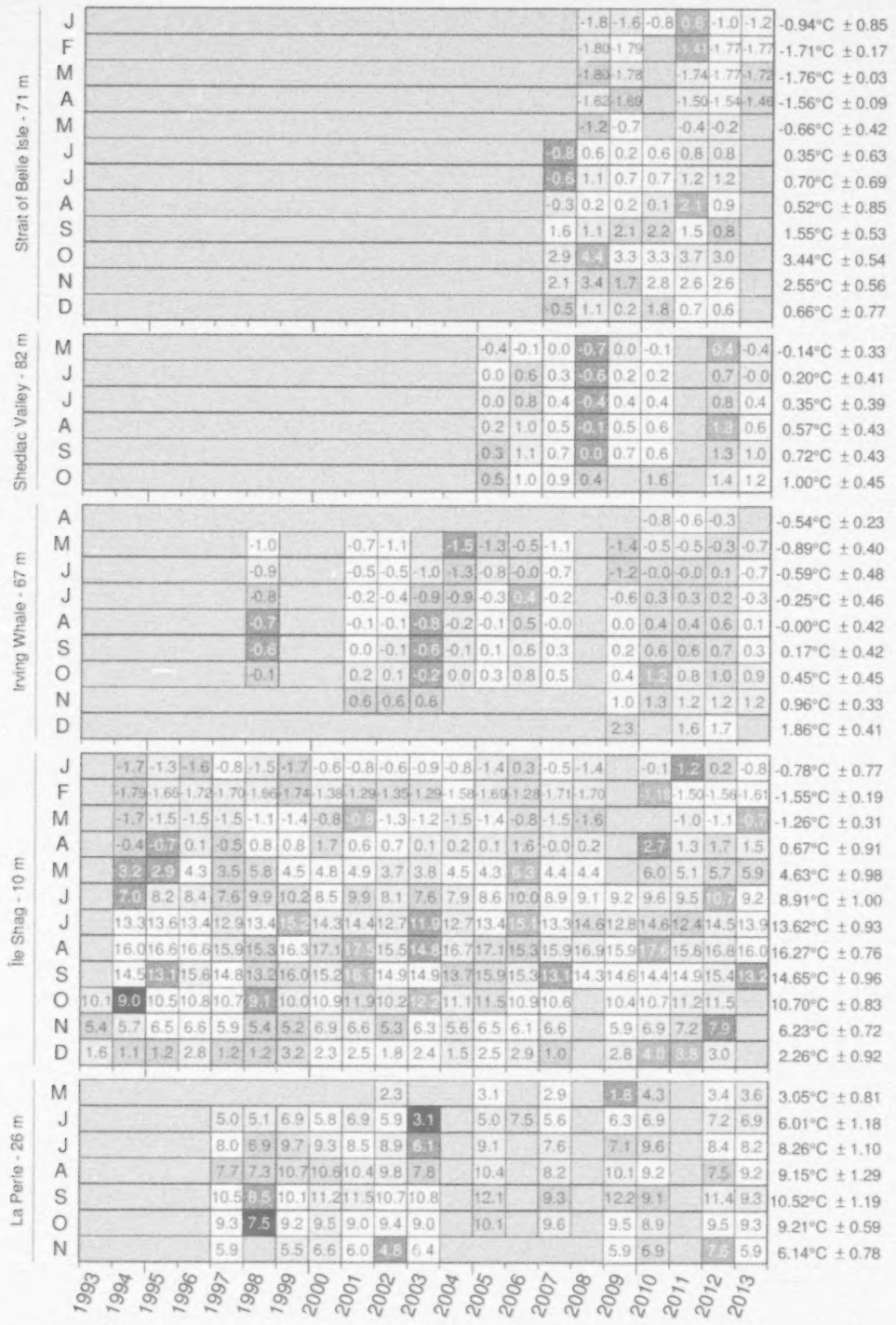

Fig. 29. Time series of the monthly averaged temperature anomalies for selected stations of the thermograph network. The colour-coding is according to the temperature anomaly relative to the climatology of each station for each month. Numbers are monthly average temperatures. The mean and standard deviation are indicated for each month on the right side of the figure.

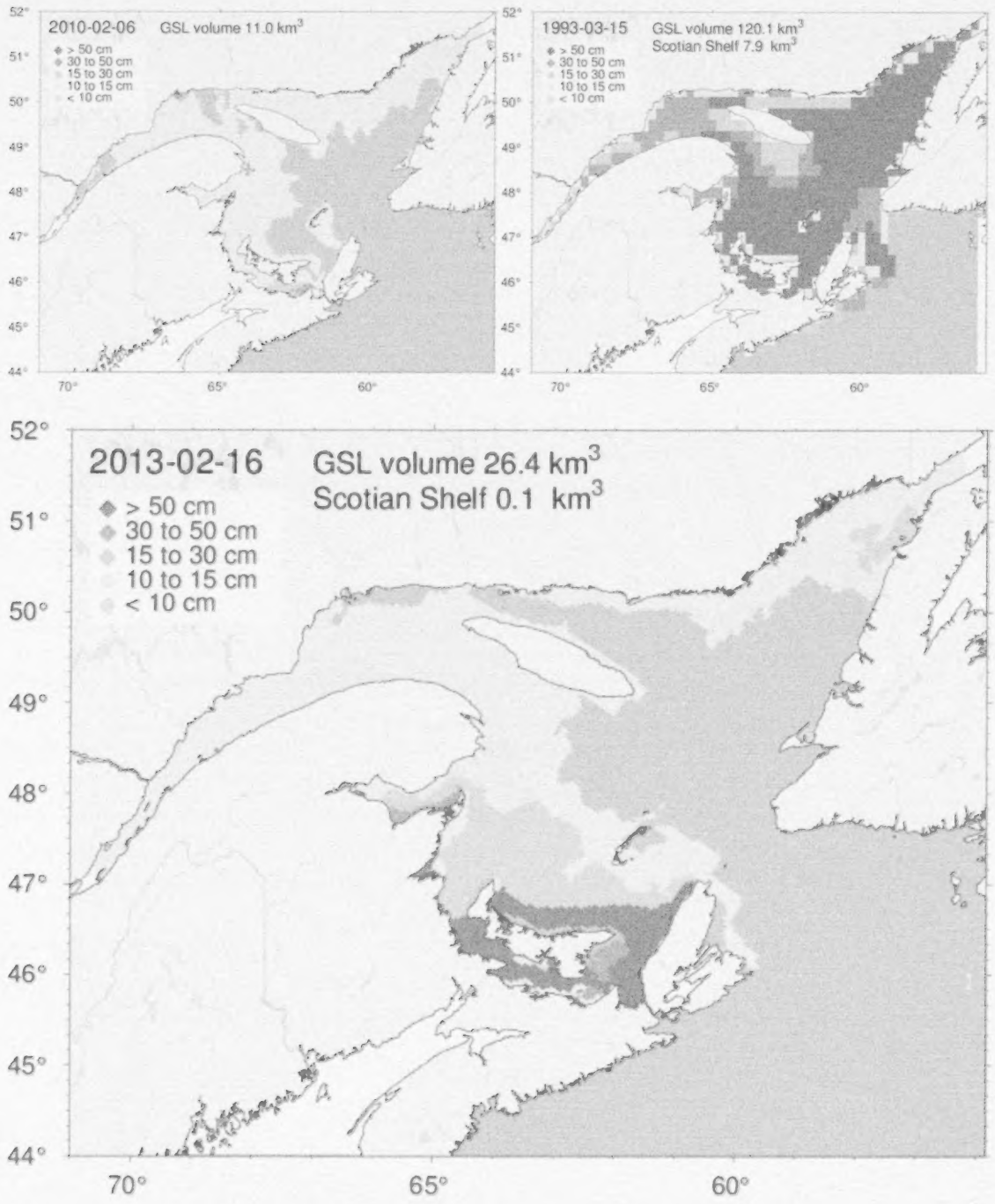

Fig. 30. Ice thickness map for 2013 for the day of the year with the maximum annual volume within the Gulf (lower panel) and similarly for 2010 and 1993, the years with the smallest and largest annual ice volumes within the Gulf, respectively. The limit of the Gulf is set at Cabot Strait. Note that the ice volume indicated for the Scotian Shelf is for that date and is not the maximum that occurred during the ice season for that area.

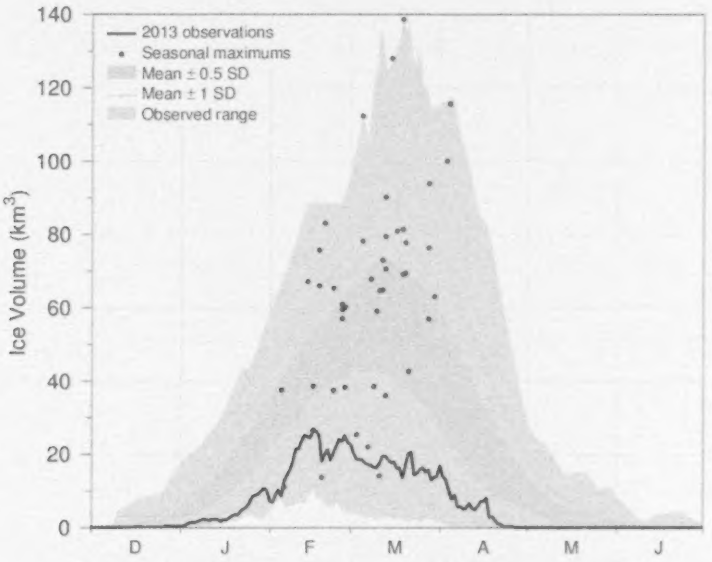

Fig. 31. Time series of the 2012-2013 daily mean ice volume for the Gulf of St. Lawrence and Scotian Shelf (black line), the 1981-2010 climatological mean volume plus and minus 0.5 and 1 SD (dark blue area and dashed line), the minimum and maximum span of 1969-2013 observations (light blue) and the date and volumes of 1969-2013 seasonal maximums (blue dots).

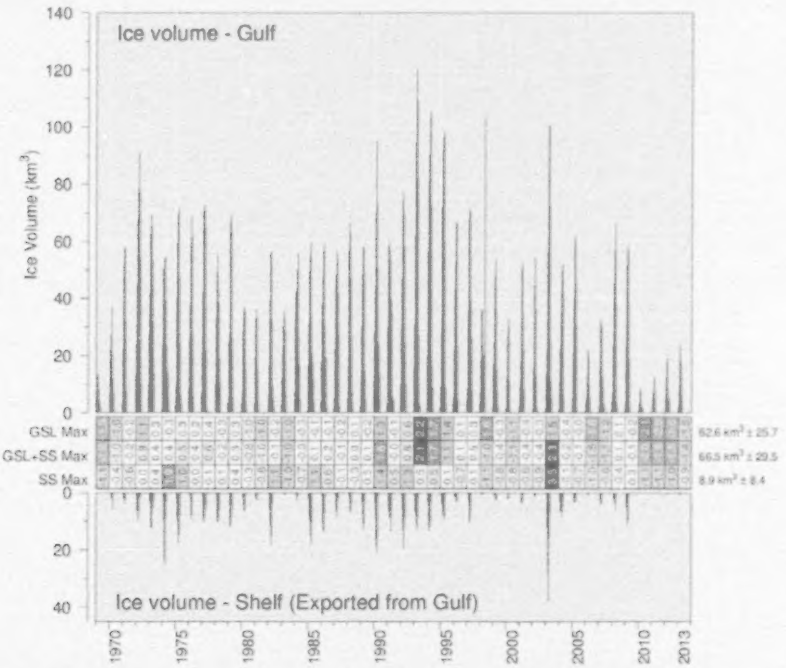

Fig. 32. Estimated ice volume in the Gulf of St. Lawrence (upper panel) and on the Scotian Shelf seaward of Cabot Strait (lower panel). Scorecards show numbered normalized anomalies for the Gulf, combined Gulf and Shelf and Shelf-only annual maximum volumes. Daily values from 1998 onward were filtered using a 7-day running mean prior to calculating the seasonal maximum. The mean and standard deviation are indicated on the right side using the 1981–2010 climatology.

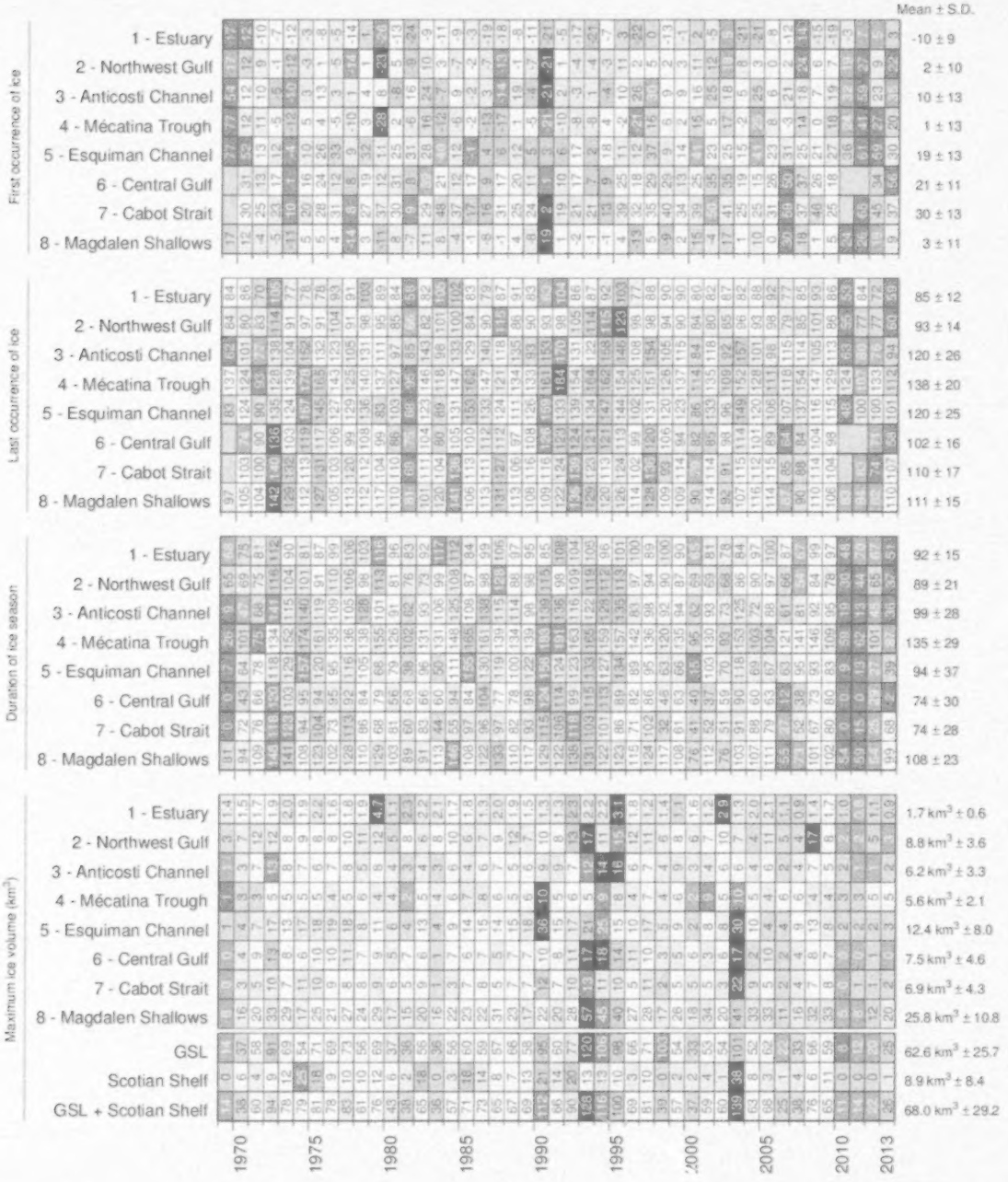

Fig. 33. First and last day of ice occurrence, ice duration, and maximum seasonal ice volume by region. The time when ice was first and last seen in days from the beginning of each year is indicated for each region, and the colour code expresses the anomaly based on the 1981–2010 climatology, with blue representing earlier first occurrence and later last occurrence. The threshold is 5% of the largest ice volume ever recorded in the region. Numbers in the table are the actual day of the year rather than the anomaly, but the colour coding is according to normalized anomalies based on the climatology of each region. Duration is the numbers of days that the threshold was exceeded. Daily values from 1998 onward were filtered using a 7-day running mean prior to calculating the seasonal maximum for the three areas of GSL, Scotian Shelf and the combination.

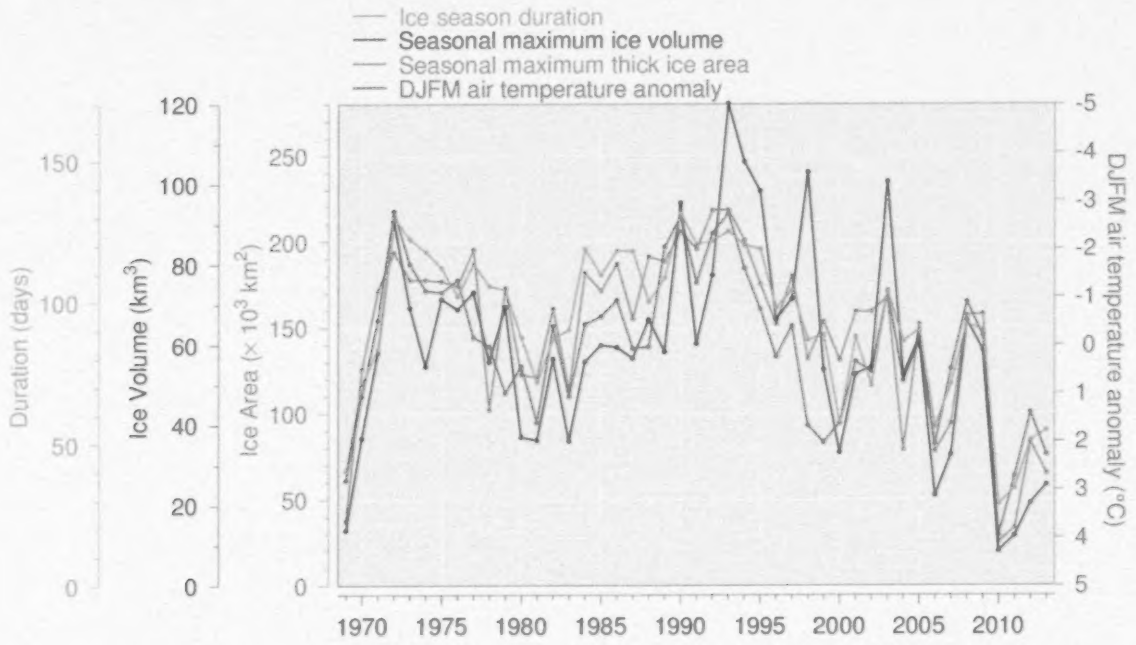

Fig. 34. Seasonal maximum ice volume and area within the Gulf (excluding ice less than 15 cm thick), ice season duration and December-to-March air temperature anomaly (Figure adapted from Hammill & Galbraith 2012).

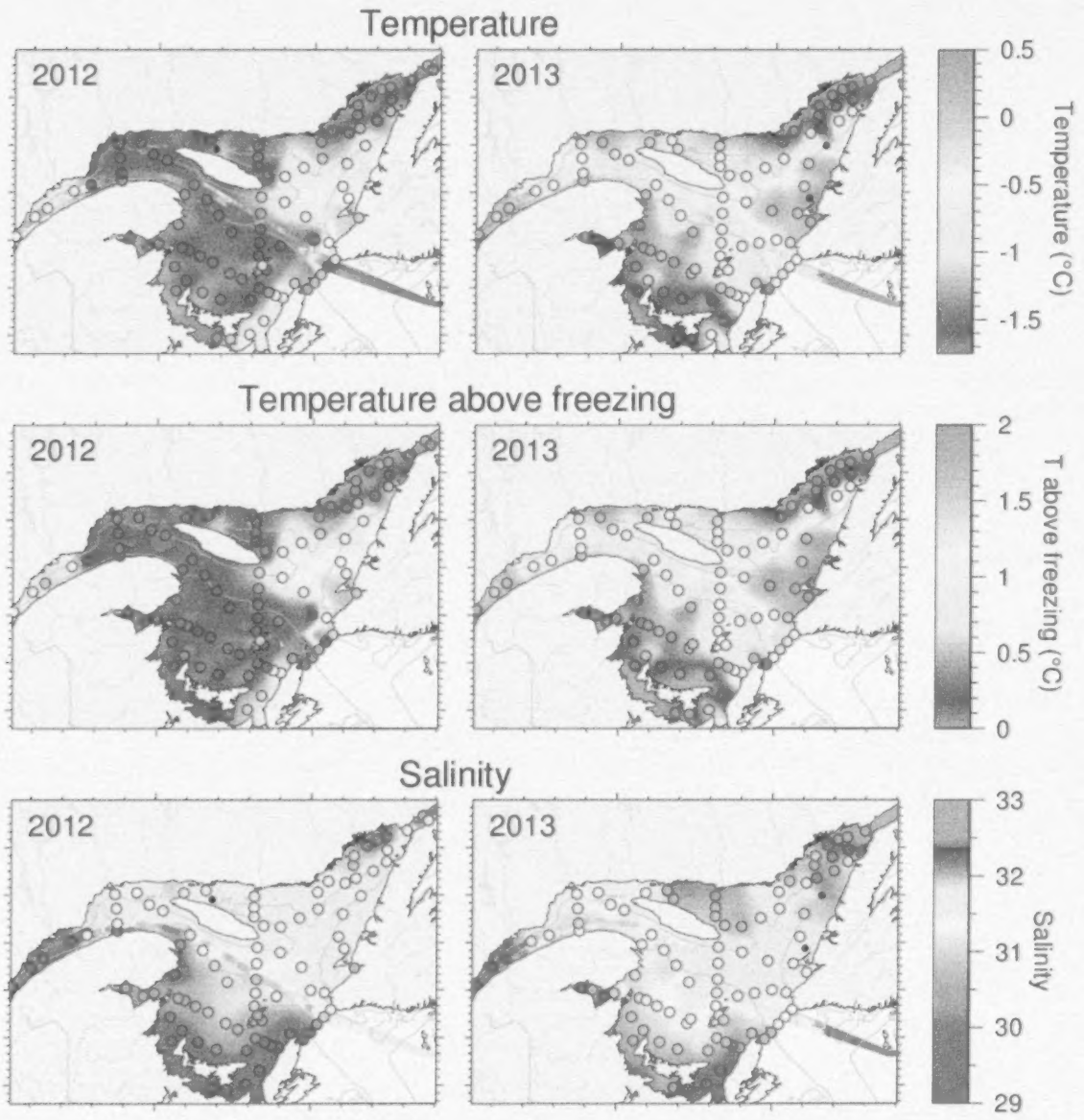

Fig. 35. Winter surface layer characteristics from the March 2012 and 2013 helicopter surveys: surface water temperature (upper panel), temperature difference between surface water temperature and the freezing point (middle panel), and salinity (lower panel). The temperature and salinity measurements from shipboard thermosalinographs taken during the surveys are also shown in the upper and lower panels. Symbols are coloured according to the value observed at the station, using the same colour palette as the interpolated image. A good match is seen between the interpolation and the station observations where the station colours blend into the background. Black symbols indicate missing or bad data.

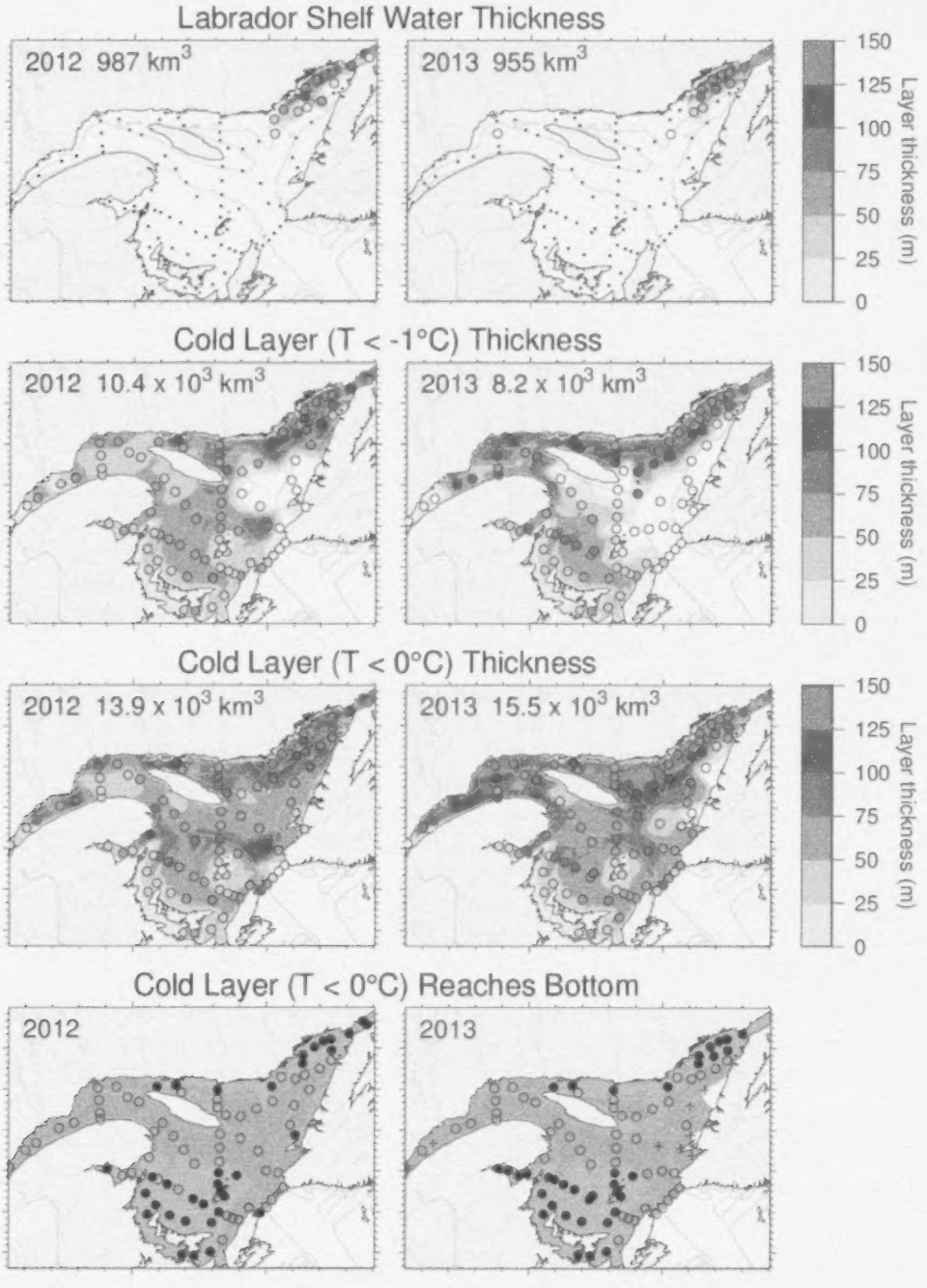

Fig. 36. Winter surface layer characteristics from the March 2012 and 2013 helicopter surveys. Estimates of the thickness of the Labrador Shelf water intrusion (upper panels), cold layer (T<-1°C, T<0°C) thickness (middle panels), and maps indicating where the cold layer (T<0°C) reaches the bottom (in brown; lower panels). Station symbols are coloured according to the observed values as in Fig. 35. For the lower panels, the stations where the cold layer reached the bottom are indicated with filled circles while open circles represent stations where the layer did not reach the bottom. Integrated volumes are indicated for the first six panels (including the Estuary but excluding the Strait of Belle Isle).

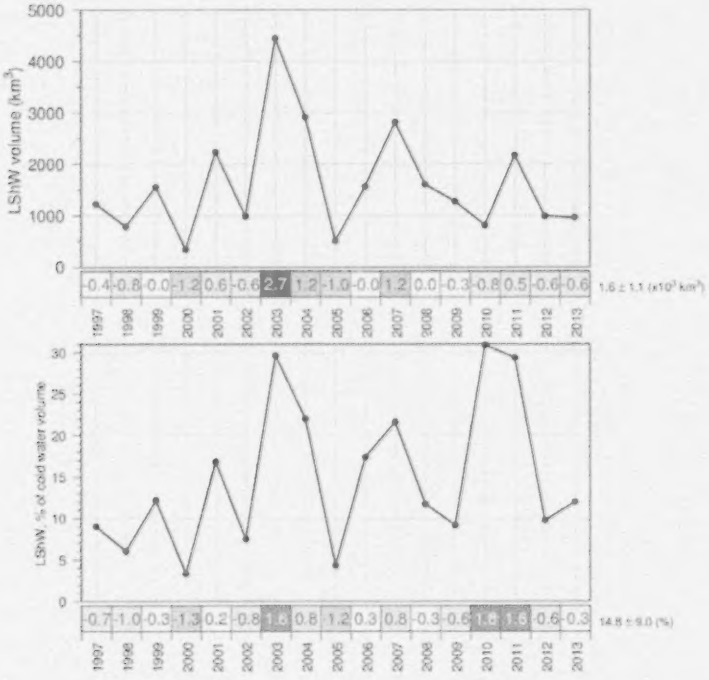

Fig. 37. Estimated volume of cold and saline Labrador Shelf water that flowed into the Gulf over the winter through the Strait of Belle Isle. The bottom panel shows the volume as a percentage of total cold-water volume (<-1°C). The numbers in the boxes are normalized anomalies.

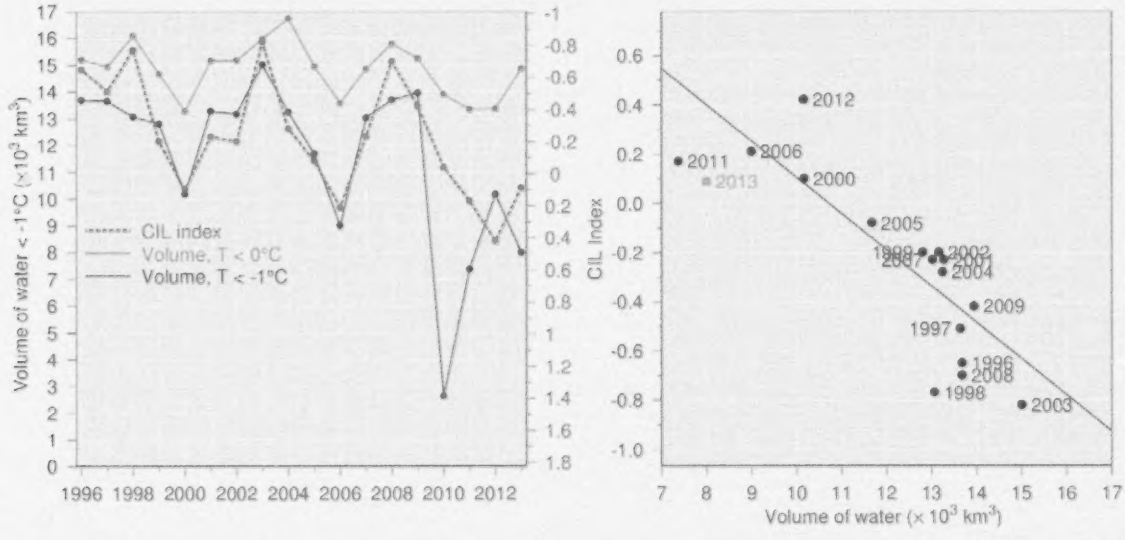

Fig. 38. Left panel: winter surface cold (T<-1°C and T<0°C) layer volume (excluding the Estuary and the Strait of Belle Isle) time series (black and grey lines) and summer CIL index (blue dashed line). Right panel: Relation between summer CIL index and winter cold-water volume with T<-1°C (regression for 1996-2009 data pairs, excluding 1998; see Galbraith 2006). Note that the CIL scale in the left panel is reversed.

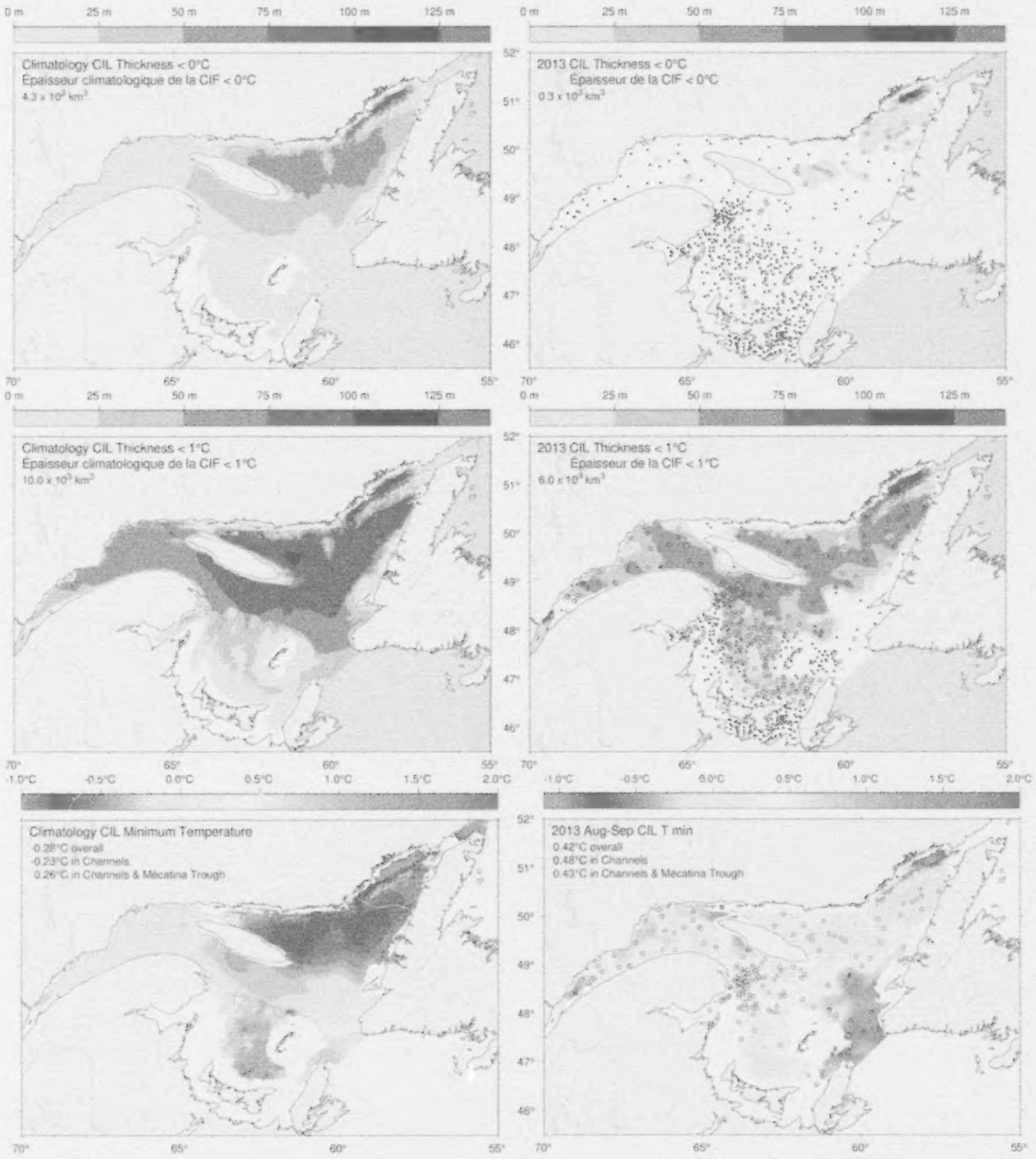

Fig. 39. Cold intermediate layer thickness (T<0°C, top panels; T<1°C, middle panels) and minimum temperature (bottom panels) in August and September 2013 (right) and 1985-2010 climatology (left). Station symbols are colour-coded according to their CIL thickness and minimum temperature. Numbers in the upper and middle panels are integrated CIL volumes and in the lower panels are monthly average temperatures.

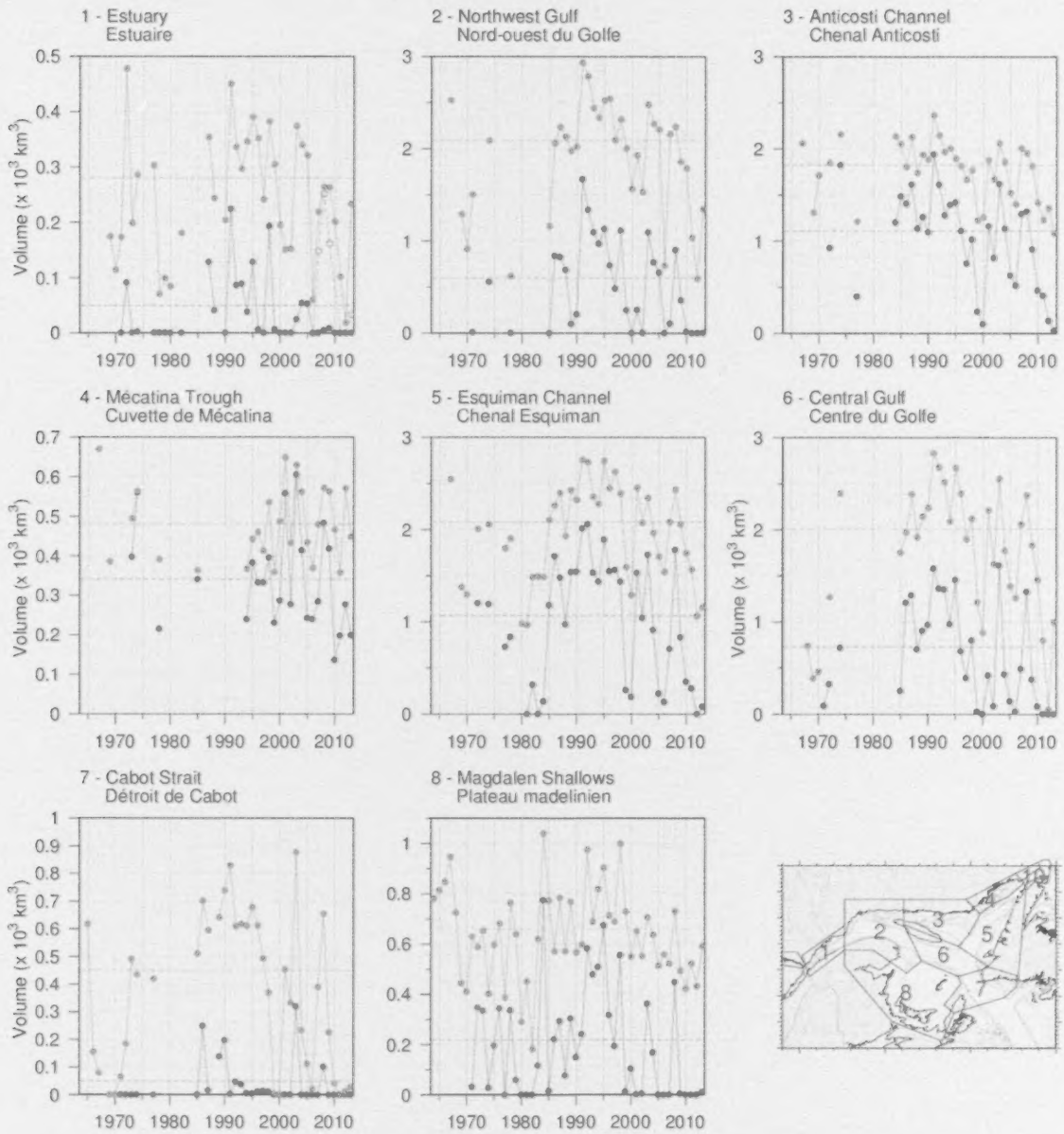

Fig. 40. Volume of the CIL colder than 0°C (blue) and colder than 1°C (red) in August and September (primarily region 8 in September). The volume of the CIL colder than 1°C in November for available years since 2006 is also shown for the St. Lawrence Estuary (dashed line).

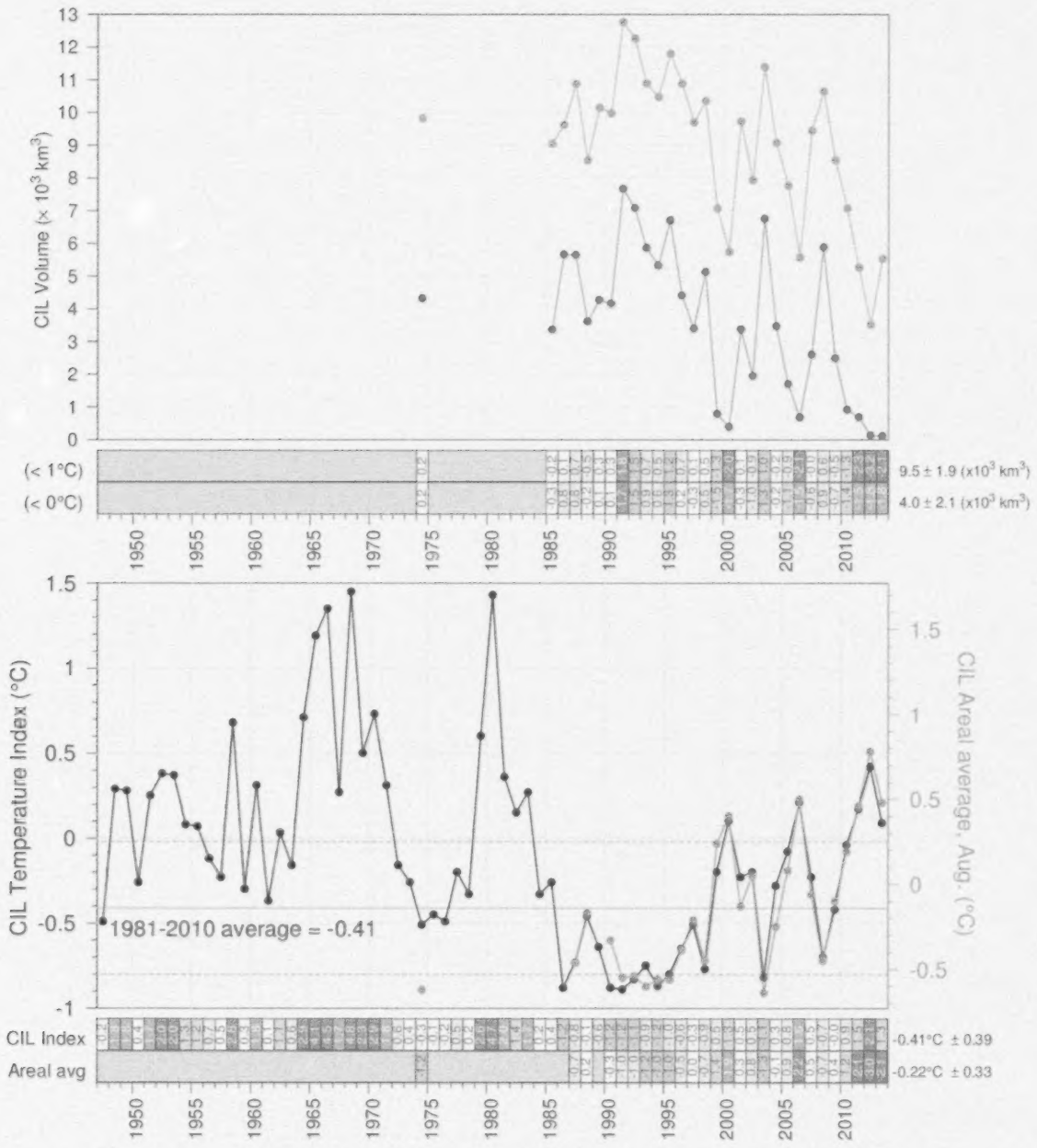

Fig. 41. CIL volume (top panel) delimited by 0°C (in blue) and 1°C (in red), and minimum temperature index (bottom panel) in the Gulf of St. Lawrence. The volumes are integrals of each of the annual interpolated thickness grids such as those shown in the top panels of Fig. 39 excluding Mécatina Trough and the Strait of Belle Isle. In the lower panel, the black line is the updated Gilbert and Pettigrew (1997) index interpolated to 15 July and the green line is the spatial average of each of the annual interpolated grid such as those shown in the two bottom panels of Fig. 39, excluding Mécatina Trough, the Strait of Belle Isle and the Magdalen Shallows. The numbers in the boxes are normalized anomalies.

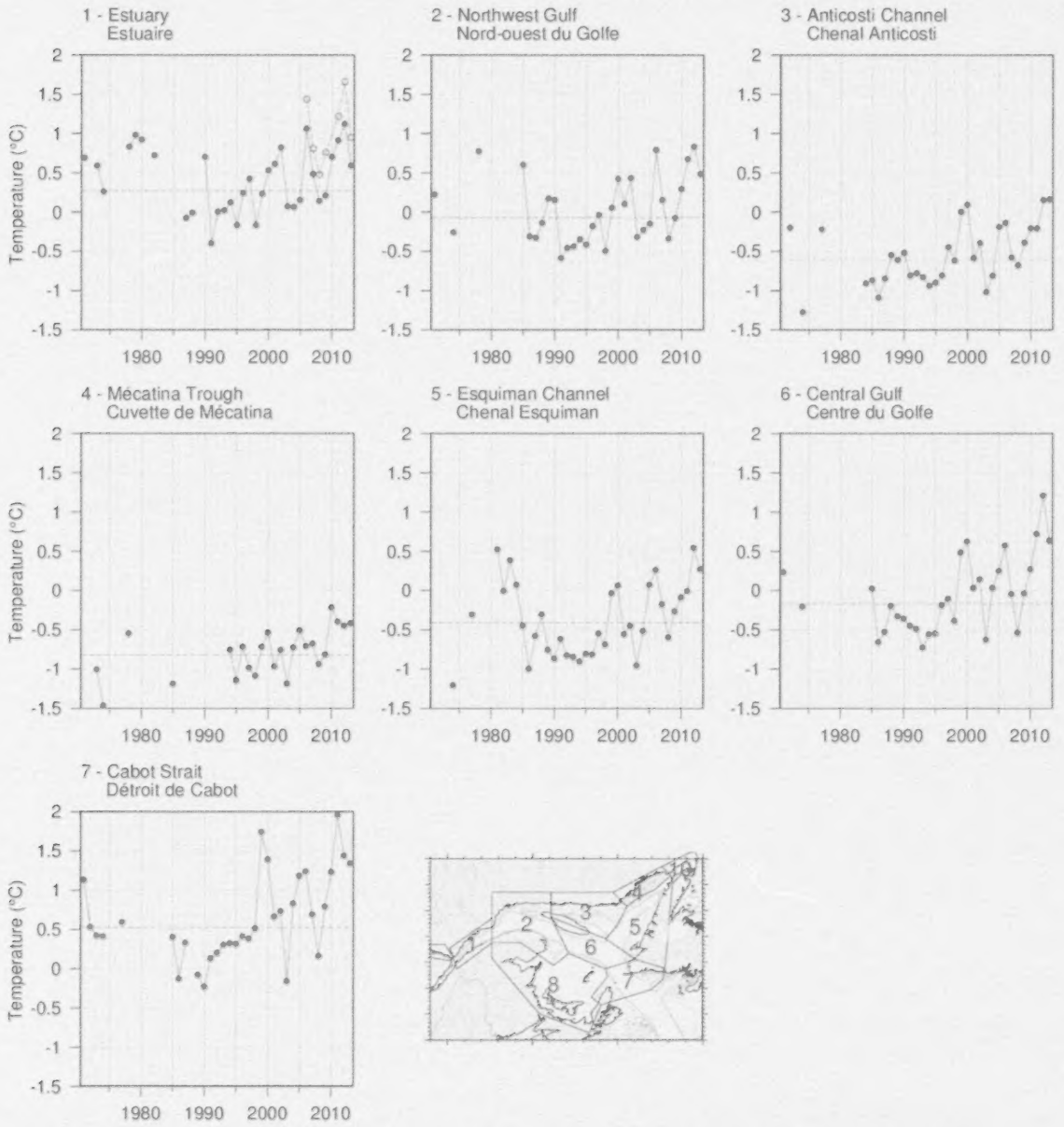

Fig. 42. Temperature minimum of the CIL spatially averaged for the seven areas where the CIL minimum temperature can be clearly identified. The spatial average of the November CIL temperature minimum for available years since 2006 is also shown for the St. Lawrence Estuary (dashed line).

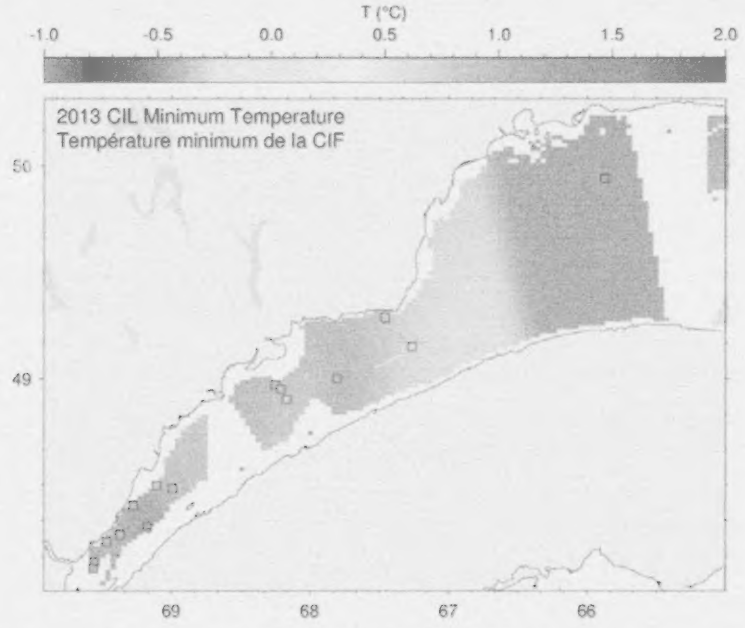

Fig. 43. Cold intermediate layer minimum temperature in November 2013 in the St. Lawrence Estuary.

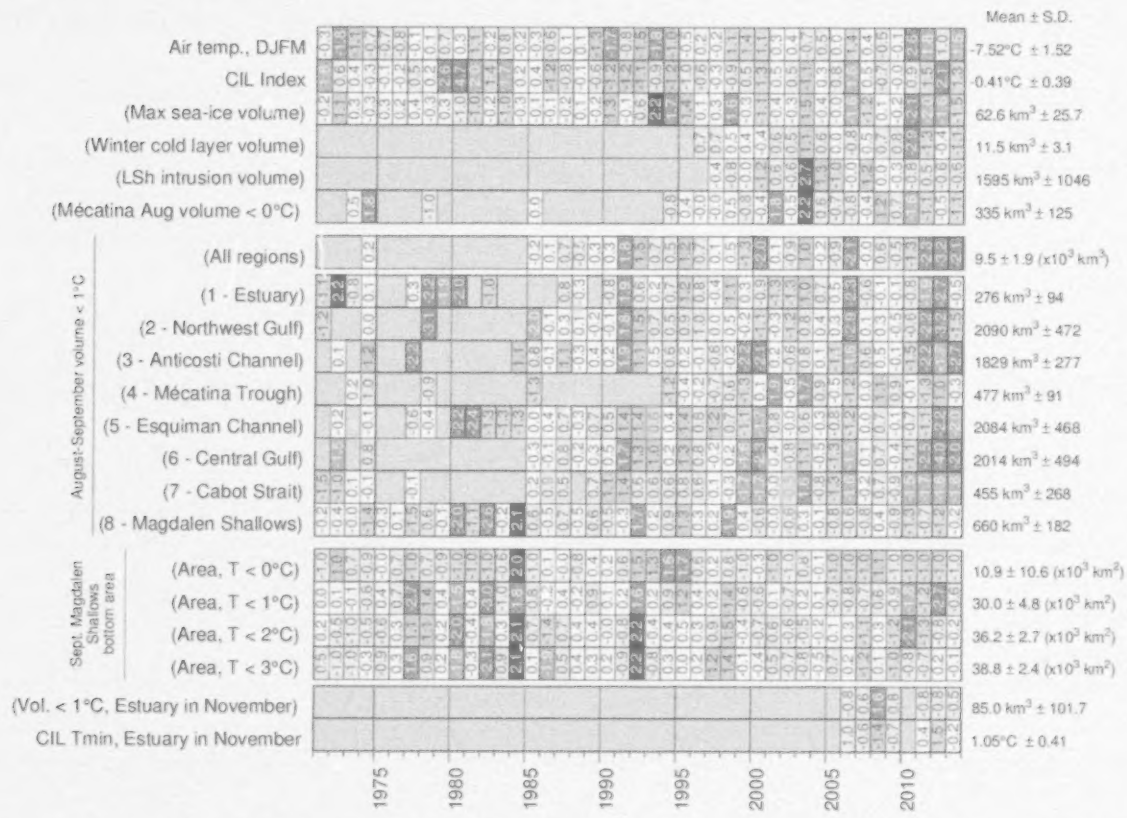

Fig. 44. Winter and summertime CIL related properties. The top block shows the scorecard time series for Dec-Jan-Feb-March air temperature (Fig. 5), the Gilbert and Pettigrew (1997) CIL index, yearly maximum sea-ice volume within the Gulf, winter (March) cold-layer (<-1°C) volume, volume of Labrador Shelf Water intrusion into the Gulf observed in March, and the August–September volume of cold water (<0°C) observed in the Mécatina Trough. Labels in parentheses have their colour coding reversed (blue for high values). The second block shows scorecard time series for August–September CIL volumes (<1°C) for all eight regions and for the entire Gulf when available. The third block shows the scorecard time series for the bottom areas of the Magdalen Shallows covered by waters colder than 0, 1, 2, and 3°C during the September survey. The last block shows the November survey CIL volume (<1°C) and average CIL minimum temperature in the Estuary.

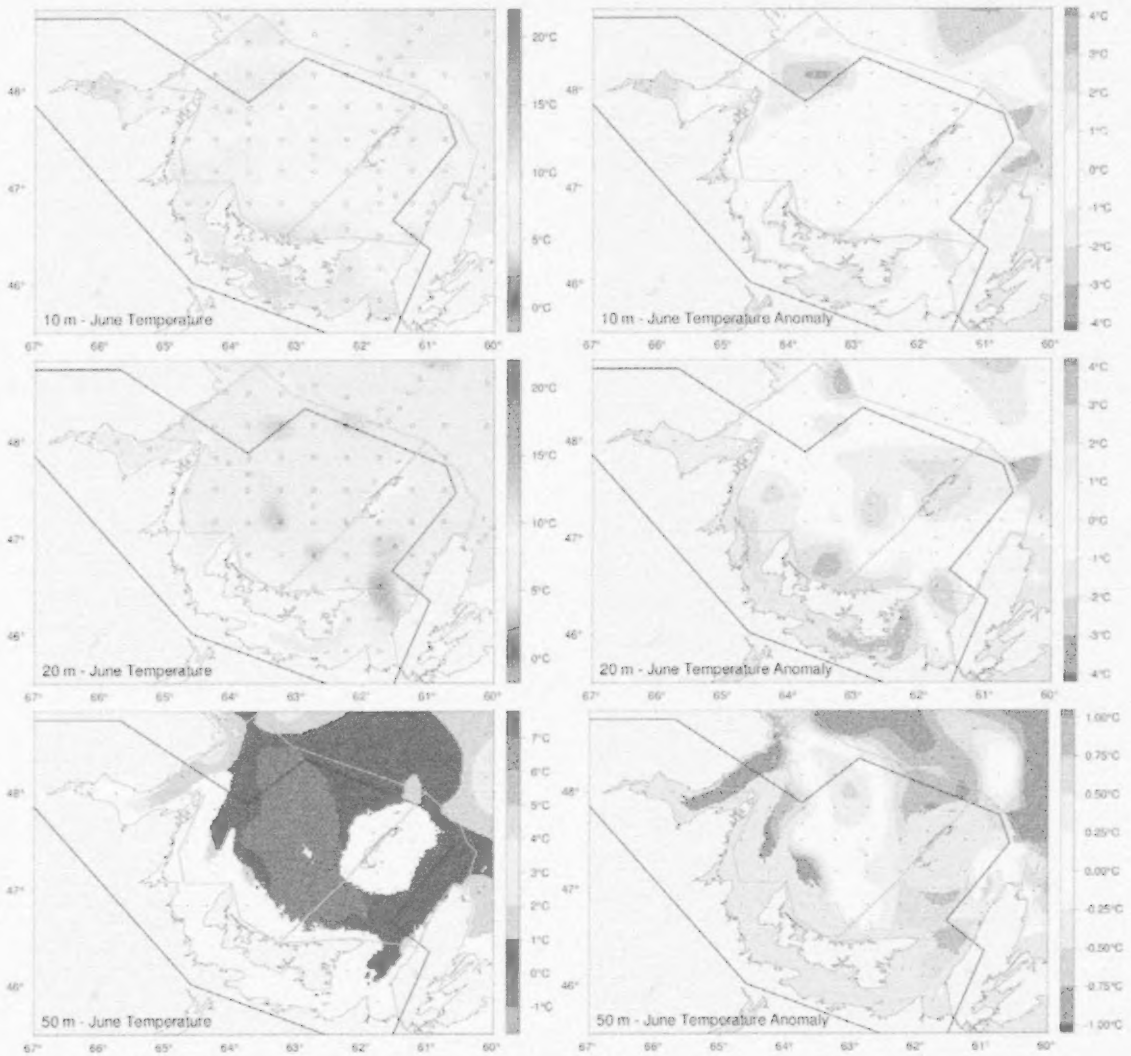

Fig. 45. June depth-layer temperature and anomaly fields on the Magdalen Shallows at 10, 20 and 50 m. Anomalies are based on 1971-2010 climatologies for all available years (appearing on Fig. 46) The black outline delimites Region 8 (Fig. 2) and the gray outlines delimit western and eastern regions of the Magdalen Shallows (Fig. 21).

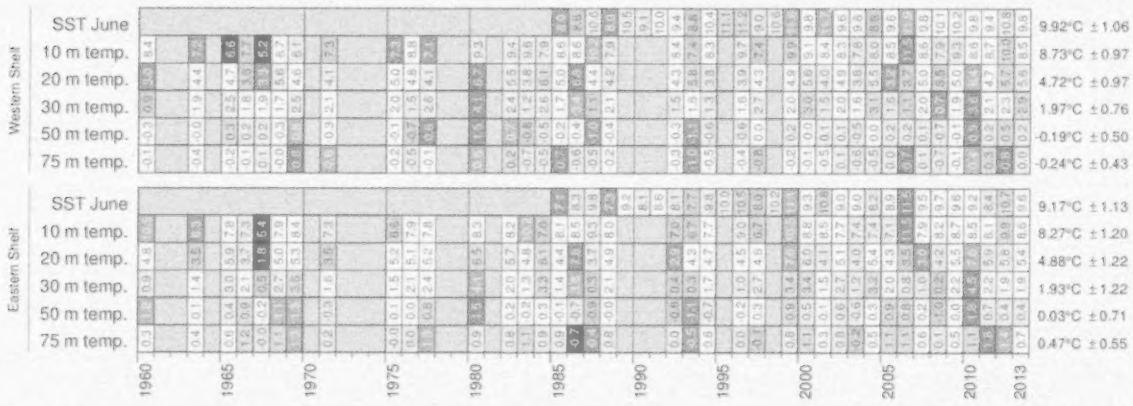

Fig. 46. Depth-layer average temperature anomalies for western and eastern Magdalen Shallows for the June mackerel survey. The SST data are June averages from NOAA remote sensing repeated from Fig. 22. The SST colour-coding is based on the 1985-2010 climatology and the numbers are mean temperatures in °C. The colour-coding of the 10 to 75 m lines are according to normalized anomalies based on the 1981-2010 climatologies, but the numbers are mean temperatures in °C.

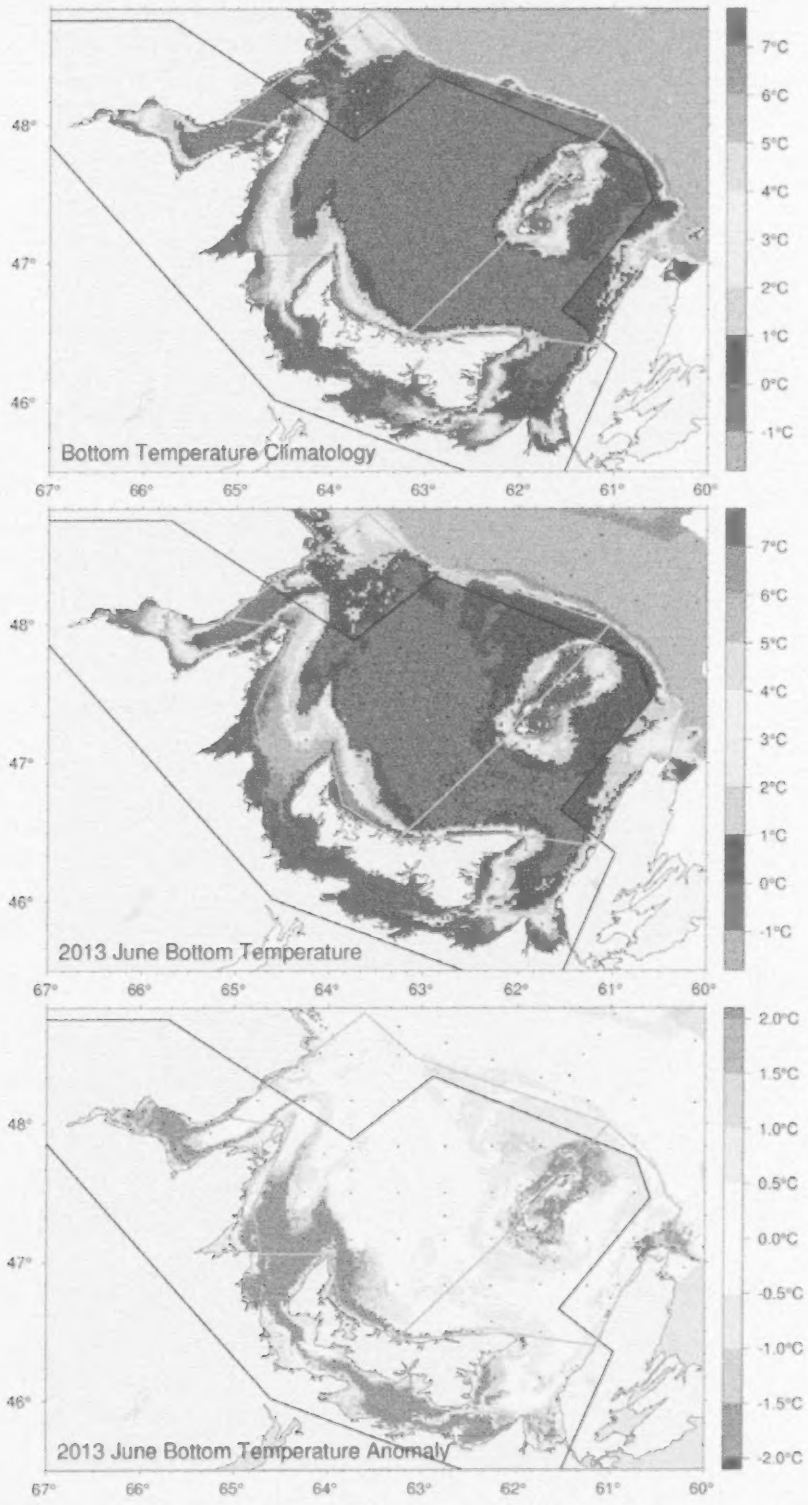

Fig. 47. June bottom temperature climatology (top), 2013 observations (middle) and anomaly (bottom).

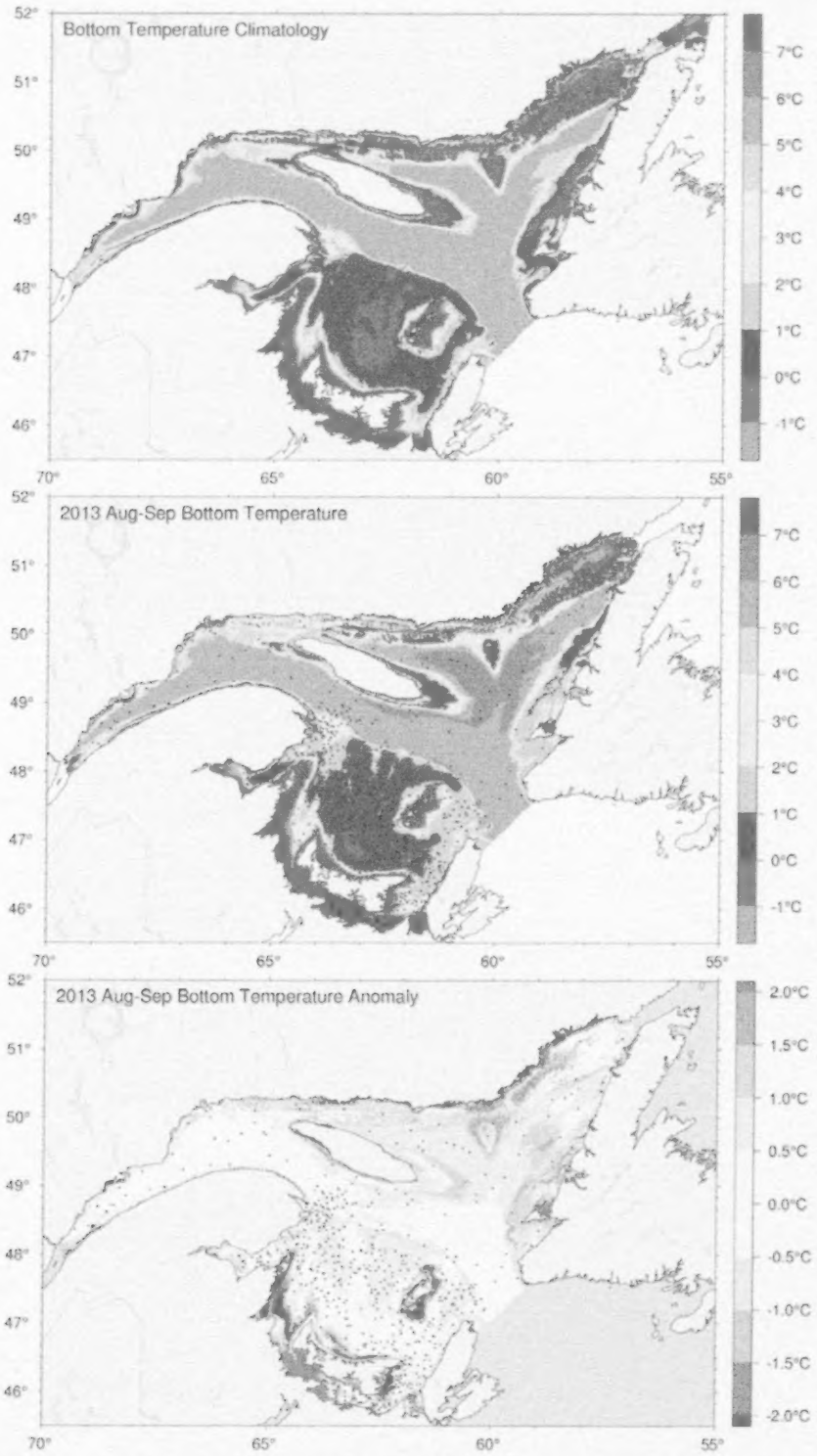

Fig. 48. August-September bottom temperature climatology (top), 2013 observations (middle) and anomaly (bottom).

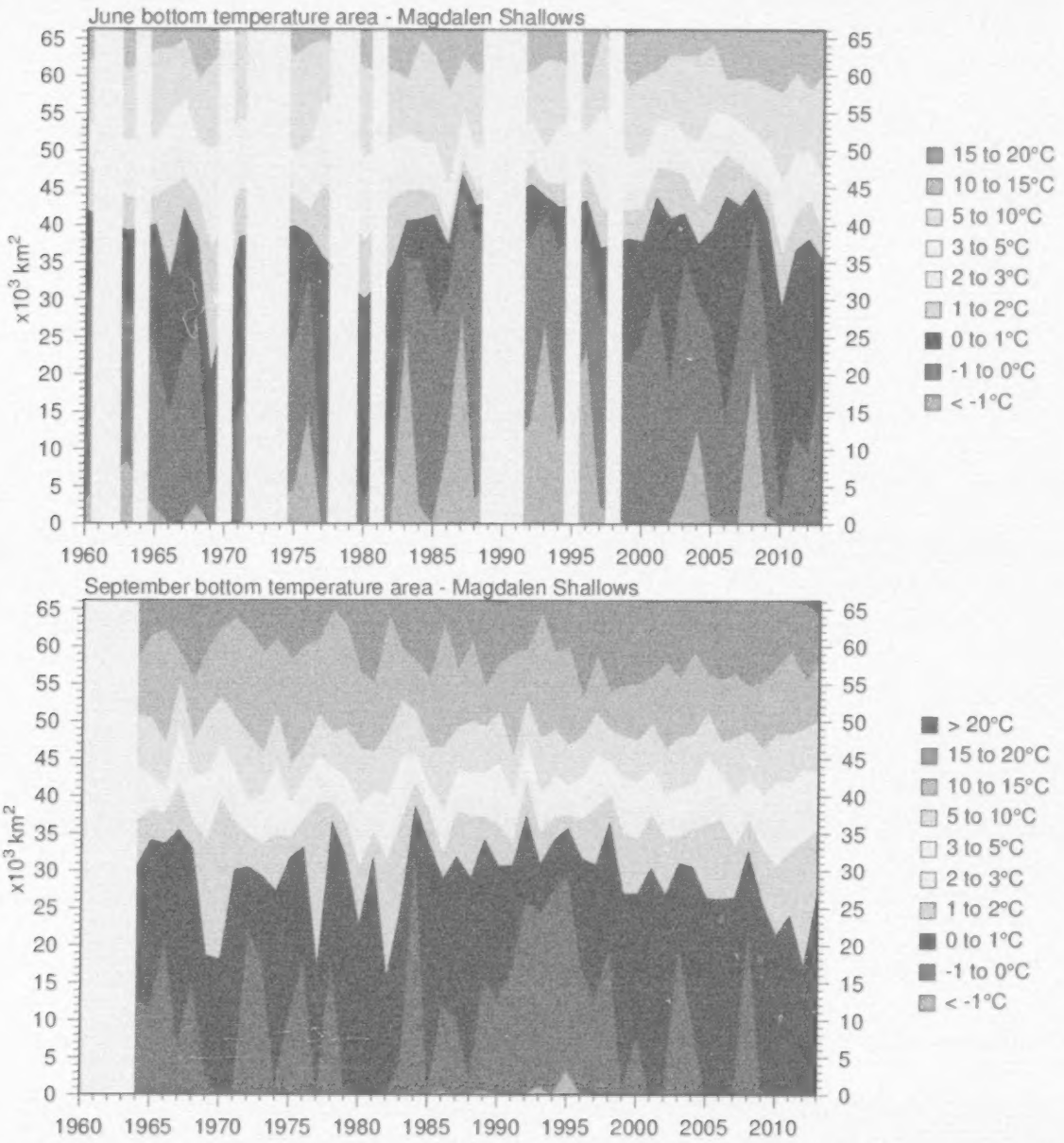

Fig. 49. Time series of the bottom areas covered by different temperature bins in June (top) and August-September (bottom) for the Magdalen Shallows (region 8). Data are majoritarily from September for the bottom panel.

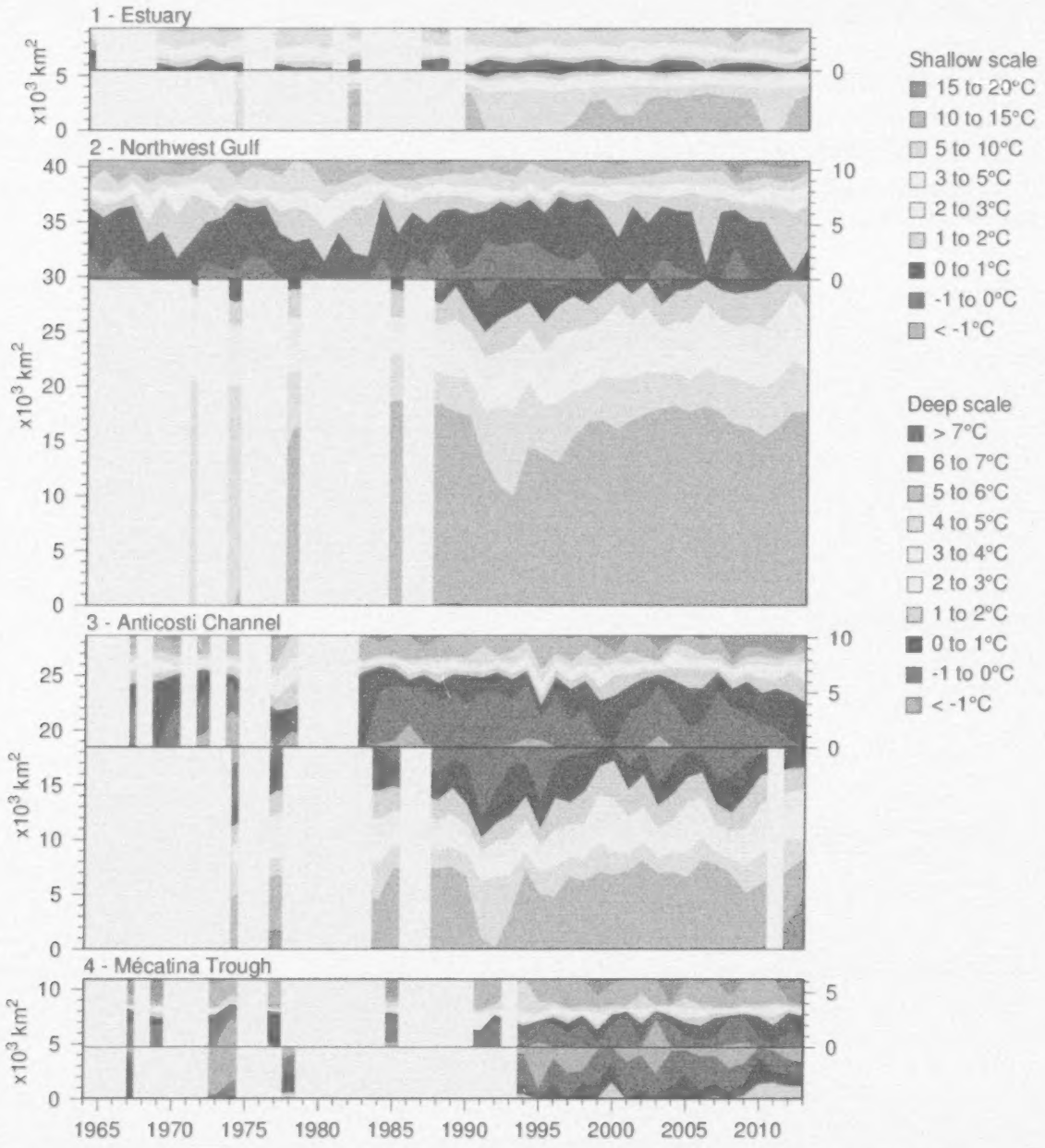

Fig. 50. Time series of the bottom areas covered by different temperature bins in August and September for regions 1 to 4. The panels are separated by a black horizontal line into shallow (<100m) and deep (>100 m) areas to distinguish between warmer waters above and below the CIL. The shallow areas are shown on top using the area scale on the right-hand side and have warmer waters shown starting from the top end. The deep areas are shown below the horizontal line and have warmer waters starting at the bottom end. The CIL areas above and below 100 m meet near the horizontal line.

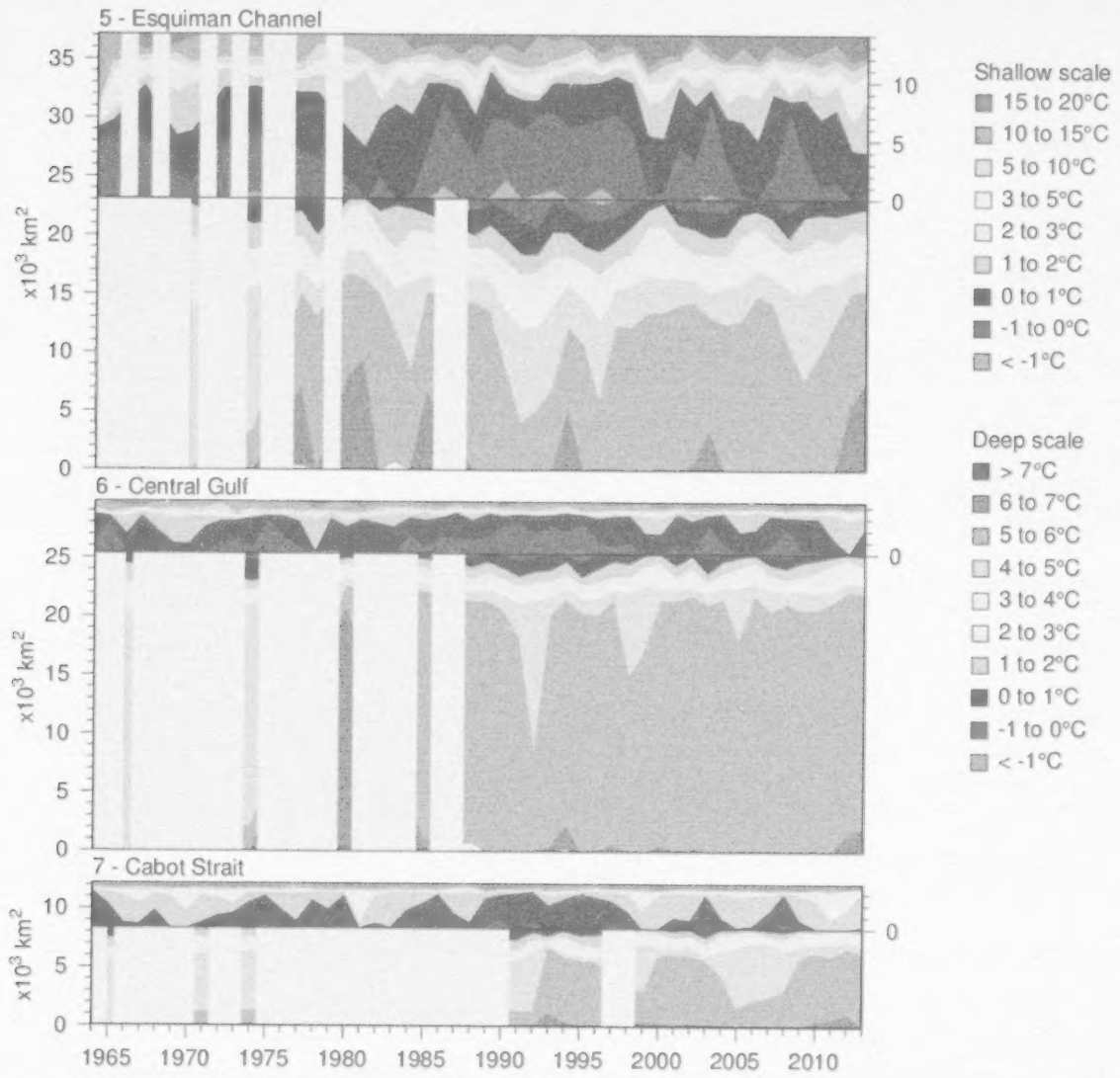

Fig. 51. Time series of the bottom areas covered by different temperature bins in August and September for regions 5 to 7. The panels are separated into shallow (<100 m) and deep (>100 m) areas to distinguish between warmer waters above and below the CIL See Fig. 50 caption.

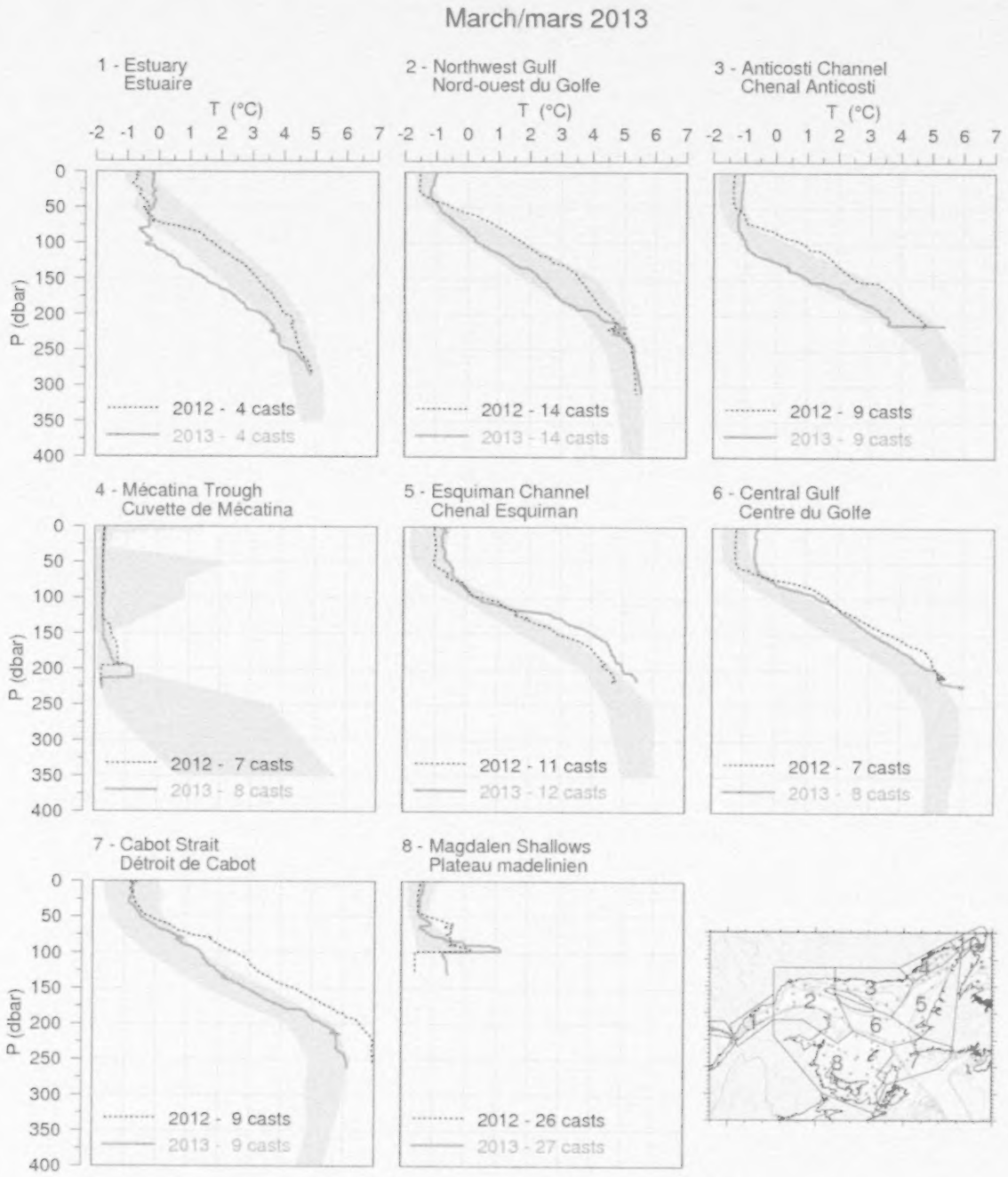

Fig. 52. Mean temperature profiles observed in each region of the Gulf during the March helicopter survey. The shaded area represents the 1981–2010 (but mostly 1996–2010) climatological monthly mean ± 1 SD. Mean profiles for 2012 are also shown for comparison.

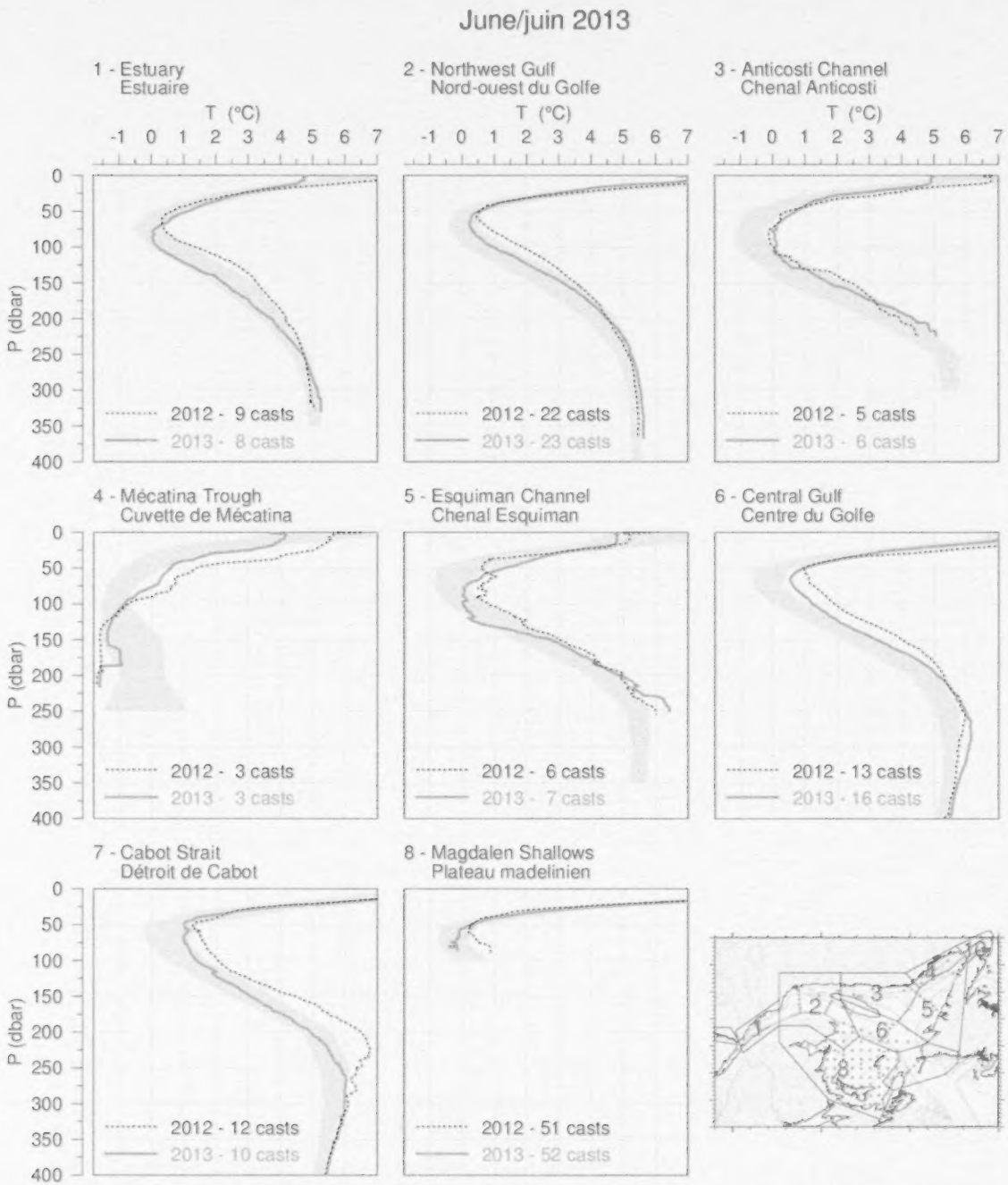

Fig. 53. Mean temperature profiles observed in each region of the Gulf during June. The shaded area represents the 1981–2010 climatological monthly mean ± 1 SD. Mean profiles for 2012 are also shown for comparison.

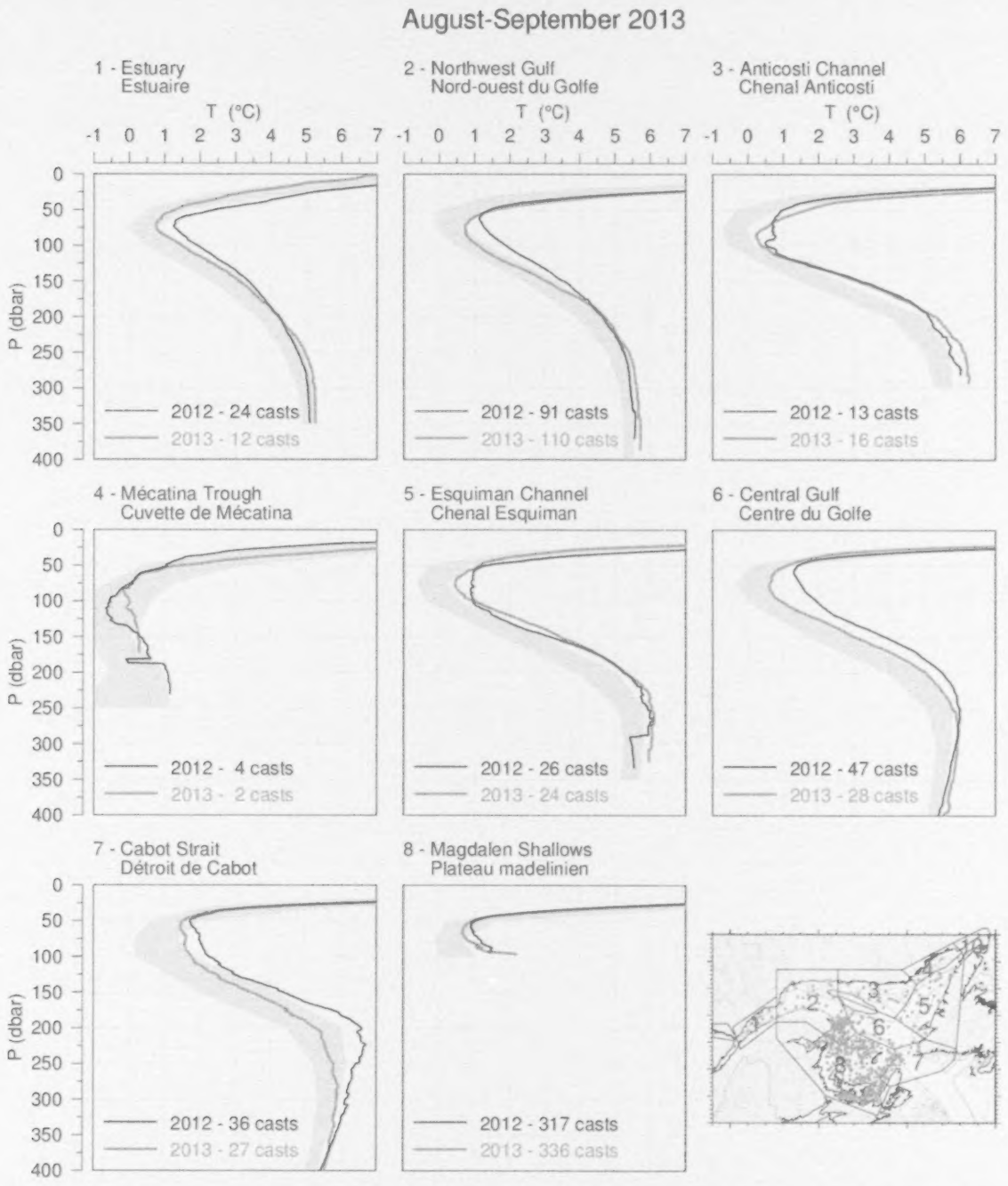

Fig. 54. Mean temperature profiles observed in each region of the Gulf during August and September. The shaded area represents the 1981–2010 climatological monthly mean ± 1 SD for August for regions 1 through 7 and for September for region 8. Mean profiles for 2012 are also shown for comparison.

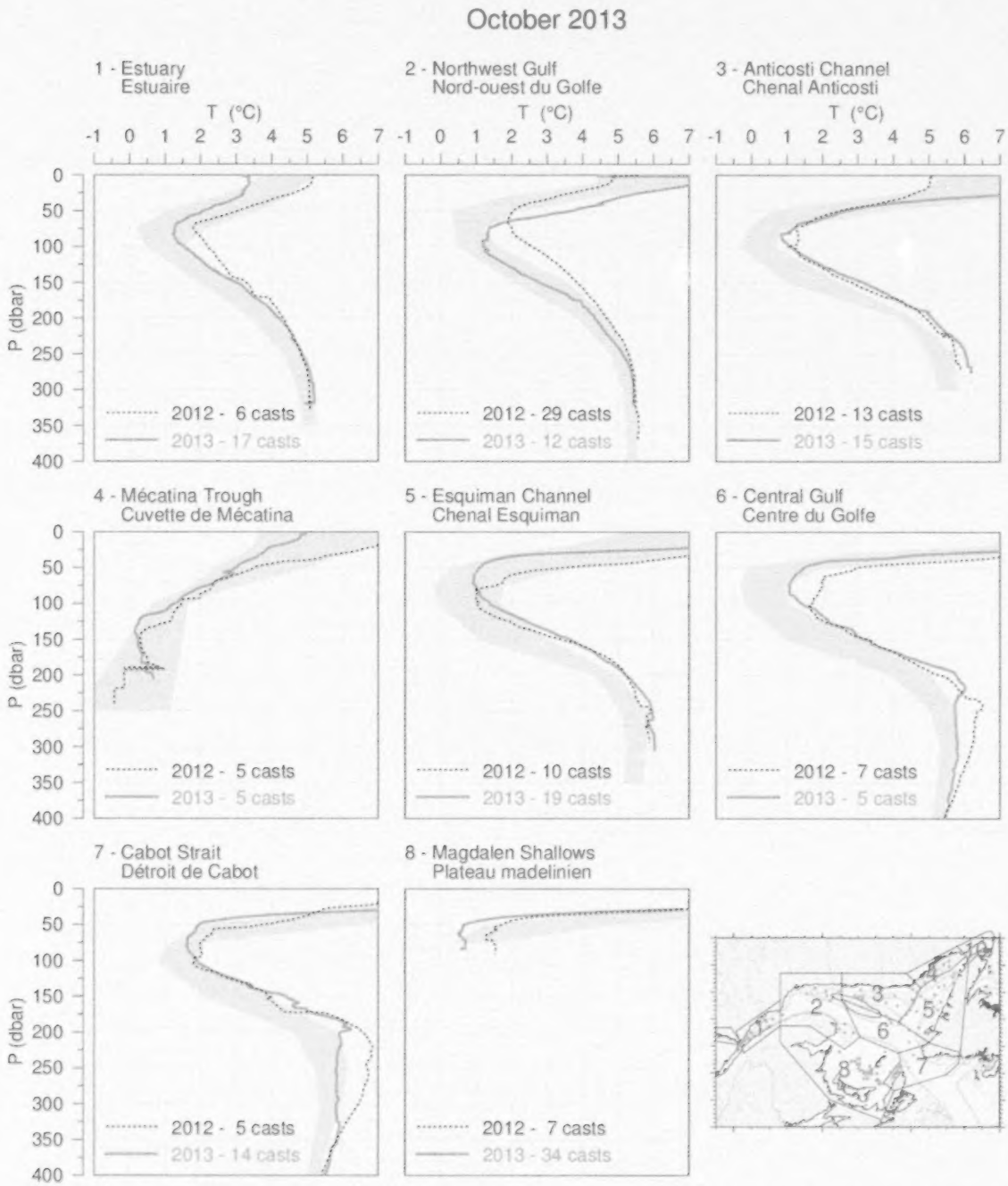

Fig. 55. Mean temperature profiles observed in each region of the Gulf during the October AZMP survey. The shaded area represents the 1981–2010 climatological monthly mean ± 1 SD. Mean profiles for 2012 are also shown for comparison.

1 - Estuary / Estuaire

	2012				2013			
	Mar	June	Aug	Nov	Mar	June	Aug	Oct
0 m	-0.64	8.3	10.6	4.4	-0.29	4.7	6.7	3.4
10 m	-0.69	6.5	8.6	4.3	-0.30	4.6	5.6	3.4
20 m	-0.77	4.0	6.3	4.1	-0.35	3.4	4.1	3.2
30 m	-0.59	2.8	4.1	3.8	-0.28	2.4	2.8	3.1
50 m	-0.30	1.2	2.5	3.2	-0.29	1.1	1.3	2.1
75 m	0.3	0.7	1.3	2.2	-0.44	0.1	0.8	1.3
100 m	1.7	1.3	1.8	2.0	-0.47	0.2	1.5	1.5
150 m	3.1	3.1	3.3	2.9	1.5	2.2	3.1	3.0
200 m	4.0	4.1	4.2	3.9	3.3	3.7	4.2	4.2
250 m	4.5	4.7	4.7	4.7	4.2	4.7	5.0	4.9
300 m	4.9	4.9	5.1	5.0	4.8	5.1	5.2	5.1
350 m		5.1	5.1	5.1		5.2	5.3	

2 - Northwest Gulf / Nord-ouest du Golfe

	2012				2013			
	Mar	June	Aug	Oct	Mar	June	Aug	Nov
0 m	-1.51	10.2	15.2	4.9	-0.99	7.6	14.3	4.9
10 m	-1.51	7.7	13.5	4.8	-1.06	6.4	12.7	4.9
20 m	-1.53	4.5	8.1	4.1	-1.11	3.7	3.2	4.5
30 m	-1.49	2.4	4.3	3.3	-1.20	2.2	4.6	3.8
50 m	-0.48	0.6	1.4	2.0	-0.90	0.5	1.5	2.0
75 m	0.9	0.9	1.3	2.0	-0.25	0.3	0.7	1.3
100 m	1.8	1.8	1.8	2.6	0.4	0.9	1.1	1.4
150 m	3.6	3.5	3.5	3.8	2.3	3.1	3.0	3.1
200 m	4.4	4.5	4.6	4.7	3.8	4.5	4.7	4.7
250 m	5.2	5.1	5.2	5.3	5.3	5.2	5.4	5.4
300 m	5.4	5.4	5.4	5.5	5.5	5.5	5.6	5.6
350 m		5.4	5.5	5.5		5.6	5.7	5.7
400 m							5.7	5.8

3 - Anticosti Channel / Chenal Anticosti

	2012				2013			
	Mar	June	Aug	Oct	Mar	June	Aug	Oct
0 m	-1.32	6.8	17.5	5.0	-1.05	4.9	14.1	8.8
10 m	-1.35	6.7	14.6	5.0	-1.05	4.9	13.6	8.7
20 m	-1.36	4.3	6.3	4.9	-1.07	3.5	8.9	8.5
30 m	-1.37	2.7	3.0	4.4	-1.09	1.7	4.6	6.2
50 m	-1.25	0.5	1.0	2.5	-1.12	0.7	1.6	2.6
75 m	-0.70	-0.1	0.7	1.5	-1.21	0.1	0.4	1.2
100 m	0.9	0.0	0.7	1.2	-0.98	0.1	0.4	1.1
150 m	2.6	2.4	2.1	2.8	1.0	1.8	3.1	3.2
200 m	4.4	3.6	5.1	4.9	3.5	4.4	5.8	5.2
250 m			5.7	5.7			6.1	6.0

4 - Mécatina Trough / Cuvette de Mécatina

	2012				2013			
	Mar	June	Aug	Oct	Mar	June	Aug	Oct
0 m	-1.68	5.7	16.4	7.6	-1.68	4.1	16.1	4.8
10 m	-1.69	5.6	12.4	7.5	-1.70	4.0	15.5	4.7
20 m	-1.69	5.2	5.7	6.9	-1.72	3.6	11.1	4.0
30 m	-1.71	4.3	2.8	6.0	-1.73	1.8	5.8	3.7
50 m	-1.73	1.4	1.1	3.5	-1.74	0.6	1.5	3.0
75 m	-1.73	0.6	0.1	2.3	-1.73	0.1	0.0	2.2
100 m	-1.73	-0.7	-0.5	1.5	-1.69	-0.8	0.0	1.3
150 m	-1.45	-1.6	0.3	0.3	-1.71	-1.4	0.2	0.2
200 m	-1.26	-1.6	1.1	1.0	-1.27	-1.5		-0.5

5 - Esquiman Channel / Chenal Esquiman

	2012				2013			
	Mar	June	Aug	Oct	Mar	June	Aug	Oct
0 m	-0.82	5.2	18.5	9.2	-0.68	4.8	16.4	8.7
10 m	-0.94	5.2	17.7	9.2	-0.64	4.8	15.9	8.7
20 m	-0.91	4.6	13.8	8.6	-0.77	4.4	8.2	7.4
30 m	-0.98	2.7	6.1	7.4	-0.72	2.9	3.4	3.0
50 m	-0.98	0.6	1.4	3.4	-0.55	1.6	1.1	1.1
75 m	-0.41	0.6	0.9	1.6	-0.27	0.1	0.5	1.0
100 m	0.4	0.8	0.9	1.0	0.3	0.0	1.1	1.4
150 m	2.9	3.0	3.1	3.4	4.1	2.7	3.4	3.6
200 m	4.6	4.9	5.2	5.2	5.0	4.9	5.3	5.2
250 m		5.0	5.8	5.7		6.4	6.0	5.9
300 m			6.0	5.9			6.0	6.0

6 - Central Gulf / Centre du Golfe

	2012				2013			
	Mar	June	Aug	Oct	Mar	June	Aug	Nov
0 m	-1.08	9.7	19.0	8.8	-0.56	7.2	15.1	6.6
10 m	-1.07	8.9	17.3	8.8	-0.66	6.9	14.3	6.6
20 m	-1.08	6.7	9.8	8.2	-0.60	5.0	8.9	6.6
30 m	-1.20	4.1	4.8	7.6	-0.65	3.2	3.3	6.0
50 m	-1.22	1.0	1.4	2.9	-0.61	1.0	1.2	1.4
75 m	-0.4	1.3	1.5	2.0	-0.10	0.7	0.6	1.0
100 m	1.8	1.9	2.0	1.7	1.4	1.5	0.8	1.2
150 m	3.8	4.0	4.0	3.3	3.2	3.2	3.0	3.5
200 m	5.1	5.3	5.5	5.3	4.9	5.2	5.0	5.3
250 m		5.9	6.1	6.4		6.0	5.9	5.9
300 m		5.8	5.9	6.2		6.1	6.0	5.9
350 m		5.6	5.7	5.9		5.8	5.8	5.7
400 m		5.5	5.4	5.4		5.6	5.6	5.6
450 m		5.3	5.3	5.4		5.5	5.4	5.4

7 - Cabot Strait / Détroit de Cabot

	2012				2013			
	Mar	June	Aug	Nov	Mar	June	Aug	Nov
0 m	-0.73	9.1	19.4	9.9	-0.70	8.3	17.2	7.2
10 m	-0.77	8.3	14.9	9.9	-0.74	7.7	15.6	7.1
20 m	-0.70	5.6	6.2	9.7	-0.77	5.4	5.8	6.8
30 m	-0.63	2.8	3.3	7.7	-0.84	2.8	4.1	6.0
50 m	-0.19	1.3	2.2	4.2	-0.46	1.0	2.4	3.0
75 m	1.1	1.5	1.6	2.3	0.6	1.0	1.6	1.7
100 m	2.5	2.1	1.9	1.9	1.4	1.4	1.8	1.6
150 m	4.4	4.5	4.3	3.6	2.9	3.1	3.1	3.6
200 m	6.3	6.5	6.5	6.2	5.2	4.9	5.4	6.1
250 m	6.9	6.5	6.7	6.6	6.1	5.8	5.8	6.2
300 m		6.1	6.3	6.4		6.0	5.8	5.9
350 m		5.8	5.8	5.7		5.7	5.7	5.7
400 m		5.4	5.5	5.4		5.4	5.5	5.4
450 m		5.2	5.3	5.1		5.4	5.4	5.1
500 m			5.2				5.4	

8 - Magdalen Shallows / Plateau madelinien

	2012				2013			
	Mar	June	Sep	Nov	Mar	June	Sep	Oct
0 m	-1.35	11.2	16.5	8.2	-1.28	9.9	14.9	12.2
10 m	-1.43	10.1	16.3	9.1	-1.32	9.1	14.6	12.2
20 m	-1.48	5.9	12.0	8.5	-1.37	6.6	11.5	11.4
30 m	-1.49	2.4	5.5	7.1	-1.43	3.2	5.5	5.3
50 m	-1.14	0.4	1.3	2.6	-1.38	0.3	1.0	0.7
75 m	-0.29	0.5	1.0	1.8	-1.08	-0.2	0.9	0.7
100 m	0.2	0.9	1.4		1.1		1.1	

Fig. 56. Depth-layer monthly average temperature summary for months during which the eight Gulf-wide oceanographic surveys took place in 2012 and 2013. The colour-coding is according to the temperature anomaly relative to the monthly 1981–2010 climatology of each region.

1 - Estuary / Estuaire

	2012				2013			
	Mar	June	Aug	Nov	Mar	June	Aug	Oct
Strat.	3.66	4.9	3.5	1.9	1.02	4.7	2.9	2.8
0 m	27.0	25.8	28.2	28.7	29.9	25.1	28.7	28.6
10 m	28.4	26.9	28.7	28.8	30.0	26.3	29.2	28.9
20 m	29.5	28.3	29.5	29.3	30.3	28.9	29.9	29.7
30 m	30.4	29.6	30.2	29.9	30.5	28.3	30.6	30.8
50 m	31.6	31.1	31.4	31.0	31.1	30.6	31.7	31.9
75 m	32.2	31.9	32.3	32.0	31.7	31.8	32.4	32.4
100 m	32.8	32.5	32.8	32.6	32.4	32.3	32.8	32.8
150 m	33.5	33.6	33.6	33.4	32.9	33.2	33.5	33.5
200 m	34.0	34.1	34.0	33.9	33.5	33.8	34.0	34.0
250 m	34.2	34.3	34.3	34.3	34.0	34.2	34.3	34.3
300 m	34.4	34.5	34.5	34.4	34.3	34.5	34.5	34.5
350 m		34.5	34.5	34.5		34.5	34.5	

2 - Northwest Gulf / Nord-ouest du Golfe

	2012				2013			
	Mar	June	Aug	Oct	Mar	June	Aug	Nov
Strat.	0.57	4.1	4.8	1.7	0.54	3.0	4.1	1.2
0 m	31.3	27.9	28.4	30.4	31.3	28.8	28.7	30.8
10 m	31.3	28.7	29.0	30.5	31.4	29.4	29.2	30.8
20 m	31.6	30.2	30.2	31.1	31.5	30.4	30.2	31.0
30 m	31.6	31.0	31.0	31.6	31.6	31.0	30.9	31.3
50 m	32.1	31.8	31.8	32.2	32.0	31.8	31.7	31.9
75 m	32.5	32.4	32.3	32.7	32.3	32.2	32.2	32.3
100 m	32.9	32.8	32.8	33.1	32.6	32.6	32.6	32.7
150 m	33.7	33.6	33.6	33.8	33.3	33.5	33.4	33.5
200 m	34.1	34.1	34.1	34.2	33.8	34.0	34.1	34.1
250 m	34.6	34.5	34.5	34.5	34.4	34.4	34.5	34.5
300 m	34.7	34.7	34.7	34.7	34.6	34.6	34.6	34.7
350 m		34.7	34.7	34.7		34.7	34.7	34.7
400 m							34.8	34.8

3 - Anticosti Channel / Chenal Anticosti

	2012				2013			
	Mar	June	Aug	Oct	Mar	June	Aug	Oct
Strat.	0.08	1.5	3.9	0.9	0.03	1.7	2.8	1.6
0 m	31.7	30.6	30.2	31.1	32.0	30.2	30.5	30.8
10 m	31.7	30.6	30.5	31.2	32.0	30.3	30.6	30.8
20 m	31.8	31.0	31.3	31.4	32.0	31.3	31.1	30.9
30 m	31.8	31.4	31.6	31.5	32.0	31.6	31.5	31.2
50 m	31.8	31.7	31.9	31.9	32.0	31.9	31.8	31.9
75 m	32.0	32.1	32.4	32.3	32.0	32.1	32.1	32.2
100 m	32.5	32.4	32.7	32.7	32.1	32.4	32.5	32.6
150 m	33.3	33.2	33.4	33.4	32.8	33.0	33.4	33.5
200 m	34.0	33.7	34.2	34.1	33.5	33.9	34.2	34.2
250 m			34.5	34.6			34.6	34.6

4 - Mécatina Trough / Cuvette de Mécatina

	2012				2013			
	Mar	June	Aug	Oct	Mar	June	Aug	Oct
Strat.	0.23	1.0	3.7	1.0	0.21	1.7	3.0	0.7
0 m	32.0	30.7	30.1	31.1	32.2	30.1	30.9	30.9
10 m	32.0	30.7	30.6	31.1	32.3	30.1	30.9	31.0
20 m	32.1	30.8	31.4	31.2	32.3	31.3	31.2	31.3
30 m	32.2	30.9	31.7	31.4	32.4	31.5	31.6	31.4
50 m	32.3	31.5	32.0	31.8	32.5	31.9	32.0	31.6
75 m	32.4	31.9	32.3	32.1	32.5	32.1	32.3	31.8
100 m	32.6	32.4	32.6	32.2	32.6	32.4	32.5	32.1
150 m	32.8	32.7	32.9	32.7	32.6	32.5	32.8	32.5
200 m	32.9	32.8	33.1	33.0	32.7	32.6		32.6

5 - Esquiman Channel / Chenal Esquiman

	2012				2013			
	Mar	June	Aug	Oct	Mar	June	Aug	Oct
Strat.	0.19	0.9	3.7	1.4	0.22	0.5	3.2	1.8
0 m	31.5	31.3	30.6	30.9	31.9	31.6	30.8	31.0
10 m	31.6	31.3	30.7	30.9	31.9	31.6	30.9	31.0
20 m	31.7	31.4	31.1	31.0	31.9	31.6	31.5	31.3
30 m	31.7	31.6	31.4	31.2	32.0	31.7	31.7	31.9
50 m	31.8	31.9	31.8	31.8	32.2	31.9	32.0	32.2
75 m	32.0	32.4	32.3	32.3	32.3	32.2	32.4	32.5
100 m	32.4	32.7	32.6	32.6	32.5	32.5	32.7	32.8
150 m	33.3	33.4	33.4	33.5	33.7	33.3	33.5	33.6
200 m	34.0	34.1	34.2	34.2	34.1	34.0	34.2	34.2
250 m		34.6	34.5	34.5		34.6	34.5	34.5
300 m			34.7	34.6			34.6	34.5

6 - Central Gulf / Centre du Golfe

	2012				2013			
	Mar	June	Aug	Oct	Mar	June	Aug	Nov
Strat.	0.08	1.9	4.4	1.5	0.18	1.1	3.1	1.3
0 m	31.5	30.7	29.9	30.9	31.7	31.3	30.6	31.1
10 m	31.5	30.8	30.1	30.9	31.7	31.3	30.7	31.1
20 m	31.5	31.1	30.8	31.0	31.8	31.5	31.2	31.1
30 m	31.5	31.4	31.4	31.1	31.8	31.6	31.7	31.2
50 m	31.6	31.9	31.9	31.9	31.9	31.9	32.0	32.1
75 m	32.0	32.3	32.4	32.4	32.1	32.4	32.3	32.4
100 m	32.6	32.8	32.8	32.7	32.7	32.7	32.6	32.7
150 m	33.6	33.7	33.7	33.4	33.4	33.4	33.4	33.5
200 m	34.3	34.2	34.3	34.2	34.0	34.1	34.1	34.2
250 m		34.6	34.6	34.6		34.6	34.5	34.6
300 m		34.7	34.8	34.8		34.7	34.7	34.7
350 m		34.8	34.8	34.8		34.8	34.8	34.8
400 m		34.9	34.9	34.9		34.9	34.9	34.9
450 m		34.9	34.9	34.9		34.9	34.9	34.9

7 - Cabot Strait / Détroit de Cabot

	2012				2013			
	Mar	June	Aug	Nov	Mar	June	Aug	Nov
Strat.	0.82	1.8	4.0	1.9	0.62	1.6	3.3	1.1
0 m	30.2	30.5	30.7	30.6	30.9	30.5	31.0	31.2
10 m	30.4	30.6	31.0	30.6	31.0	30.7	31.1	31.2
20 m	30.7	30.9	31.4	30.8	31.2	31.0	31.7	31.3
30 m	30.9	31.2	31.7	31.3	31.4	31.3	31.9	31.5
50 m	31.3	31.6	32.1	32.1	31.7	31.7	32.2	32.0
75 m	32.0	32.3	32.4	32.6	32.2	32.1	32.4	32.5
100 m	32.7	32.8	32.8	32.7	32.6	32.5	32.7	32.7
150 m	33.8	33.7	33.6	33.4	33.3	33.4	33.4	33.6
200 m	34.4	34.4	34.4	34.3	34.1	34.1	34.2	34.4
250 m	34.6	34.6	34.7	34.7	34.5	34.5	34.5	34.6
300 m		34.8	34.9	34.8		34.7	34.7	34.7
350 m		34.8	34.9	34.9		34.9	34.8	34.8
400 m		34.9	34.9	34.9		34.9	34.9	34.9
450 m		34.9	34.9	34.9		34.9	34.9	34.9
500 m			34.9				34.9	

8 - Magdalen Shallows / Plateau madelinien

	2012				2013			
	Mar	June	Sep	Nov	Mar	June	Sep	Oct
Strat.	0.57	2.8	4.3	2.2	0.52	2.5	4.1	3.0
0 m	30.1	29.3	28.9	29.5	30.7	29.5	28.7	29.3
10 m	30.1	29.6	29.0	29.6	30.8	29.7	28.8	29.4
20 m	30.2	30.1	29.5	29.9	31.0	30.2	29.4	29.6
30 m	30.3	30.6	30.4	30.3	31.1	30.7	30.4	30.5
50 m	30.6	31.3	31.5	31.4	31.4	31.3	31.5	31.4
75 m	31.5	32.0	32.0	32.0	31.7	31.8	32.2	31.9
100 m	31.9	32.2	32.5		32.6		32.3	

Fig. 57. Depth-layer monthly average stratification and salinity summary for months during whichthe eight Gulf-wide oceanographic surveys took place in 2012 and 2013. Stratification is defined as the density difference between 50 m and the surface and its colour-coding is reversed (blue for positive anomaly).

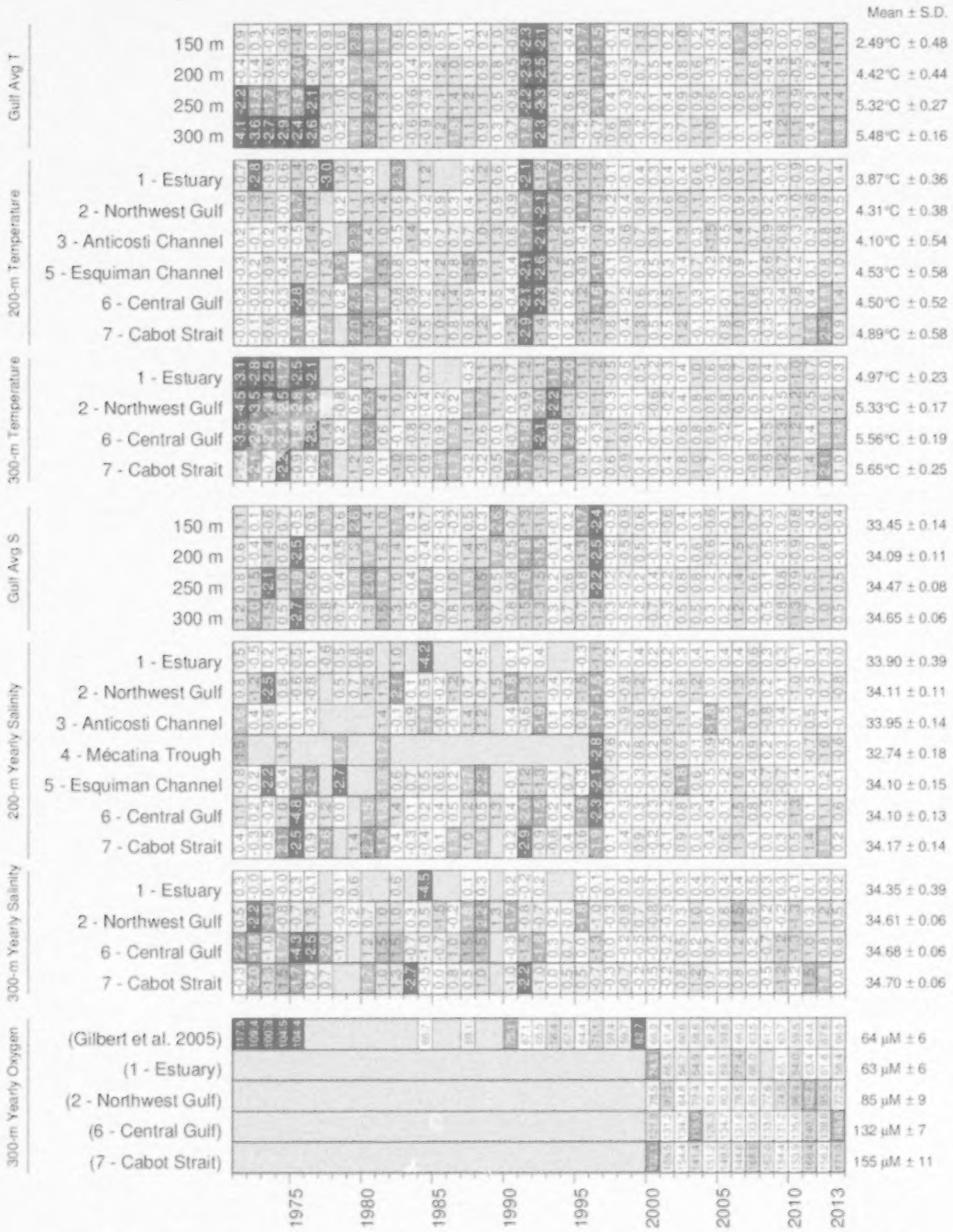

Fig. 58. Deep layer temperature, salinity, and dissolved oxygen. Gulf averages for temperature and salinity are shown for 150, 200, 250, and 300 m, and regional averages are shown for 200 and 300m. Dissolved oxygen is shown with an inverted colour scheme for the updated Gilbert et al. 2005 time series as well as recent regional averages at 300 m obtained using a Seabird SBE43 CTD sensor. The numbers on the right are the 1981–2010 climatological means and standard deviations. The numbers in the boxes are normalized anomalies, except for oxygen where physical values are shown for easier comparison between the Gilbert et al. 2005 time series and the CTD data.

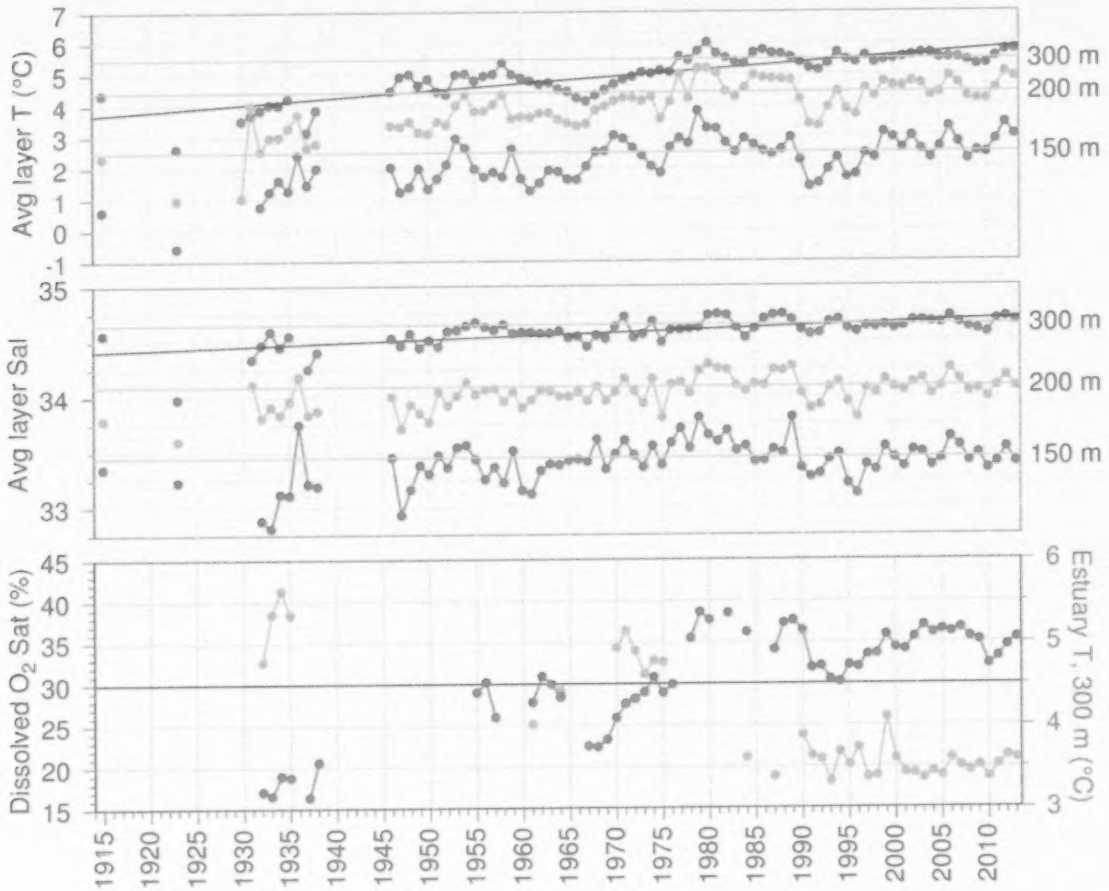

Fig. 59. Layer-averaged temperature and salinity time series for the Gulf of St. Lawrence and dissolved oxygen between 295 m and the bottom in the deep central basin of the St. Lawrence Estuary. The temperature and salinity panels show the 150 m, 200 m, and 300 m annual averages and the horizontal lines are 1981–2010 means. Sloped lines show linear regressions for temperature and salinity at 300 m of respectively 2.2°C and 0.3 per century. The horizontal line in the oxygen panel corresponds roughly to 30% saturation and marks the threshold of hypoxic conditions. In addition to the oxygen percent saturation time series (light blue), the lower panel also shows temperature (dark blue) at 300 m in the Estuary.

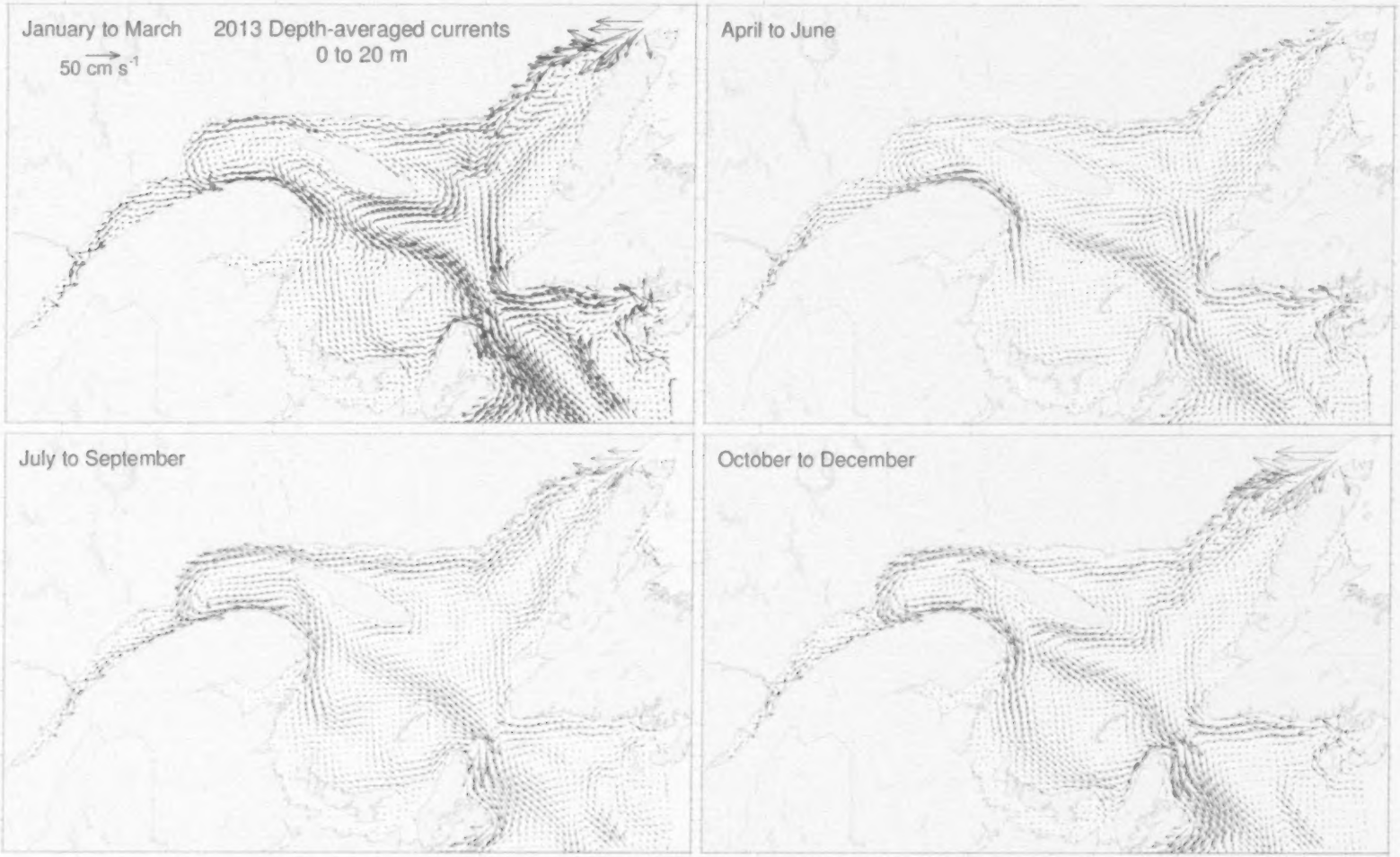

Fig. 60. Depth-averaged currents from 0 to 20 m for each three-month period of 2013.

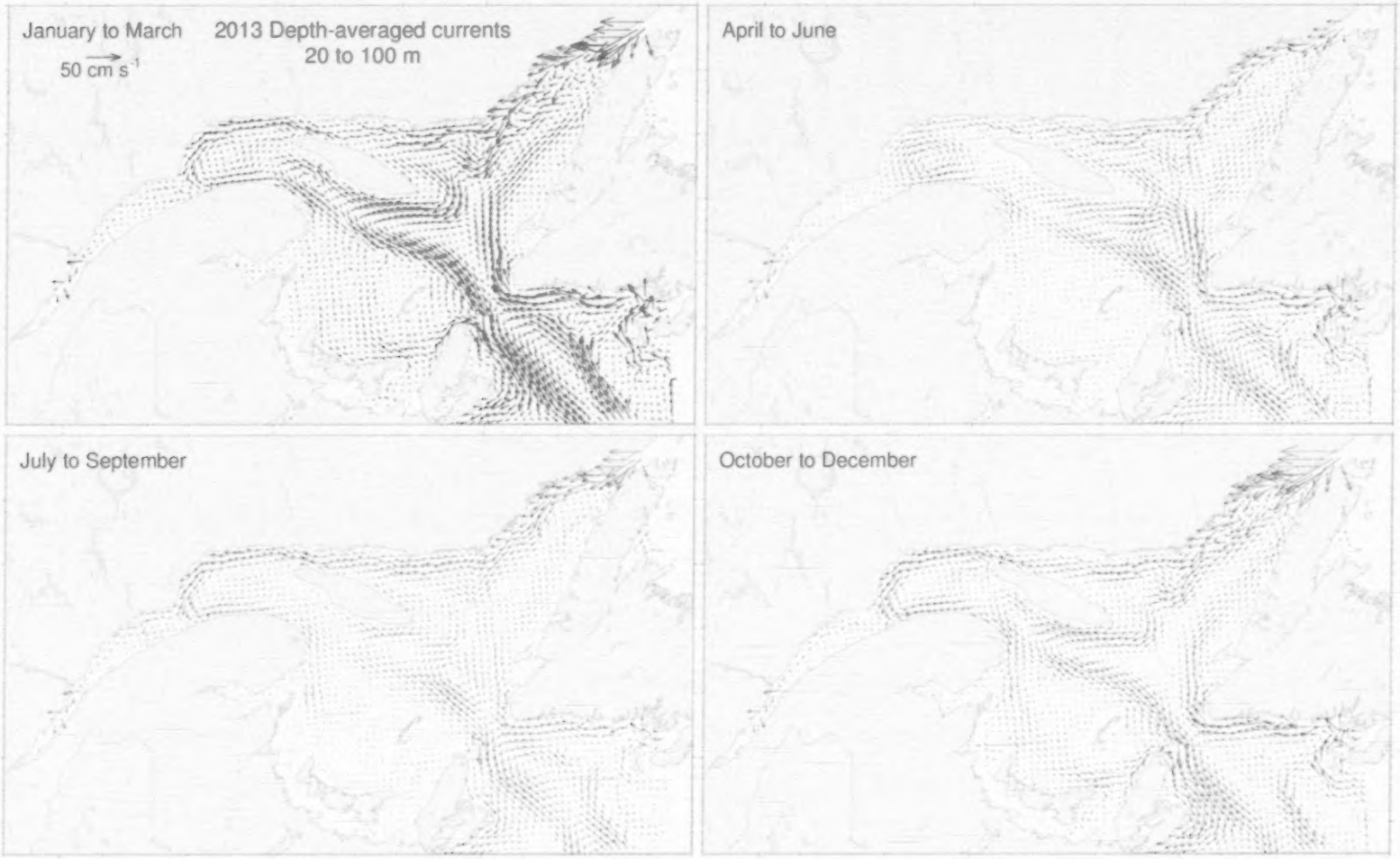

Fig. 61. Depth-averaged currents from 20 to 100 m for each three-month period of 2013.

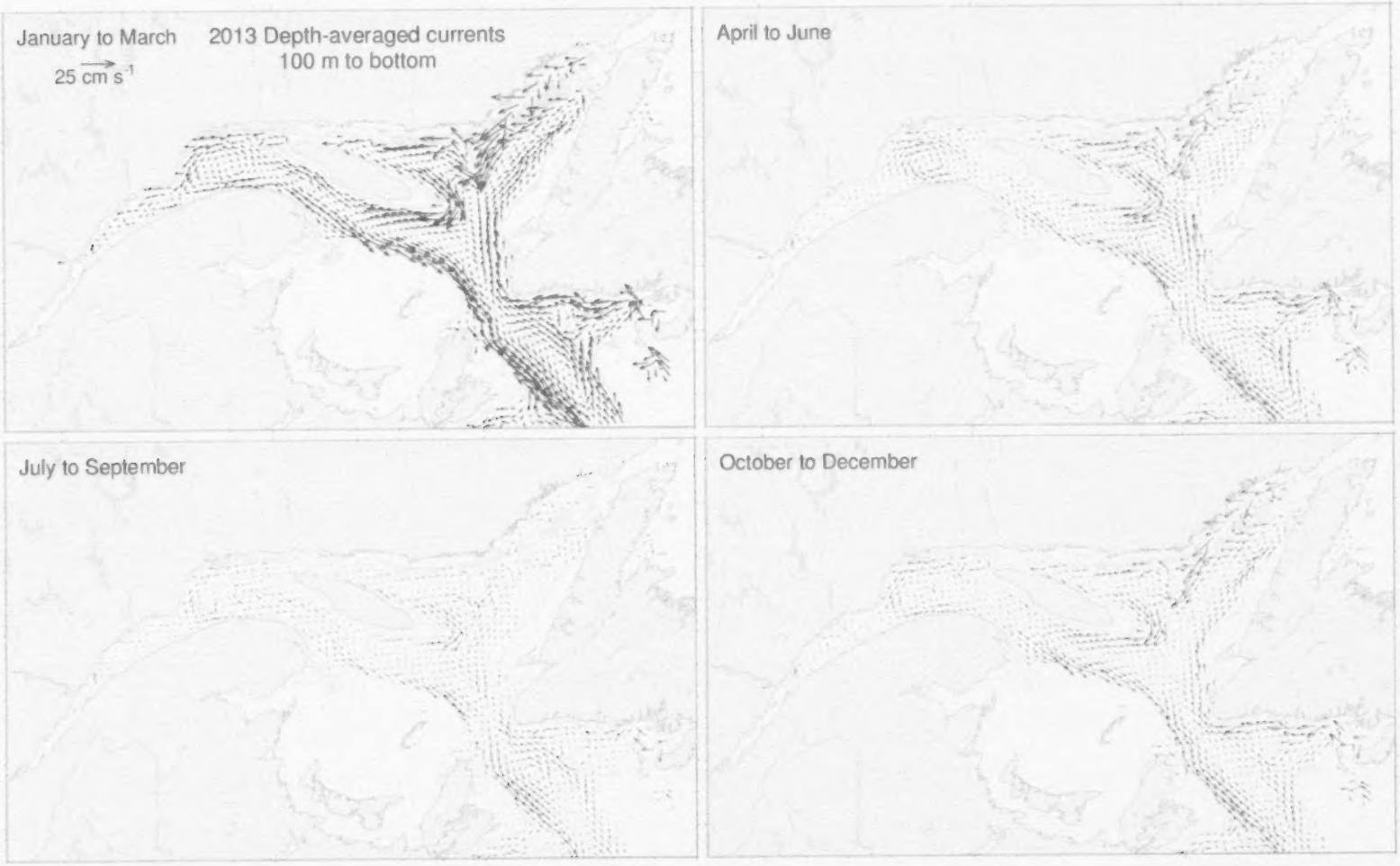

Fig. 62. Depth-averaged currents from 100 m to the bottom for each three-month period of 2013.

Fig. 63. Monthly averaged modelled transports and estuarine ratio across sections of the Gulf of St. Lawrence since 2006. The numbers on the right are the 2006–2013 means and standard deviations. The numbers in the boxes are normalized anomalies. Colours indicate the magnitude of the anomaly. Sv (Sverdrup) are units of transport equal to 10^6 $m^3 s^{-1}$.

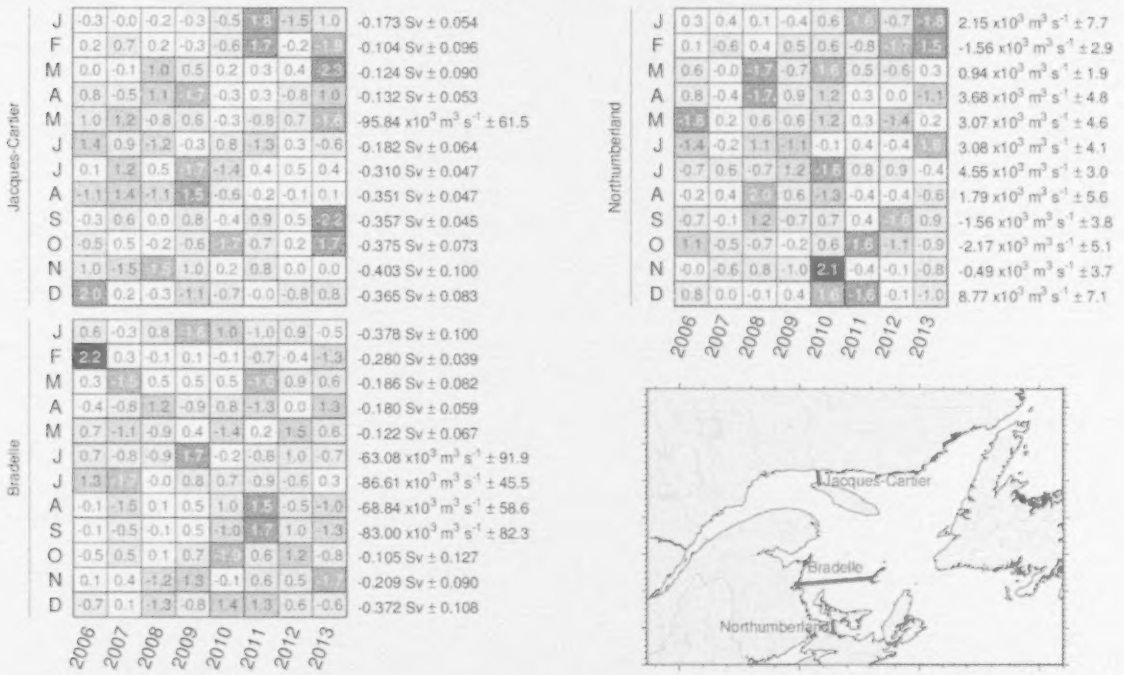

Fig. 64. Monthly averaged modelled transports across sections of the Gulf of St. Lawrence since 2006. The numbers on the right are the 2006–2013 means and standard deviations, with positive values toward east and north. The numbers in the boxes are normalized anomalies. Colours indicate the magnitude of the anomaly (e.g., negative anomalies are still shown in red when the mean transport is negative across the section).

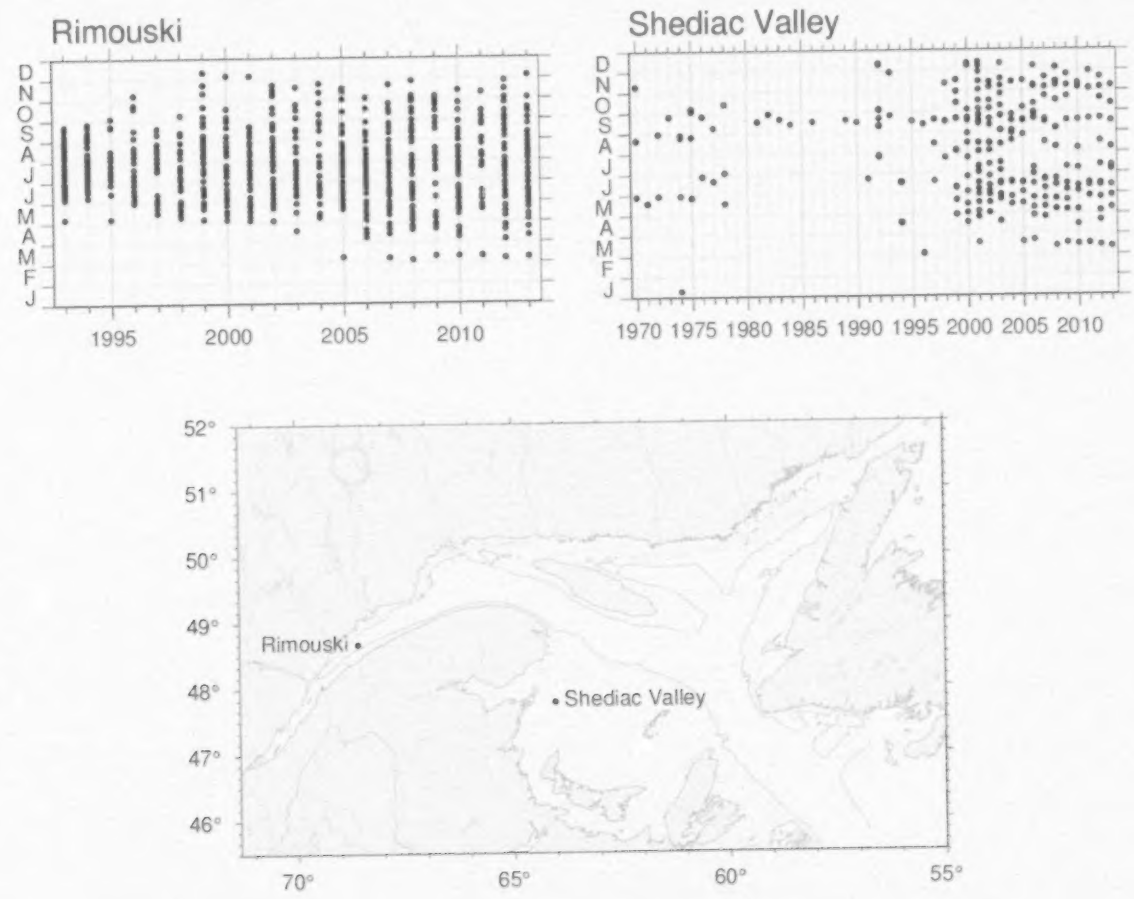

Fig. 65. Sampling frequency and positions of the AZMP stations Rimouski and Shediac Valley.

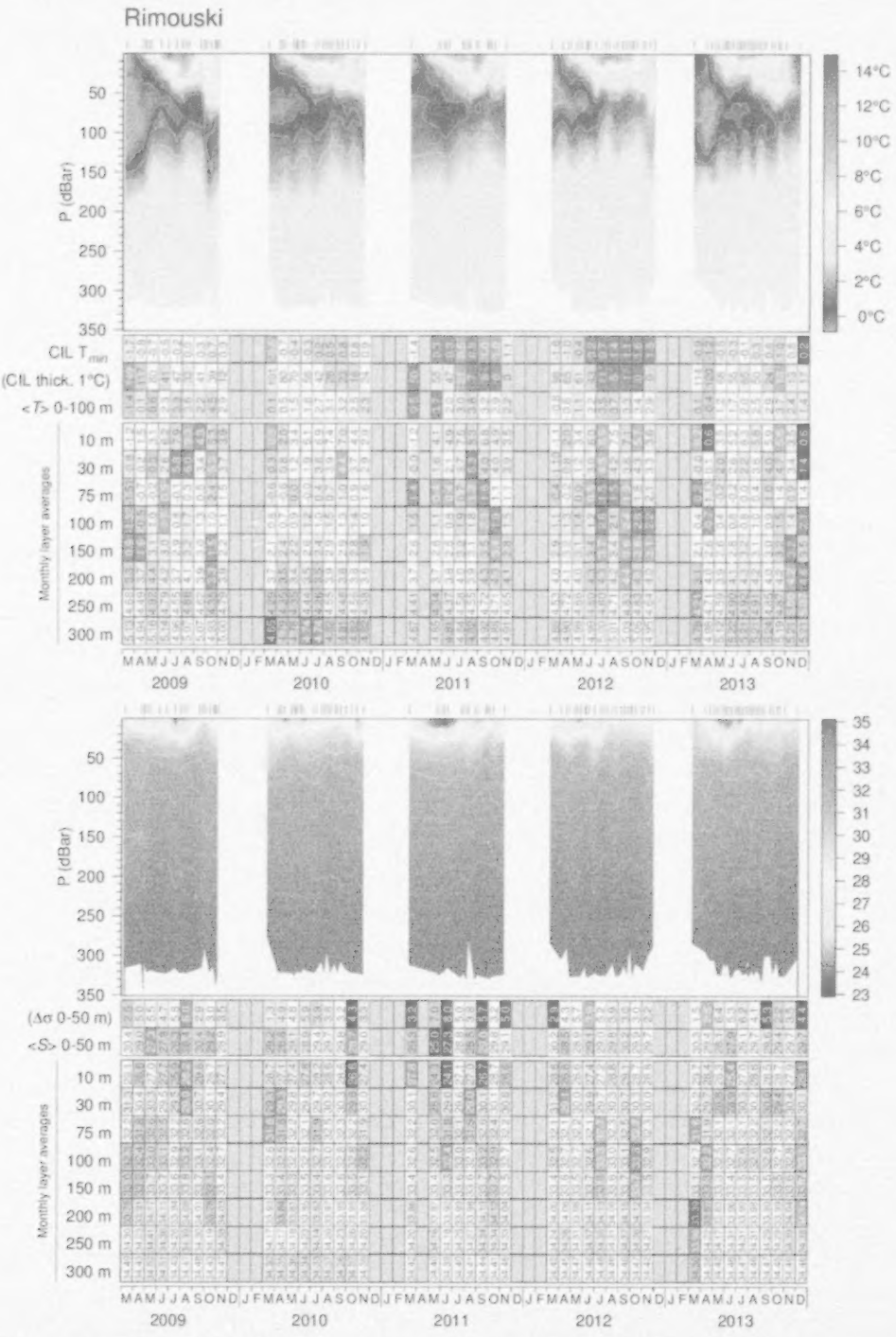

Fig. 66. Isotherm (top) and isohaline (bottom) time series at the Rimouski station; tick marks above indicate sample dates. The scorecard tables are monthly layer averages colour-coded according to the anomaly relative to the 1993–2010 monthly climatology for the station (yearly climatology for 250 m and deeper). Thickness of the CIL and stratification have reversed colour codes where red indicates thinner CIL (warmer water) and less stratification (higher surface salinity).

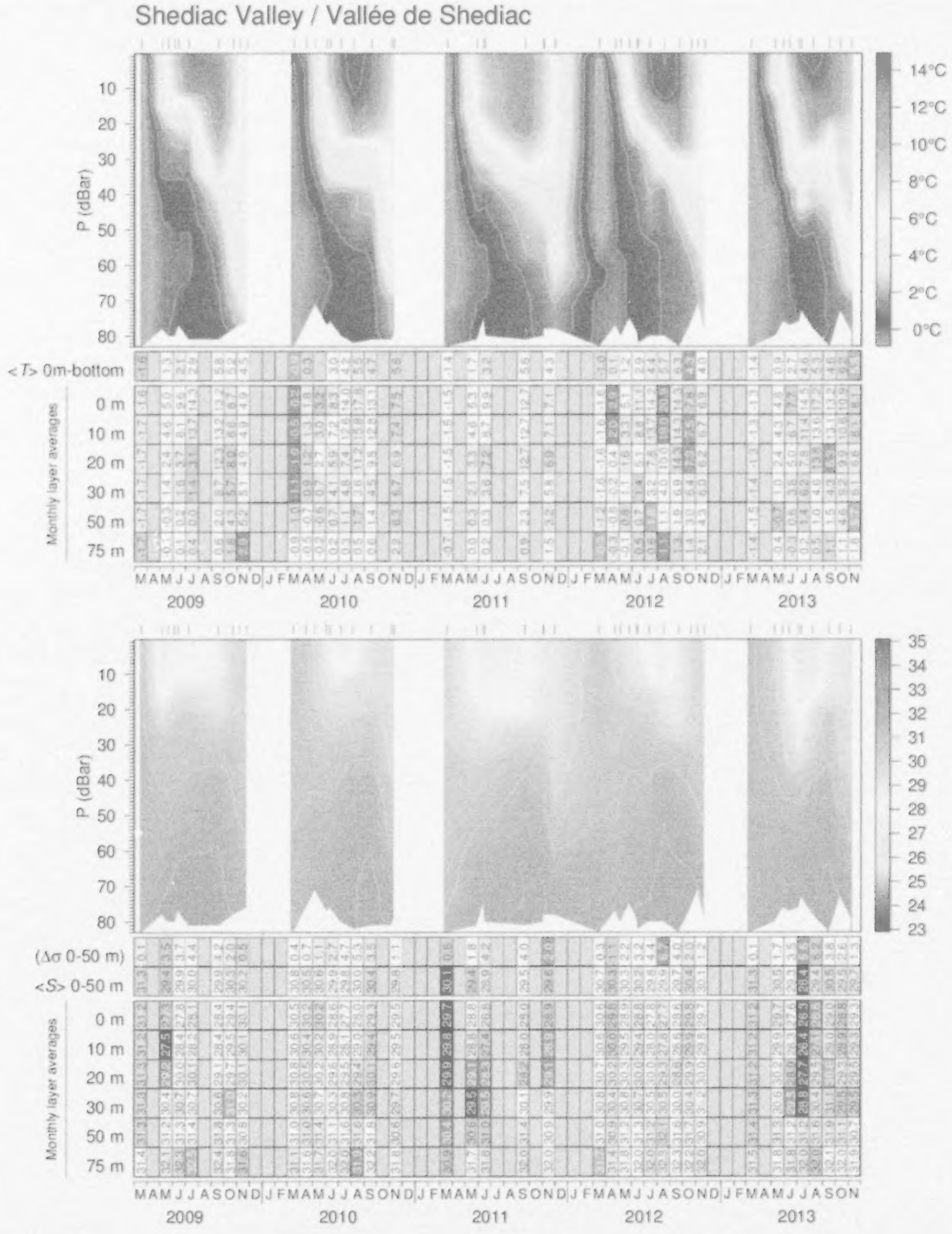

Fig. 67. Isotherm (top) and isohaline (bottom) time series at the Shediac Valley station; tick marks above indicate sample dates. Scorecard tables are monthly layer averages colour-coded according to the anomaly relative to the 1981–2010 monthly climatology for the station (input to climatology is sparse prior to 1999).

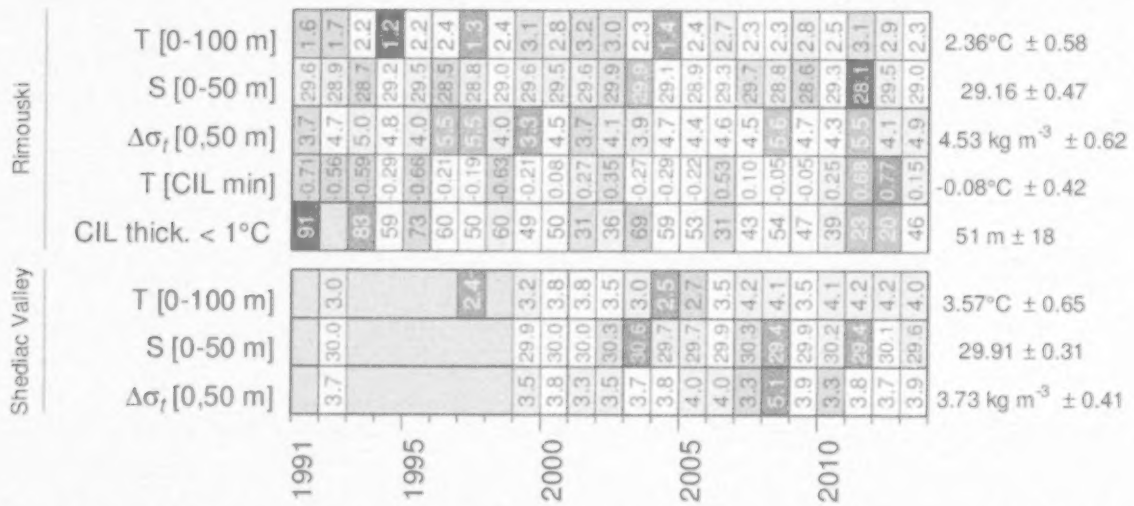

Fig. 68. May to October temperature and salinity layer averages, stratification expressed as the density difference between 0 and 50 m, and CIL temperature minimum and thickness (T<1°C) for the fixed monitoring stations. Numbers in panels are monthly average values colour-coded according to the anomaly relative to the 1991–2013 time series. Three months of anomaly data, between May and October, are required to show an average anomaly for any given year.

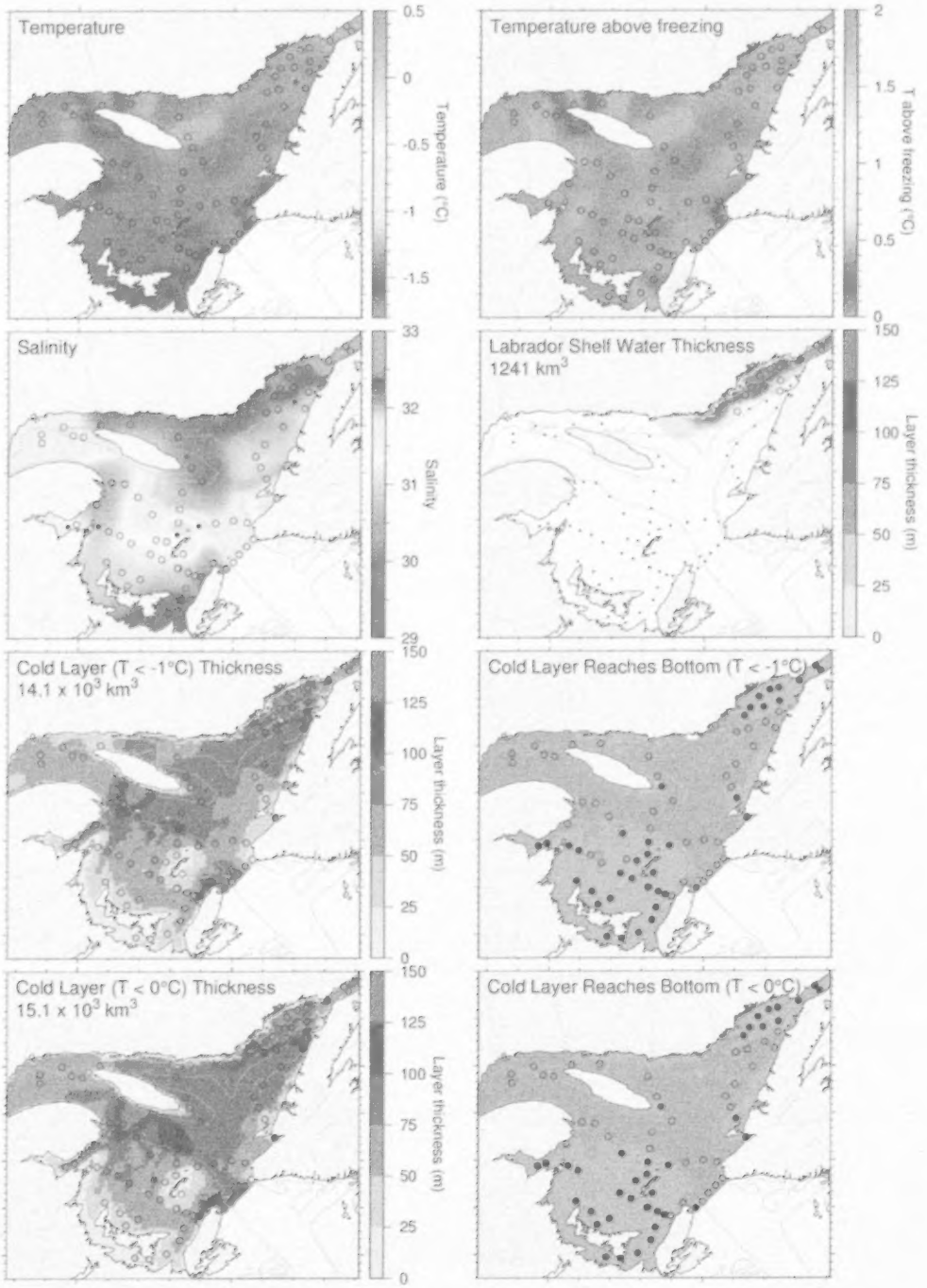

Fig. 69. March 2014 surface cold layer characteristics: surface water temperature (upper left), temperature difference with the freezing point (upper right), salinity (second row left), estimate of the thickness of the Labrador Shelf water intrusion (second row right), and cold layer (T<-1°C and <0°C) thicknesses and where they reach bottom. The symbols are coloured according to the value observed at the station, using the same colour palette as the interpolated image. A good match is seen between the interpolation and the station observations where the station colours blend into the background.

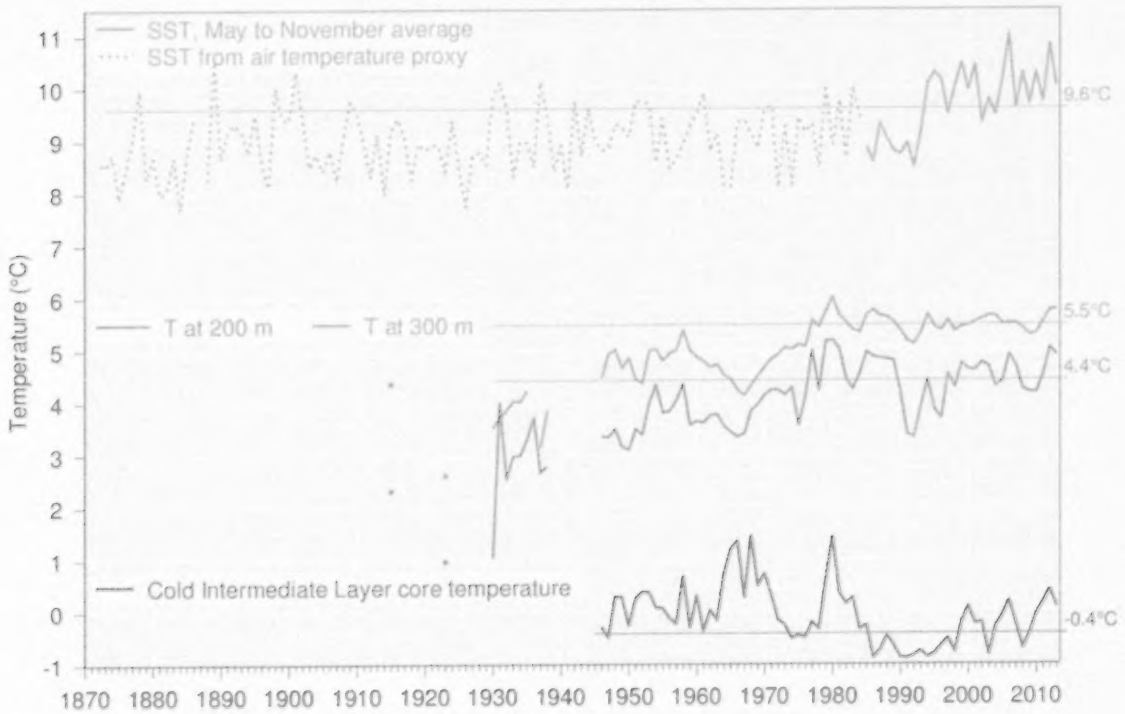

Fig. 70. Water temperatures in the Gulf of St. Lawrence. May–November SST averaged over the Gulf excluding the Estuary (1985–2013, red line), completed by a proxy based on April–November air temperature (1873–1984, red dashed line; average of all AHCCD stations in Fig. 4 but excluding Estuary stations at Baie Comeau and Mont-Joli). Layer-averaged temperature for the Gulf of St. Lawrence at 200 and 300 m (green lines). Cold intermediate layer minimum temperature index in the Gulf of St. Lawrence (blueline). SST air temperature proxy is similar to that of Galbraith et al. (2012). Climatological averages based on the 1981-2010 period are indicated by thin lines labeled on the right side. Figure adapted from (Benoît et al. 2012).

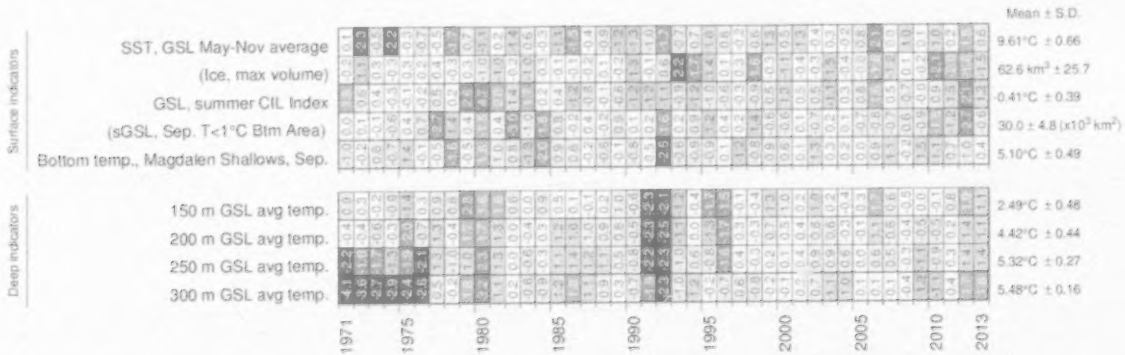

Fig. 71. Surface and deep indicators used in the composite climate index (Fig. 72)

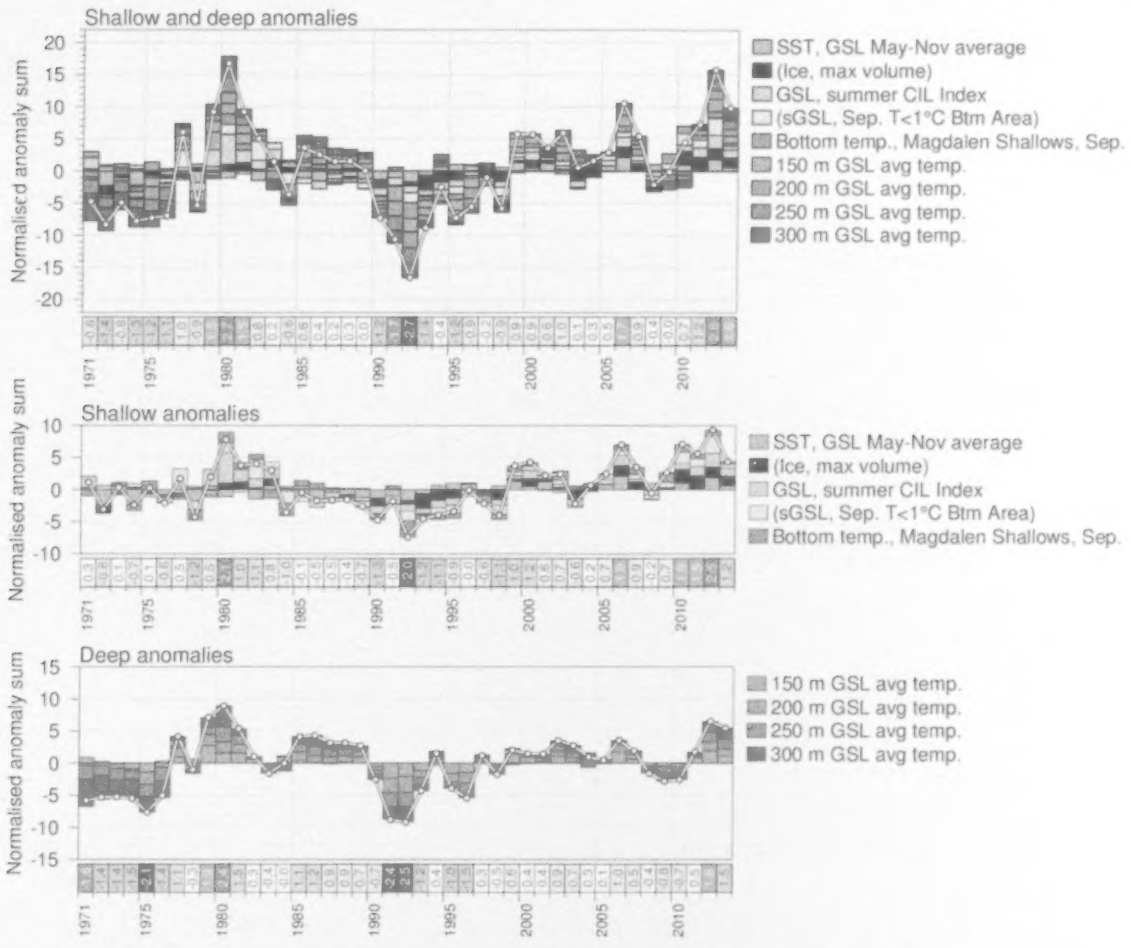

Fig. 72. Composite climate indices (white lines and dots) derived by summing various normalized anomalies from different parts of the environment (colored boxes stacked above the abscissa are positive anomalies, and below are negative). Top panel sums anomalies representing the entire water column, middle panel sums shallow anomalies and bottom panel sums deep anomalies.